EXPERIMENTAL EVALUATION OF GEOMEMBRANE / GEOTEXTILE INTERFACE AS BASE ISOLATING SYSTEM

A THESIS SUBMITTED TO
THE GRADUATE SCHOOL OF NATURAL AND APPLIED SCIENCES
OF
MIDDLE EAST TECHNICAL UNIVERSITY

BY

AMIN TAHERI BONAB

IN PARTIAL FULFILLMENT OF THE REQUIREMENTS
FOR
THE DEGREE OF MASTER OF SCIENCE
IN
CIVIL ENGINEERING

APRIL 2016

Approval of the thesis:

EXPERIMENTAL EVALUATION OF GEOMEMBRANE / GEOTEXTILE INTERFACE AS BASE ISOLATING SYSTEM

submitted by **AMIN TAHERI BONAB** in partial fulfillment of requirement for the degree of **Master of Science** in **Civil Engineering Department**, **Middle East Technical University** by:

Prof. Dr. Gülbin Dural Ünver
Dean, Graduate School of **Natural and Applied Sciences** _____

Prof. Dr. İsmail Özgür Yaman
Head of Department, **Civil Engineering** _____

Assoc. Prof. Dr. Zeynep Gülerce
Supervisor, **Civil Engineering Dept., METU** _____

Asst. Prof. Dr. Volkan Kalpakcı
Co-Supervisor, **Civil Engineering Dept., HKU** _____

Examining Committee Members:

Prof. Dr. Erdal Çokça
Civil Engineering Dept., METU _____

Assoc. Prof. Dr. Zeynep Gülerce
Civil Engineering Dept., METU _____

Asst. Prof. Dr. Volkan Kalpakcı
Civil Engineering Dept., HKU _____

Asst. Prof. Dr. Nabi Kartal Toker
Civil Engineering Dept., METU _____

Asst. Prof. Dr. Nejan Huvaj Sarıhan
Civil Engineering Dept., METU _____

Date: _____

I hereby declare that all information in this document has been obtained and presented in accordance with academic rules and ethical conduct. I also declare that, as required by these rules and conduct, I have fully cited and referenced all material and results that are not original to this work.

Name, Last Name: Amin, TAHERI BONAB

Signature:

ABSTRACT

EXPERIMENTAL EVALUATION OF GEOMEMBRANE / GEOTEXTILE INTERFACE AS BASE ISOLATING SYSTEM

Taheri Bonab, Amin

M.S., Department of Civil Engineering

Supervisor: Assoc. Prof. Dr. Zeynep Gülerce

Co-Supervisor: Asst. Prof. Dr. Volkan Kalpakcı

April 2016, 82 pages

The objective of this study is to evaluate the effect of the composite liner seismic isolation system on the seismic response of small-to-moderate height structures. For this purpose, a building model with the natural frequency of 3.13 Hz (representing 3-4 story structures) was tested with and without the addition of composite liner system using the shaking table test set-up by employing harmonic and modified/ scaled ground motions. Experiment results showed that the composite liner seismic isolation system significantly reduced the floor accelerations, especially in moderate-to-high ground shaking levels. The interaction between the natural frequency of the model and the frequency of the loading is evaluated by integrating the test results obtained here with previously conducted experiments on similar models by Kalpakcı (2013). Analysis results displayed that the composite liner system is most effective when these two frequencies are close to each other. Based on the test results discussed here, a mean spectrum was derived to define the behavior of the isolation system in frequency domain under ground motion excitation.

Keywords: Seismic isolation, composite liner, geotextile, geomembrane, dynamic tests, shaking table, building response.

ÖZ

GEOMEMBRAN / GEOTEKSTİL ARAYÜZÜNÜN TEMEL IZOLASYONU OLARAK KULLANILMASININ DENEYSEL OLARAK İNCELENMESİ

Taheri Bonab, Amin
Yüksek Lisans, İnşaat Mühendisliği Bölümü
Tez Yöneticisi: Doç. Dr. Zeynep Gülerce
Ortak Tez Yöneticisi: Yrd. Doç. Dr. Volkan Kalpakcı

Nisan 2016, 82 sayfa

Bu çalışmanın amacı kompozit sismik izolasyon sisteminin küçükten orta yüksekliğe kadar olan yapıların sismik tepkileri üzerindeki etkisini değerlendirmektir. Bu amaçla, 3-4 katlı yapıları temsil eden (doğal frekansı 3.13 Hz olan) bir bina modeli, kompozit sistemin eklenmesiyle ve kompozit sistem olmadan sarsma tablası üzerinde harmonik ve uyarlanmış yer hareketleri kullanarak test edilmiştir. Deney sonuçları, kompozit sismik izolasyon sisteminin katlarda ölçülen ivmeleri özellikle orta/yüksek yer hareketi seviyelerinde önemli ölçüde azalttığını göstermiştir. Modelin doğal frekansı ile uygulanan hareketin frekansı arasındaki etkileşimin incelenmesi için bu deney setinin sonuçları benzer modellerle daha önce yapılmış deney sonuçları (Kalpakcı, 2013) ile birleştirilerek tekrar analiz edilmiştir. Analiz sonuçları, bu iki frekansın birbirine yakın olduğu durumlarda kompozit sistemin etkinliğinin arttığını işaret etmektedir. Test sonuçları kullanılarak, sismik izolasyon sisteminin kuvvetli yer hareketleri altındaki davranışını tanımlayan ortalama bir tepki spektrumu elde edilmiştir.

Anahtar Kelimeler: Sismik izolasyon, kompozit sistem, geotesktil, geomembran, dinamik deneyler, sarsma tablası, tepki spektrumu.

To my beloved family

ACKNOWLEDGMENTS

The author wishes to express his sincere appreciation to his precious supervisor
Prof. Dr. Zeynep GÜLERCE
for her guidance, advice and encouragements throughout the research.

Asst. Prof. Dr. Volkan KALPAKCI
is sincerely acknowledged for his valuable support and contributions.

Finally, the author is grateful for the continuous support and encouragement
he has received from his family.

TABLE OF CONTENTS

LIST OF FIGURES

LIST OF TABLES

LIST OF SYMBOLS

A_b: Base area

D: Critical damping ratio

d_i= amplitude at i^{th} cycle

FB: Fixed base condition

H: Height of story at which acceleration was measured

IB: Isolated base condition

L: Total height of model

P_m: base pressure of model

W_m: weight of model

CHAPTER 1

INTRODUCTION

Turkey and other earthquake-prone countries frequently experience moderate to large magnitude earthquakes. These earthquakes mostly result in loss of lives and collapse of most of the improperly built structures, especially in developing countries (e.g. 2010 Chile Earthquake). Isolating the building from the ground shaking is one of the methods that has been proposed to avoid such collapses. Various types of seismic isolators (e.g. elastomeric bearings, sliding bearings) have been designed for special structures all around the world; however, the use of these seismic isolators have still not become a standard practice in Turkey and in other developing countries mainly due to their high initial costs and difficulties in their installation. In the last two decades, many research efforts were focused on designing innovative seismic isolators with lower costs and application ease. One of the recently developed systems, known as the "composite liner system", combines geotextiles and geomembranes to be used as base isolators. Shaking table studies that test the dynamic properties of composite liners with rigid blocks on top are available in the literature and the details of these experiments are provided in **Chapter 2**. Similar tests on composite liner system were also conducted on the shaking table test set-up located in the Middle East Technical University Soil Mechanics Laboratory, using 2-story and 4-story building models since the blocks in previous studies were rigid and consequently had a higher natural frequency than typical buildings (Kalpakcı, 2013). **Chapter 2** also includes a detailed summary of the tests performed by Kalpakcı (2013).

Kalpakcı (2013) noted that the frequency of the loading has a significant effect on the efficiency of the composite liner system. Since the previous tests are limited with only two models, 2-story and 4-story models with the scale of 1:12, the results could not be fully utilized to analyze these effects in a systematic manner. One of the objectives of this study is to complement the test results of Kalpakcı (2013) by adding more data using a building model with a different natural frequency.

Therefore, a 3-story building model with the natural frequency of 3.13 Hz was designed and tested by employing harmonic and modified ground motions in both fixed base and isolated base conditions. The shaking table test set up, 3-story building model, and the harmonic and modified ground motions used in the tests are presented in **Chapter 3**. 69 experiments under different loading and base conditions were performed and the acceleration time history of each floor was recorded during these experiments. Tests results are given and thoroughly discussed in **Chapter 4**.

To understand the relation between the frequency of the harmonic load and the natural frequency of the model, the test results gathered in this study was combined with the results of 2-story and 4-story tests. The reduction in the floor accelerations in the isolated base case when compared to the fixed base case is analyzed in **Chapter 5**. Analysis results showed that the interaction between these two frequencies has a significant effect on the efficiency of the composite liner system, especially for harmonic loads. However, for modified and scaled ground motions, this effect is not that substantial and the test results from all models can be combined to analyze the reduction in the response. Combined results of tests with modified ground motions are also presented in **Chapter 5**. The efficiency of the composite liner system in reducing the spectral accelerations in a range of frequencies were evaluated and a mean response spectra was derived to define the behavior of the isolation system under ground motion excitation. Main conclusions of this study and recommendations for future studies are provided in **Chapter 6**.

CHAPTER 2

PREVIOUS STUDIES ON THE SEISMIC RESPONSE OF COMPOSITE LINER SYSTEM USED AS BASE ISOLATION

Seismic isolation of foundation systems from the base of the structure is not a new idea and studies on this subject return to the 1960s. The basic definition of seismic isolation is *a system for decoupling the motions of ground from motions of superstructure in order to decrease earthquakes' destructive effects to the structure*. In fact, seismic base isolation dissipates the earthquake energy by reducing the transmission of acceleration from ground to the superstructure (Figure 2.1).

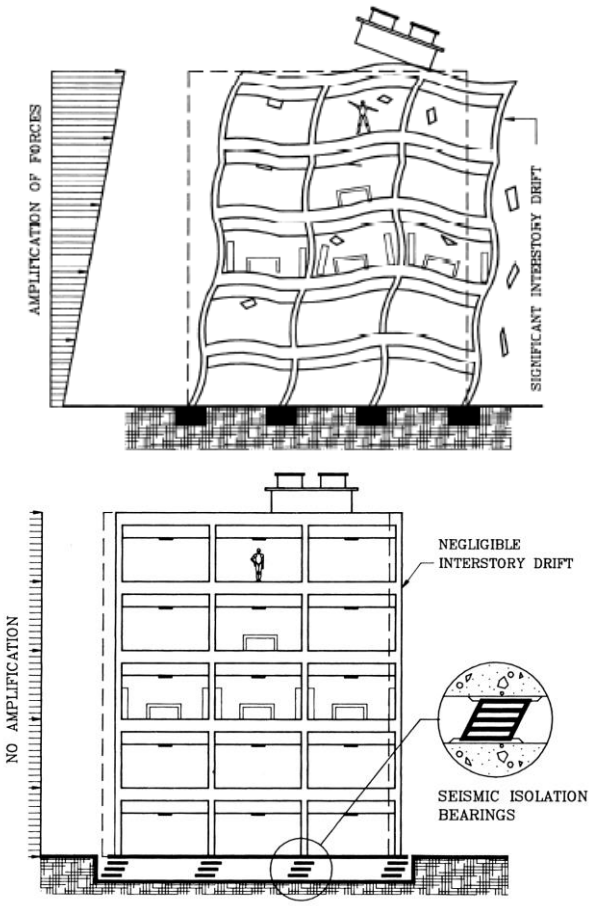

Figure 2.1 Conventional structures and base isolated structures (Naeim and Mayes, 2001)

Various types of seismic isolation systems have been developed and used for this purpose. Elastomeric and sliding isolators are the major types of seismic isolators, which are used in developed countries (Figure 2.2). 'Lead Rubber Bearing' (LRB) and 'High Damping Rubber Bearing' (HDRB) are mainly two types of elastomeric isolators. 'Sliding Support with Rubber-pad' (SSR) and 'Friction Pendulum System' (FPS) are the types of sliding bearing systems.

(a) (b)

Figure 2.2 (a) Elastomeric and (b) Sliding isolators

Since the application and implementation of seismic base isolation systems are costly and requires expert and experienced staff to install, their application is limited to public housing, schools, hospitals and structures with major importance. Therefore, researchers have been attempting to find an easy-to-use, innovative and cost effective approach to solve this problem. Using geomembrane and geotextile as a seismic isolator is one of these new systems that researchers have been investigating for the past few decades. In a study by Yegian and Lahlaf (1992), the static and dynamic interface properties of geomembrane and geotextile was investigated. In their study, static shear tests were performed in order to measure the static angle of friction (Table 2.1). And also different shaking table tests with different frequencies and normal stresses was performed on the selected geosynthetic combination in both dry and submerged condition in order to measure the dynamic friction angle (Table 2.2).

Table 2.1 Static friction angle (Yegian and Lahlaf, 1992)

Interface condition (1)	Peak angle of friction ϕ (2)	tan ϕ (3)	Residual angle of friction ϕ (4)	tan ϕ (5)
Geomembrane[a]/geotextile[b] dry	10.7°	0.19	10.0°	0.18
Geomembrane[a]/geotextile[b] submerged	9.6°	0.17	8.5°	0.15

[a]Gundle HD60: hard, smooth HDPE.
[b]Polyfelt TS700: Nonwoven, continuous filament, needlepunched geotextile.

Table 2.2 Dynamic friction angle (Yegian and Lahlaf, 1992)

Interface condition (1)	Acceleration transmitted to block at first observation of sliding (2)	Peak dynamic friction angle (3)	Acceleration transmitted to the block after sliding is initiated (4)	Residual dynamic friction angle (5)
Geomembrane[a]/geotextile[b] dry	0.2 g	11.3°	0.19 g[c]–.24 g[d]	10.7–13.5°
Geomembrane[a]/geotextile[b] submerged	0.19 g	10.7°	0.17 g[c]–.23 g[d]	9.6–13°

[a]Gundle HD60: hard, smooth HDPE.
[b]Polyfelt TS700: Nonwoven, continuous filament, needlepunched geotextile.
[c]At first observation of sliding.
[d]At table acceleration of 0.4 g.

The following conclusions were made Yegian and Lahlaf (1992):

- As the induced forces exceeded the shear strength of the geosynthetic interface, the transferred acceleration slightly increased by increasing the applied acceleration and the amount of this increment was independent of the frequency of input motion. (Figure 2.3 and Figure 2.4)
- Angle of friction measured under dynamic tests were slightly larger compared to angle of friction under static tests. The residual angle of friction under dynamic loadings was approximately equal to peak angle of friction under static loading. In addition to this, measured angle of friction in dry condition was larger than the one in submerged condition.

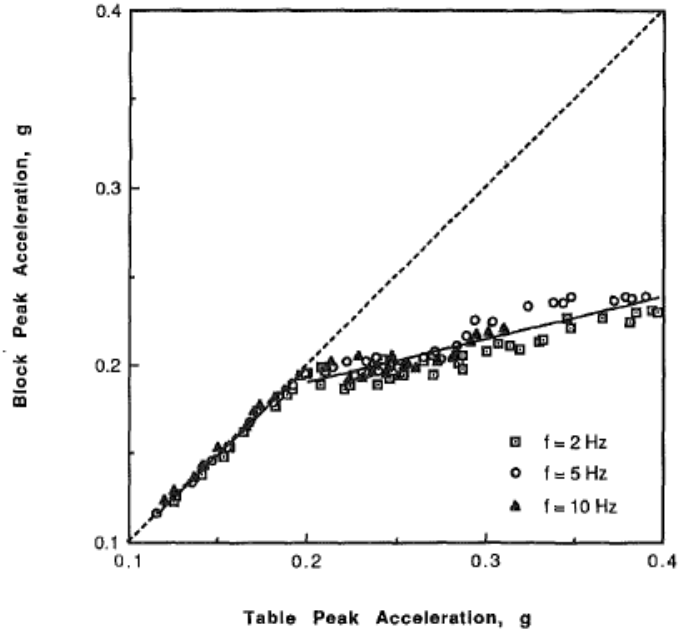

Figure 2.3 Experiments using shaking table for geosynthetic interface in dry condition with normal stress 1.2 psi (8.5 kPa) and for motions f=2,5,10 Hz (Yegian and Lahlaf, 1992)

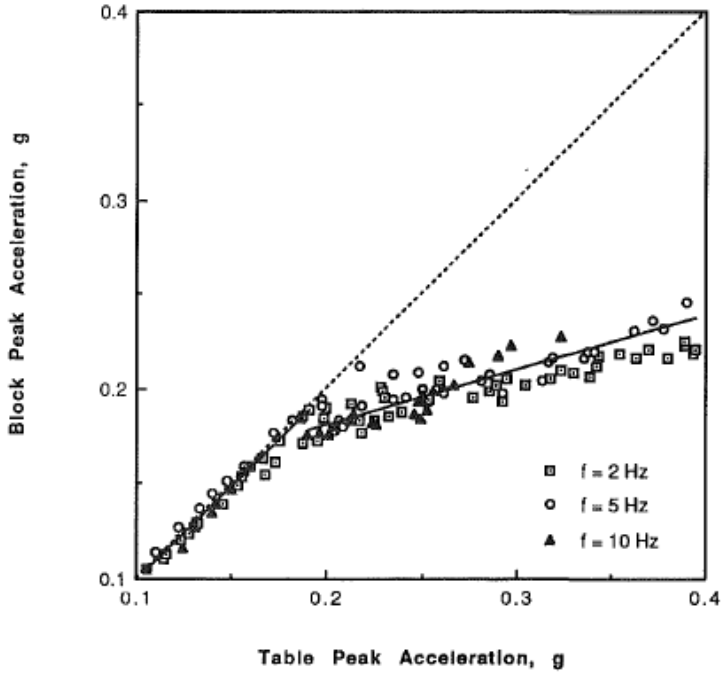

Figure 2.4 Experiments using shaking table for geosynthetic interface in submerged condition with normal stress 1.2 psi (8.5 kPa) and for motions f=2,5,10 Hz (Yegian and Lahlaf, 1992)

In a study by Yegian et al. (1999), the use of geosynthetic materials as seismic energy dissipation system was investigated. Geosynthetic or related materials that are placed under foundations can absorb seismic energy, and hence transmit limited shear forces and consequently smaller levels of excitation to an overlying structure. Three following combinations of interfaces were chosen for shaking table tests:

- Smooth HDPE/HDPE;
- Smooth HDPE/Nonwoven spun-bonded Geotextile;
- Polytetrafluoroethylene (PTFE)/PTFE.

In order to determine friction coefficients of tested interfaces, shaking table tests were carried out and the interface with minimum friction coefficient was chosen, since the minimum friction causes the maximum decrease in earthquake induced forces. However, the interface's friction coefficient had to be independent of the slip rate. Results of shaking table tests under cyclic loading utilizing these three combinations of different interfaces showed that the transmitted acceleration through UHMWPE/Geotextile interface was lower than other combinations (Figure 2.5). The 'Ultra High Molecular Weight Polyethylene' (UHMWPE)/Geotextile interface which has the lower friction coefficient (independent of slip rate), was chosen for the future shaking table tests.

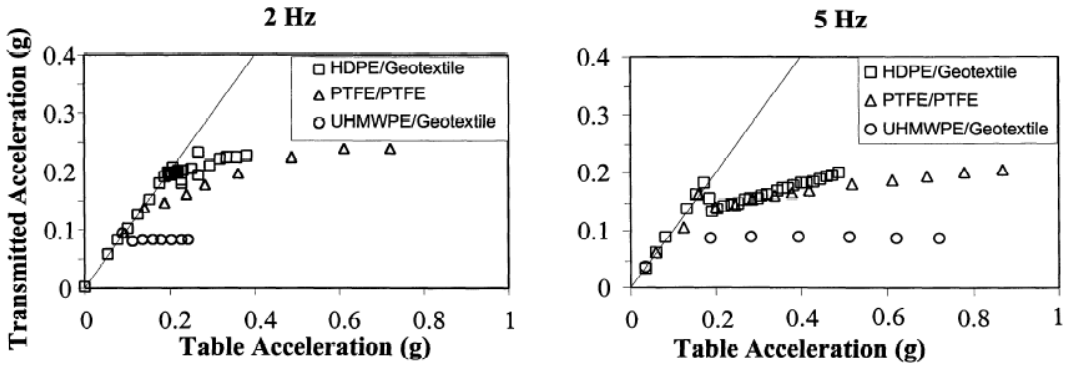

Figure 2.5 Accelerations transmitted through geosynthetic interfaces tested at 2 and 5 Hz (Yegian et al., 1999)

A single-story building model was tested on shaking table and UHMWPE/Geotextile interface used as seismic isolator beneath the foundation of the model (Figure 2.6). Acceleration at the top, base level and at the shaking table and the displacement were

measured. In order to evaluate the efficiency of UHMWPE/Geotextile, the model was also tested in a fixed condition (without isolator). Three acceleration time history records were used as input ground motion. Figure 2.7 shows that the PGA of input ground motion, which was 0.35g was amplified to 0.77g at the top level when it was fixed to the shaking table and the PGA at the top level decreased to 0.33g when it was placed on UHMWPE/Geotextile interface, showing a reduction of 60% compared to fixed base condition.

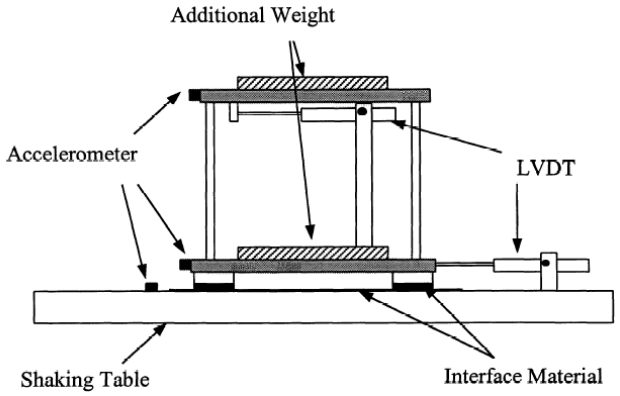

Figure 2.6 Single Story experimental model used in Yegian et al, 1999.

In another study by Yegian and Kadakal (2004), more combinations and more tests were conducted in order to evaluate the efficiency and applicability of this seismic isolator. Table 2.3 shows the combinations that were used in order to find the minimum friction coefficient, which results in minimum earthquake force transmission. The combinations were tested under different normal stresses. Figure 2.8 shows the effect of normal stress on the friction angle. As it was seen from that figure, the combination Geotextile/UHMWPE has lower friction coefficient compared to other combinations and consequently this interface would be a suitable liner for this purpose.

After the suitable geosynthetic interface was determined, shaking table tests were conducted by using this geosynthetic combination on a rigid block. The tests were performed by applying harmonic excitation with frequencies in the range of f= 1-5 Hz. Figure 2.9 shows the transmitted acceleration from shaking table to rigid block. This graph demonstrates that by increasing the acceleration of the shaking table, the maximum acceleration that could be measured on rigid block was 0.08g and this was independent of the frequency of input motion.

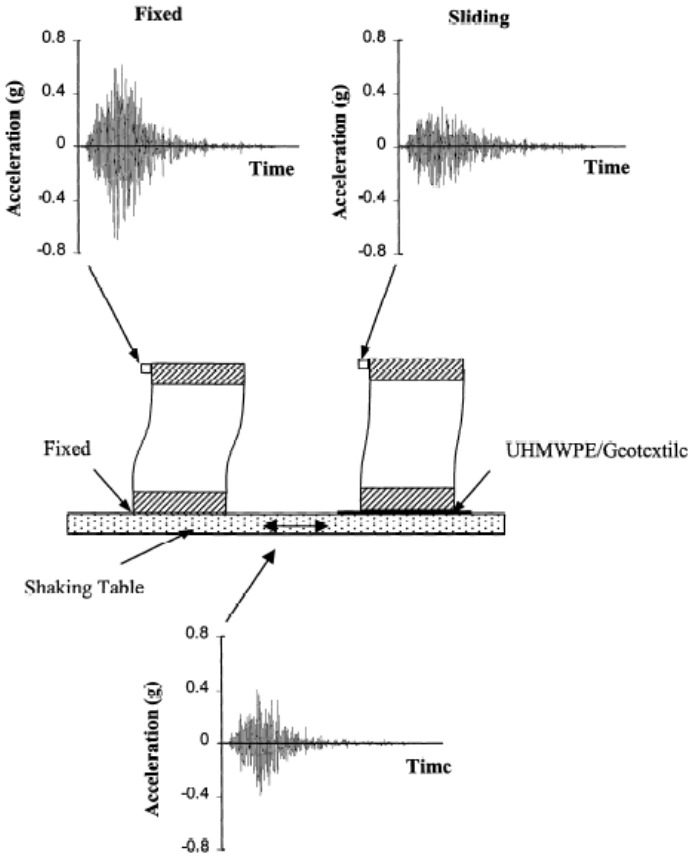

Figure 2.7 Comparison of model responses with and without geosynthetic foundation isolation. (Yegian et al, 1999)

Table 2.3 Interfaces and their friction coefficient used in Yegian and Kadakal, 2004.

Interface	Description	Friction coefficient
Geotextile/HDPE	A high-strength nonwoven geotextile, "Typar 3601" against 1.5 mm smooth HDPE (high density polyethylene)	0.15–0.3
PTFE/PTFE	Two sheets of 1.5 mm thickness PTFE (polypropylene)	0.08– 0.15
UHMWPE/UHMWPE	Two layers of 6.4 mm thick UHMWPE (ultrahigh molecular weight polyethylene) "TIVAR 88-2 AntiStatic"	0.09–0.25
Geotextile/UHMWPE	Typar 3601 geotextile against TIVAR 88-2, 6.4 mm thick UHMWPE	0.06–0.08

Additionally, ground motion tests were applied on the rigid block. Capitola earthquake which contains frequencies in a wide band and Corralitos and Santa Cruz earthquake which contain low and high frequencies respectively, in narrow bands. Figure 2.10 shows the transmitted maximum acceleration from shaking table. As shown on the graph the transmitted accelerations are about 0.11g in all of the tests and they are independent of frequency content and peak acceleration of input motions.

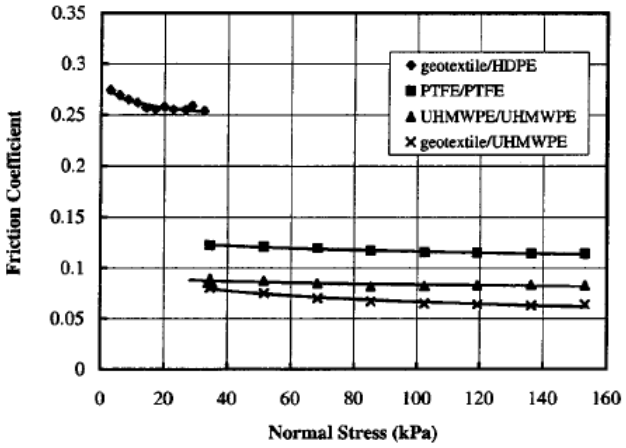

Figure 2.8 Friction Coefficient vs. Normal Stress (Yegian and Kadakal, 2004)

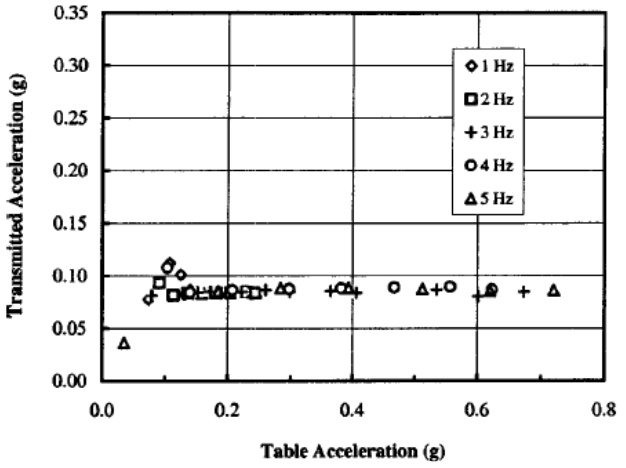

Figure 2.9 Maximum shaking table acceleration vs. transmitted acceleration during harmonic excitation (Yegian and Kadakal, 2004)

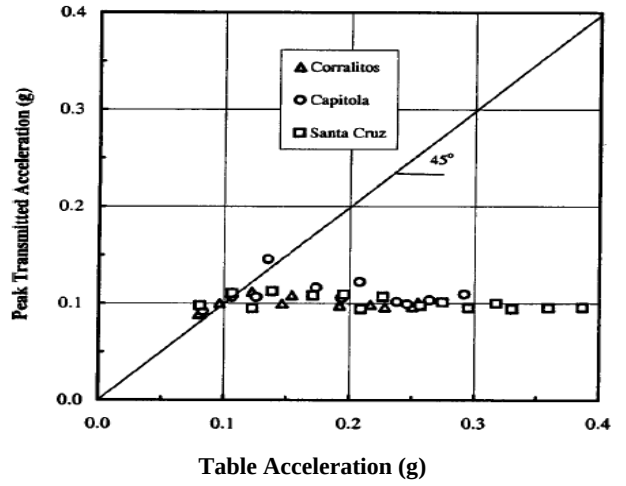

Figure 2.10 Maximum shaking table acceleration vs. transmitted acceleration during earthquake excitation (Yegian and Kadakal, 2004)

Finally, all of ground motion tests were conducted on a one-story model in order to investigate the effect of the geosynthetic combination on the drift. These tests were conducted for fixed base and isolated base mode. Figure 2.11 shows that by increasing the peak acceleration of input motion, model drift increases in fixed base mode whereas in isolated base mode drift values are smaller than those in the fixed base mode and remain constant.

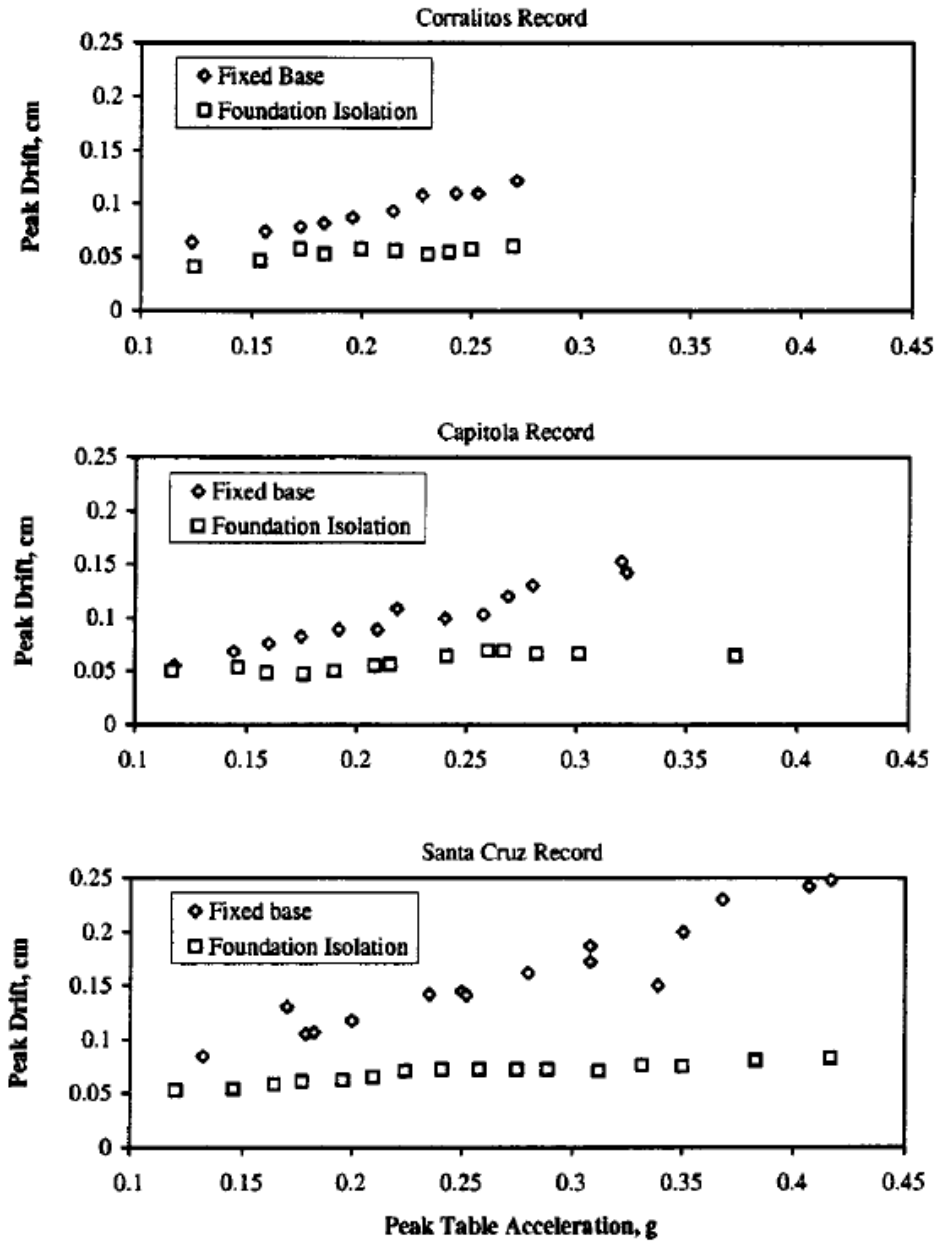

Figure 2.11 Maximum acceleration of shaking table vs. model drift (Yegian and Kadakal, 2004)

In the study performed by Kalpakcı (2013), the efficiency of geosynthetic liner similar to the one used in Yegian and Kadakal (2004) was investigated on two different experimental models. 2-Story model with natural frequency of f_n=4.35 Hz and 4-Story model with the natural frequency of f_n=2.33 Hz with the scale of 1:12 were prepared for this purpose (Figure 2.12). The models were tested in both fixed base (FB) and isolated base (IB) conditions in order to evaluate the efficiency of the geosynthetic liner, which was composed of UHMWPE (Ultra High Molecular Weight Polyethylene) and nonwoven heat-bonded geotextile.

(a) (b)

Figure 2.12 (a) 2-story and (b) 4-story model used in Kalpakcı (2013)

These models were tested under both harmonic motions and modified ground motions. Harmonic motions were chosen with frequency of f=1 to 4 Hz in order to cover the natural frequency of the experimental models. 4 different amplitudes were combined with different frequencies of the harmonic motions in order to provide the maximum acceleration of a_{max}= 0.08, 0.16, 0.24 and 0.3 g. Table 2.4 shows the details of harmonic motions used in Kalpakcı (2013).

Table 2.4 Properties of input harmonic motions used in Kalpakcı (2013)

Frequency (Hz)	**Displacement (mm)**			
1	20	40	60	75
2	5	10	15	18.75
3	2.22	4.44	6.66	8.33
4	1.25	2.5	3.75	4.69
Acceleration (g)	0.08	0.16	0.24	0.3

In addition to harmonic motions, these models also were tested under modified ground motions. 6 earthquake recordings, three with strike-slip mechanism and three with reverse mechanism were chosen in a way that predominant frequency of the input motion is approximately equal to f_n= 1, 2 and 4 Hz (Table 2.5). Amplitude of these motions were scaled to a_{max}= 0.1, 0.2 and 0.3g; therefore, each ground motion is applied more than once with different scale factors.

Table 2.5 Properties of input modified ground motions used in Kalpakcı (2013)

Mechanism	No	Earthquake	Date	Station	f (Hz)
Strike-Slip	1	Landers	28.06.1992	Arcadia Av	1
	2	Chalfant Valley	21.07.1986	Tinemaha Res	2
	3	Loma Prieta	18.10.1989	Capitola	4
Reverse	1	Coalinga	02.05.1983	Park Field	1
	2	Northridge	17.01.1994	Sylmar-County Hospital	2
	3	San Fernando	09.02.1971	Carbon Canyon Dam	4

Figures 2.13 (a-d) and Figures 2.14 (a-d) demonstrate acceleration at each story vs. H/L (H represents the height of story and L represents the total height of model) for 2-story and 4-story models respectively under harmonic motions. According to these figures, triggering the system and the reduction of the acceleration depends on the frequency of the input motion and independent of the a_{max} of input motion. The system is more efficient when the frequency of input motion is close to the natural frequency of the experimental model.

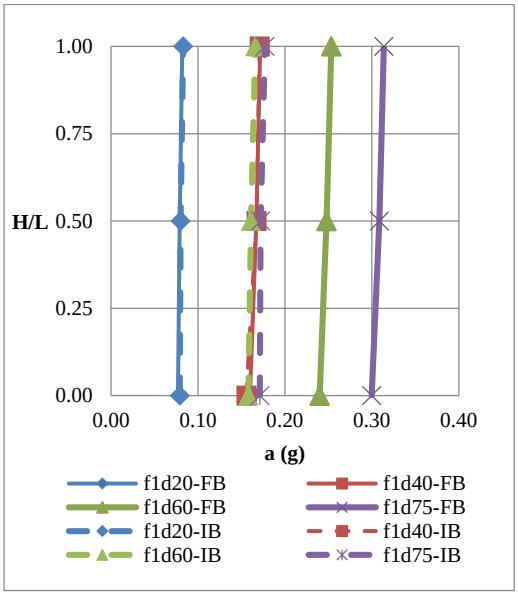

(a)

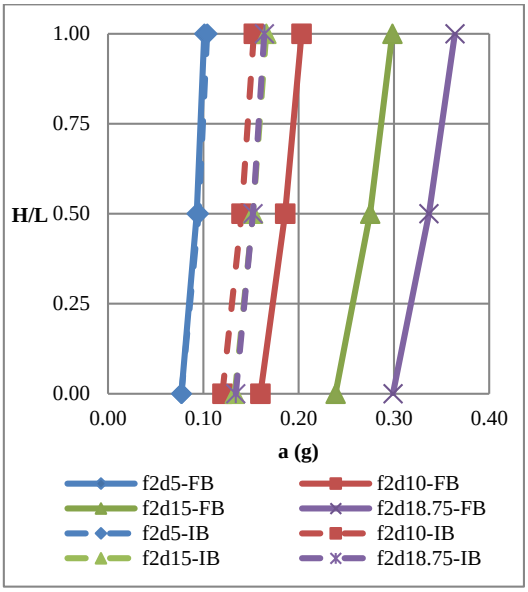

(b)

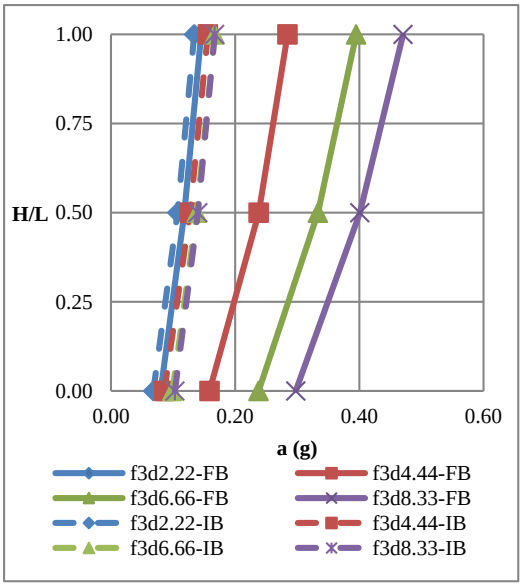

(c)

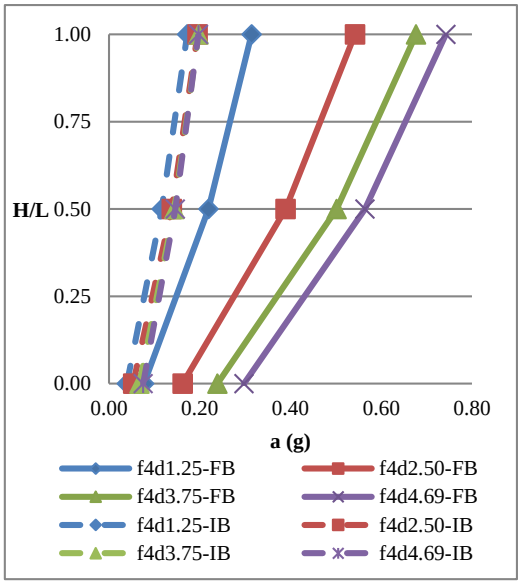

(d)

Figure 2.13 H/L vs. Acceleration for 2-Story Model (a) f= 1 Hz, (b) f= 2 Hz, (c) f= 3 Hz and (d) f= 4 Hz

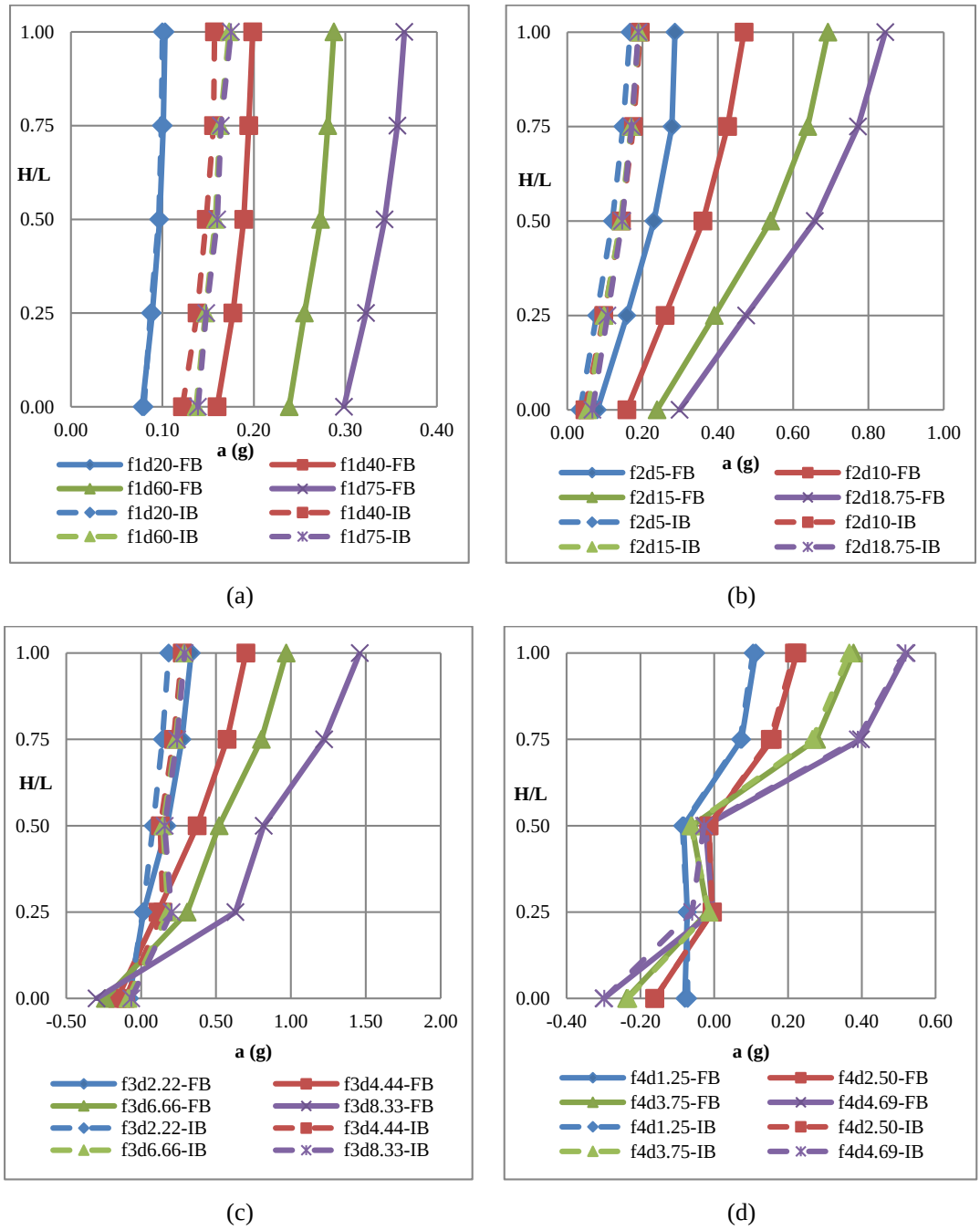

Figure 2.14 H/L vs. Acceleration for 4-Story Model (a) f= 1Hz, (b) f= 2 Hz, (c) f= 3 Hz and (d) f= 4 Hz

The figures show that application of seismic isolator does not change the mode of vibration. The seismic isolator was triggered in all ground motion experiments and this result was independent of the predominant frequency of input motion. In order to evaluate the efficiency of this system in the modified ground motion tests, the following equation was defined as:

$$\eta = 1 - (\frac{\Delta a_I}{\Delta a_F}) \qquad (2.1)$$

In which,

Δa_F : The difference between acceleration of top and base floors, for FB condition;

Δa_I : The difference between acceleration of top and base floors, for IB condition.

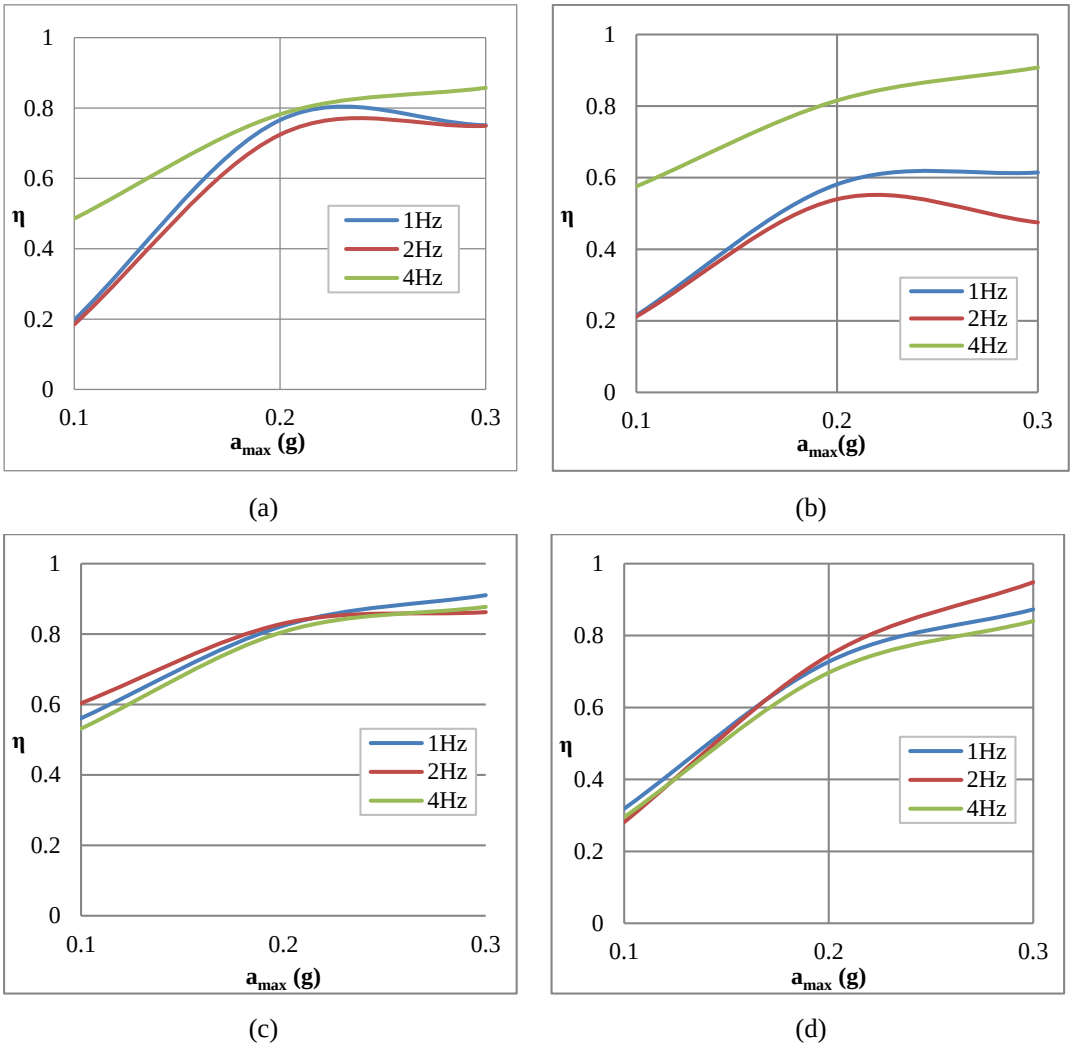

Figure 2.15 η vs. a_{max} for (a) 2-story model (strike-slip), (b) 2-story model (reverse) , (c) 4-story model (strike-slip), (d) 4-story model (reverse)

Figure 2.15 (a-d) shows the efficiency of the isolator for 2-story and 4-story models respectively. As it can be seen in the graphs, the efficiency of the isolator system is independent of predominant frequency of input motion however in experiments on the 2-story model the system worked with higher efficiency as it coincides with

natural frequency of the model. Similar to the 2-story model, the seismic isolator is also triggered for 4-story model and also was independent of predominant frequency of the model. Another conclusion that could be drawn from the figures is that by increasing the a_{max} of input motion the efficiency of the system increases.

CHAPTER 3

EXPERIMENTAL SETUP AND TESTING PROGRAM

The shaking table test set-up used in this study is located in the Middle East Technical University Soil Mechanics Laboratory. Design and production stages of the shaking table along with its specifications were given in Kalpakcı (2013) and Kalpakcı et al. (2014); therefore, only a brief summary will be provided in this section. The servo-engine shaking table shown in Figure 3.1 is capable of performing dynamic tests with harmonic and random motions along a single axis. However, the applied motions are limited with the maximum frequency of 5 – 7 Hz (depending on the payload, maximum 2 tons) and the maximum acceleration (a_{max}) of 0.3g. Two switches control the amplitude of shaking table and shut down the system completely when the displacement of the table reaches to the limiting amplitude (±300 mm). The external dimensions of the shaking table are 2m x 4m and its platform is 1m x 1.5m. A laminar box of the same size in plan view can be attached to the table.

2.1 Experimental Model Properties

A 3-story model (composed of 3 stories and a base slab) that is consistent with the experimental models of Kalpakcı (2013) was prepared with the scale of 1:12 for this study (Figure 3.2). Slabs are made of fiberglass plates with dimensions of 35x50 cm and with the thickness of 10 mm. These fiberglass plates were attached to 4 aluminum plates with the thickness of 1.5 mm and width of 3.5 cm at corners in a way that the longer dimension the of aluminum plates are perpendicular to the direction of motion to reduce the transverse and torsional movements during the tests (as shown in Figure 3.3).

For recording the acceleration-time history at each story, four strain-gauge based accelerometers with 1g measurement range were installed at the center of each floor. Before each test, all of the accelerometers were re-calibrated and re-mounted on the model since these accelerometers are highly sensitive to the voltage of the current in the laboratory. In order to reduce the measurement errors; each test was performed

more than once on different days. The measured accelerations were collected by the 16-channel 24-bit resolution TDS TESTBOX2010 data acquisition system at the sampling speed of 250 Hz (Figure 3.4).

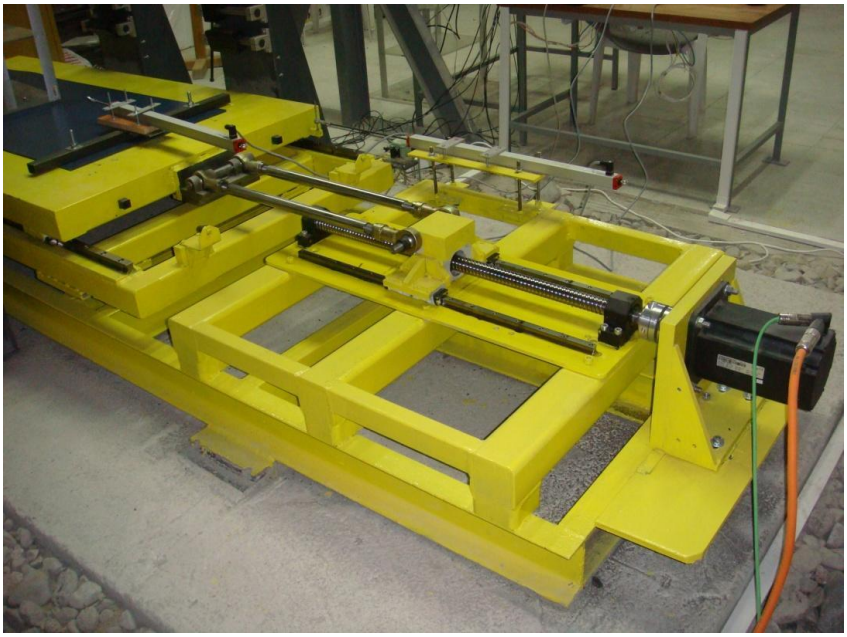

Figure 0.1 Shaking table in soil laboratory of METU

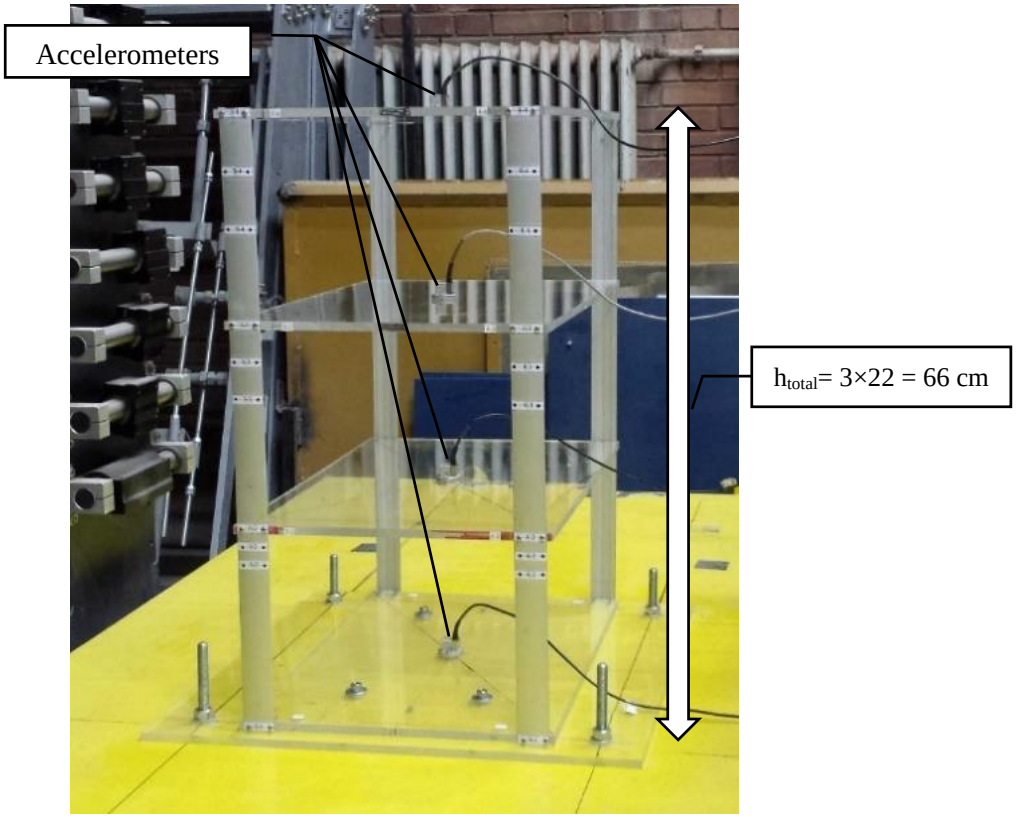

Figure 0.2 3-story model in fixed base mode

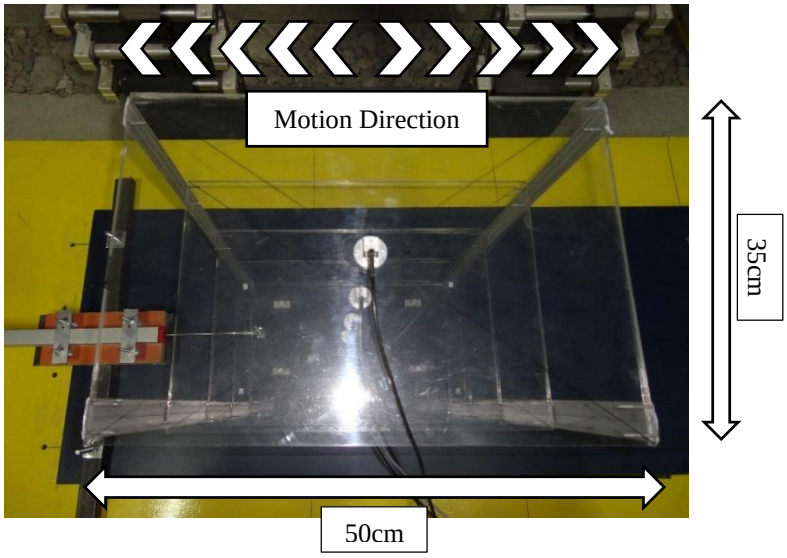

Figure 0.3 Aluminum plates and the motion direction

Figure 0.4 TDG Testbox 2010 data logger

In order to evaluate the efficiency of the composite liners for the purpose of seismic base isolation, the model was tested on the shaking table both in 'fixed base' mode (FB, Figure 3.2) and in 'isolated base' mode (IB, Figure 3.5). In FB experiments, the model was fixed directly to the shaking table. During IB tests, a piece of UHMWPE geomembrane (Figure 3.6) in 60x160 cm dimensions with the thickness of 6.4 mm was fixed to the shaking table and 4 small blocks of fiberglass (Figure 3.7) covered with nonwoven heat-bonded geotextile (Figure 3.8) were mounted to the base of the model. Therefore, IB experiments utilize the friction between the geomembrane and geotextile, not between the structure and the composite liner system. Specifications of UHMWPE geomembrane and nonwoven heat-bonded geotextile are provided in Appendix C.

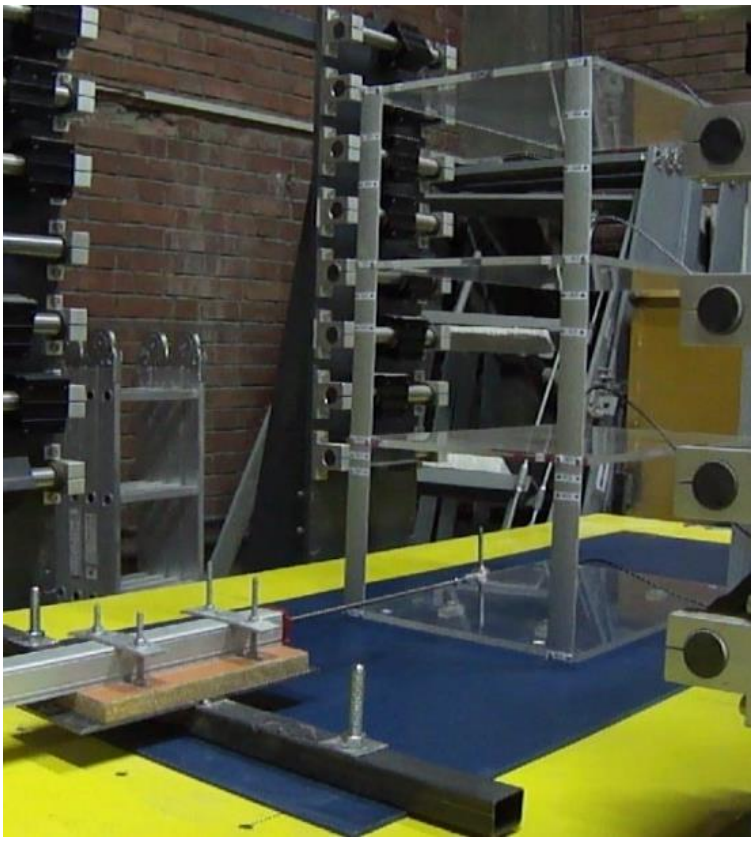

Figure 0.5 Model in isolated base condition

The base pressure beneath the foundation of the model assumed to be as 40 kPa. In order to simulate this pressure beneath the model in IB condition, the model was weighed as 0.084 kN and the area of geotextile which will be in contact with geomembrane was calculated as follows:

$$P_m = W_m / A_b \qquad (3.1)$$

P_m: base pressure of model
W_m: weight of model
A_b: base area

$$A_b = 0.084 \div 40 = 2100 \text{ mm}^2 \qquad (3.2)$$

The size of the four small fiberglass blocks used for attaching the geotextiles are calculated as:

$$A_{block} = 2100 \div 4 = 525 \text{ mm}^2 \rightarrow 15 \text{ mm} \times 35 \text{ mm} \qquad (3.3)$$

Figure 0.6 UHMWPE geomembrane

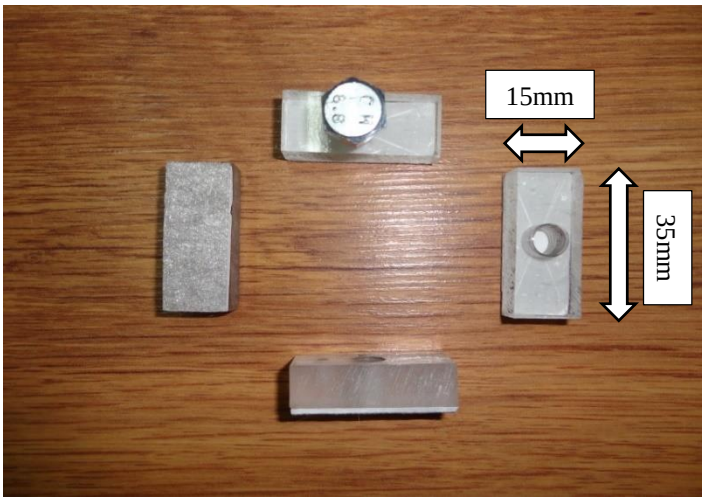

Figure 0.7 Small blocks of fiberglass covered with nonwoven heat-bonded geotextile

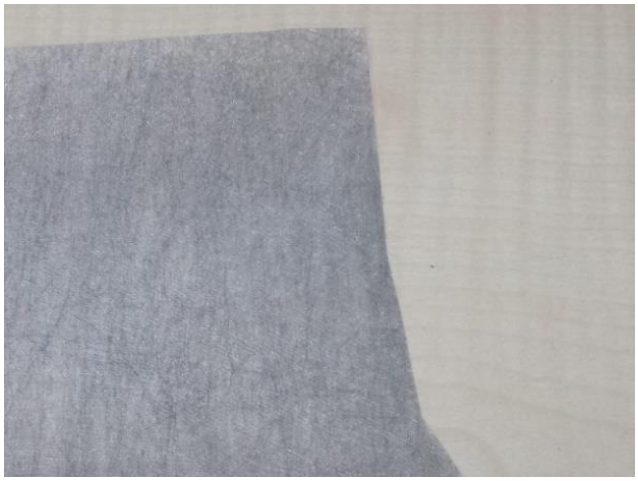

Figure 0.8 Nonwoven heat-bonded geotextile

2.1.1 Free Vibration Test

As discussed in the previous chapter, the dimensions of the model were selected to achieve a natural period that lies within 0.28-0.32 second range to complement the previously conducted experiments. Free vibration tests were performed to determine the natural period and the damping ratio of the models with different dimensions. In these tests, the motion of the model was initiated by applying a small displacement to the top of the model and the acceleration-time history of the top slab is recorded as shown in Figure 3.9. Recorded time history is processed in SeismoSignal software to estimate the natural frequency of the system. After a trial-and-error phase, the height of each story was chosen as 22 cm and the natural frequency of the model is measured as f_n=3.13 Hz (T_n=0.32sec).

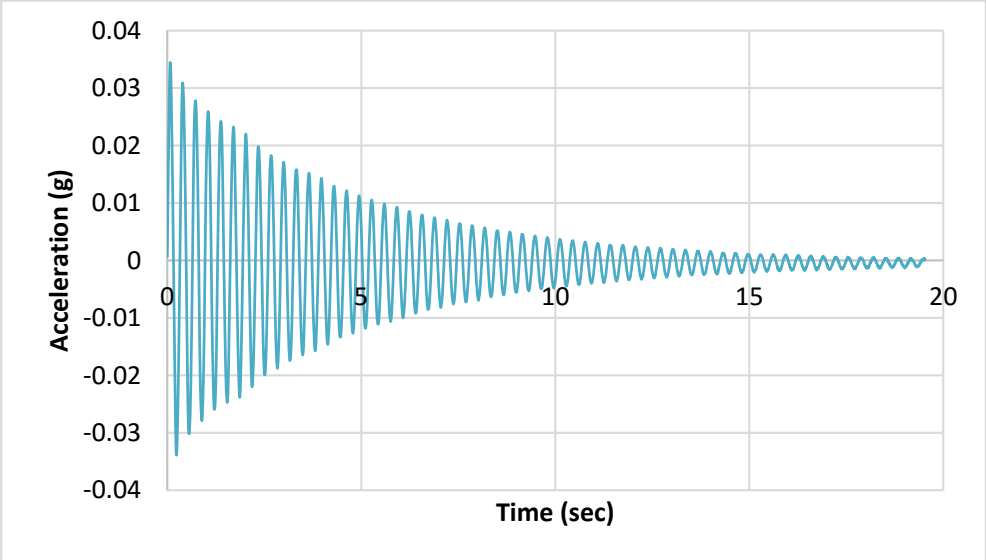

Figure 0.9 Acceleration time history of model under free vibration test

The damping ratio of the model is calculated as shown:

$$\ln (d_i / d_{i+n}) = 2\pi nD$$

where, d_i is the amplitude at i^{th} cycle, d_{i+n} is the amplitude at $(i+n)^{th}$ cycle, D is the critical damping ratio. For this model, d_3 = 0.0278 at t = 0.728 sec and d_{30} = 0.0043 at t = 9.476 sec (n = 30-3 = 27); therefore, the damping ratio is:

$$\ln (0.0278 / 0.0043) = 2\pi \times 27 \times D \rightarrow D = 1.10\ \%$$

2.2 Input Motions

The model was tested in FB and IB conditions by employing harmonic and modified/scaled ground motions. 16 different combinations of harmonic motions were created with different frequencies and maximum accelerations as shown in Table 3.1. It is notable that these combinations were selected by Kalpakcı (2013) to cover a large range of loading frequencies without violating the frequency limit of the shaking table set-up. The natural frequency of the model tested in this study (f_n=3.13 Hz) is also within the covered range of loading frequencies; therefore, the characteristics of the harmonic motions chosen by Kalpakcı (2013) were not modified. In order to apply a particular maximum acceleration level, corresponding displacement values were determined and applied for 30 loading cycles as listed in the following table:

Table 0.1 Frequencies and amplitudes of selected harmonic motion combinations

Frequency (Hz)	**Displacement (mm)**			
1	20	40	60	75
2	5	10	15	18.75
3	2.22	4.44	6.66	8.33
4	1.25	2.5	3.75	4.69
Acceleration (g)	0.08	0.16	0.24	0.3

In addition to the harmonic motions, recorded ground motions were also employed in FB and IB tests. Again, the ground motions selected and modified by Kalpakcı (2013) were used in this study. Characteristics of six ground motions chosen by Kalpakcı (2013) are provided in Table 3.2 and response spectra of the scaled ground motions are shown in Figure 3.10. Table 3.2 indicates that the record properties, especially the predominant frequency of the motion were considered in this selection. As the peaks of the spectra in Figure 3.10(a-f) show, the predominant frequencies of the selected motions are in within the same frequency range of the harmonic motions. Since the mechanism of the earthquake changes the ground motion with the same magnitude and distance, different style-of-faulting (SS for Strike-Slip and R for Reverse earthquakes) conditions werte considered in record selection. The ground

motions are downloaded from the Pacific Earthquake Engineering Research Center (PEER) Next Generation Attenuation – West 1 (NGA-W1) database (Chiou et al., 2008) and formatted for the shaking table test set-up. The shaking table is fully computer controlled and the motions are uploaded to the machine as a text file with a specific format: in the text file, the first column shows the position of the shaking table (in mm) and the second column is the velocity of table (See Appendix A). Each ground motion recording was scaled to a_{max}= 0.1, 0.2 and 0.3g, therefore, 18 loading combinations are created based on the ground motion and the scale factor. Please note that when the original recordings are scaled in amplitude, the original scaling with magnitude, distance, and style-of-faulting effects are modified.

Table 0.2 Summary of Input Ground Motions

Mechanism	No	Earthquake	Abbr. *	Date	Station	Magnitude	R_{rup} (km)	Vs_{30} (m/s)	F (Hz)
Strike-Slip	1	Landers	LND	28.06.1992	Arcadia Av	7.28	137.25	330.5	1
	2	Chalfant Valley	CHL	21.07.1986	Tinemaha Res	6.19	51.98	467.62	2
	3	Loma Prieta	LMP	18.10.1989	Capitola	6.93	15.23	288.62	4
Reverse	1	Coalinga	CLN	02.05.1983	Park Field	6.36	55.77	359.03	1
	2	Northridge	NRT	17.01.1994	Sylmar-County Hospital	5.13	24.79	420.81	2
	3	San Fernando	SNF	09.02.1971	Carbon Canyon Dam	6.61	61.79	235.0	4

* Note: To prevent using long names of input ground motions the abbreviations will be used in charts and tables presented in this stud.

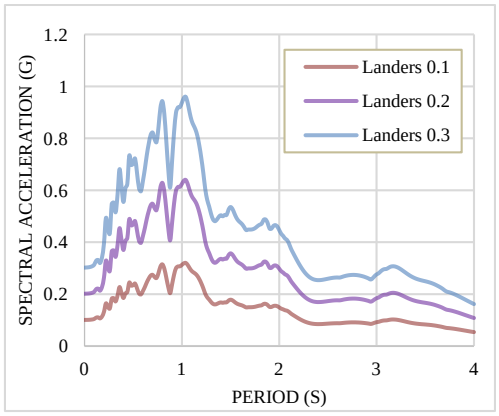

(a)

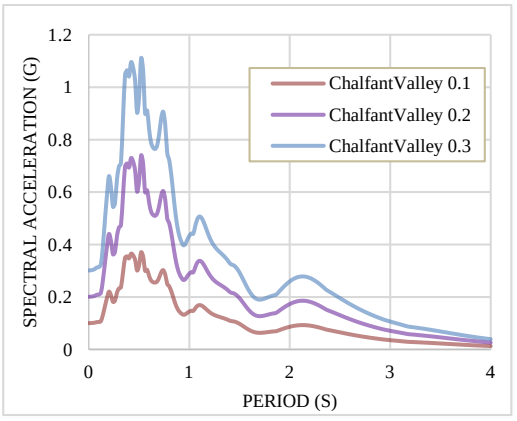

(b)

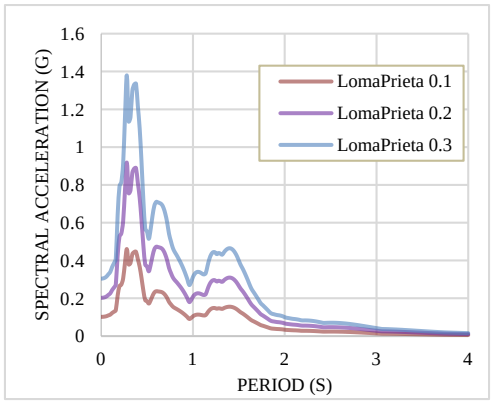

(c)

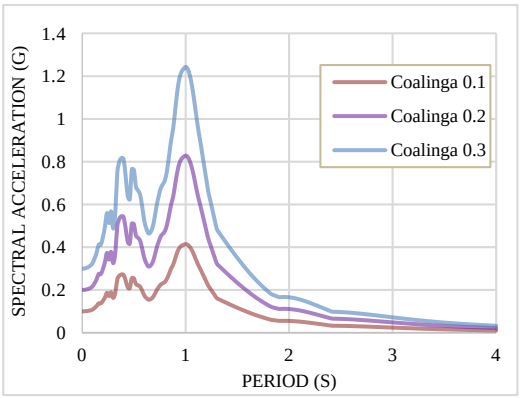

(d)

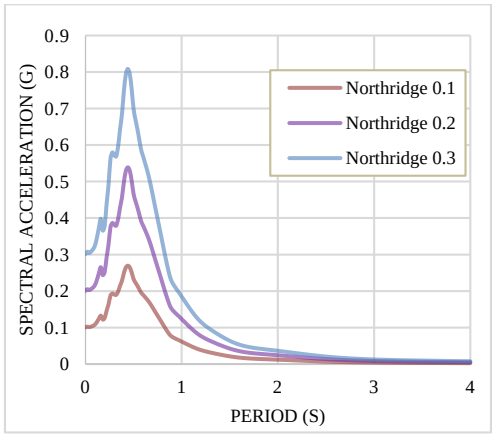

(e)

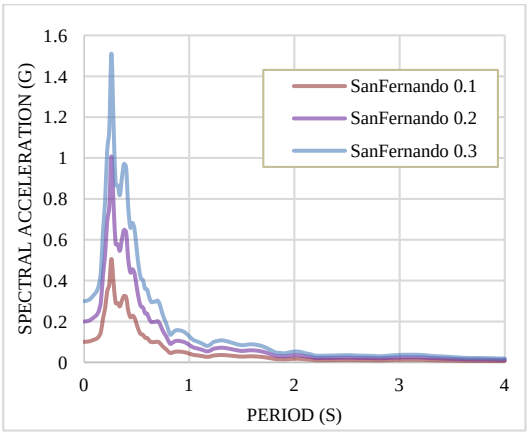

(f)

Figure 0.10 Scaled response spectra for the recordings taken from (a) Landers, (b) Chalfant Valley, (c) Loma Prieta, (d) Coalinga, (e) Northridge, and (f) San Fernando Earthquakes (Each scaled to 0.1, 0.2 and 0.3g)

CHAPTER 4

EXPERIMENT RESULTS FOR 3-STORY BUILDING MODEL

The 3-story building model described in Chapter 3 was tested by employing 16 different harmonic loading combinations and 18 different modified and scaled ground motions in fixed base (FB) and isolated base (IB) conditions (68 experiments in total). During these experiments, acceleration-time history at each floor is recorded by accelerometers attached to the middle of the floors. Recorded raw time histories include some measurement errors due to the vibration of the shaking table set-up, minor time lag between the applied and recorded shaking, and the fluctuations in the electrical current in the soil mechanics laboratory. The example provided in Figure 4.1 clearly shows the measurement errors in the raw time history recorded at the top story of the model during a harmonic motion experiment.

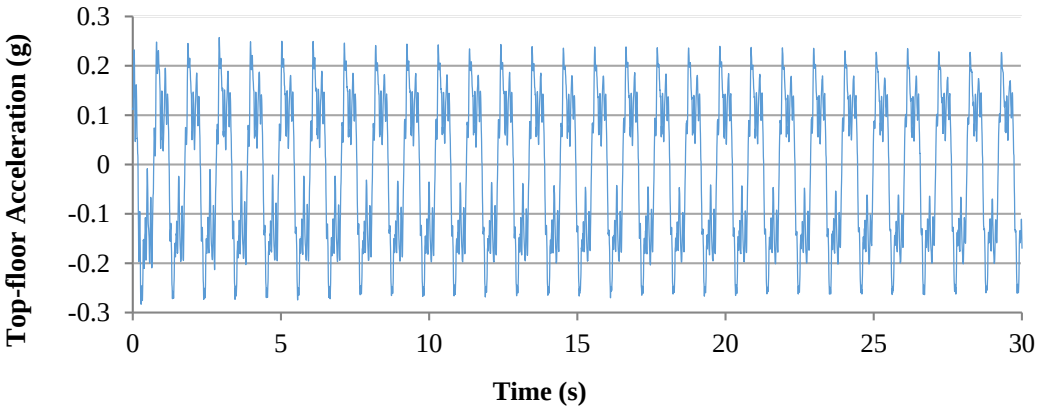

Figure 4.1 Time history recorded at top slab under f1a0.16 motion before filtration

To eliminate these errors, recorded raw accelerograms are filtered and baseline-corrected using SeismoSignal and SeismoSpect software (http://www.seismosoft.com). For this purpose, a-causal Butterforth filter with high-pass and low-pass frequencies of 0.2 Hz and 6 Hz, respectively is used according to criteria described by Douglas and Boore (2011) and Akkar et al. (2011) for modified and scaled ground motions (Figure 4.2). For harmonic motions, the initial frequency

range of the a-casual filter is chosen to be consistent with the predominant frequency of input motion (generally within ±0.5 Hz) but modified for each recording to produce a smooth and harmonic form of the recorded motion as shown in Figure 4.3.

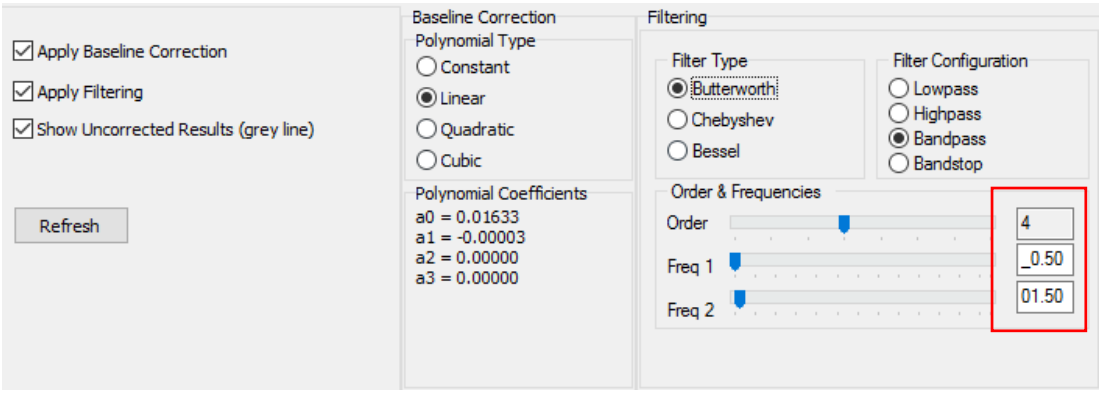

Figure 4.2 Filters applied in SeismoSignal software

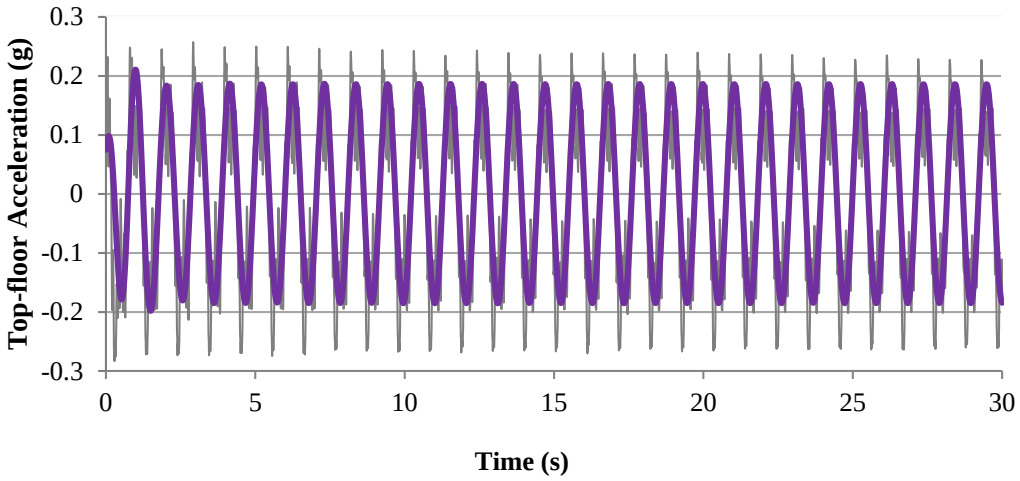

Figure 4.3 Time history recorded at top story under f1a0.16 motion after filtration

As it was mentioned before, in order to reduce the measurement errors, each test was performed more than once on different days. Figure 4.4 shows the result of test under harmonic motion with frequency of f=4 Hz and a_{max}=0.30g performed on two different days. It is clear from that there is not much difference between results of these two experiments. Figures 4.5 and 4.6 shows the raw and filtered acceleration, velocity and displacement time histories recorded at the base slab during San Fernando ground motion scaled to 0.3g.

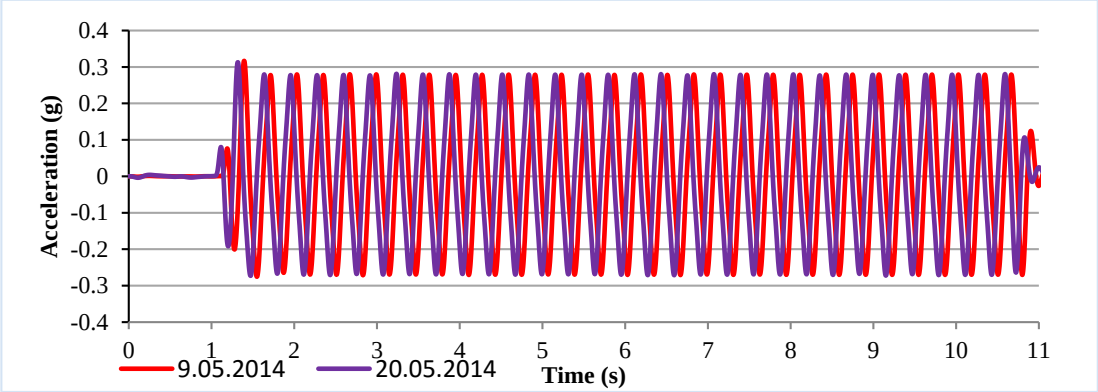

Figure 4.4 Acceleration recorded in different days during f4a0.30 motion at base slab

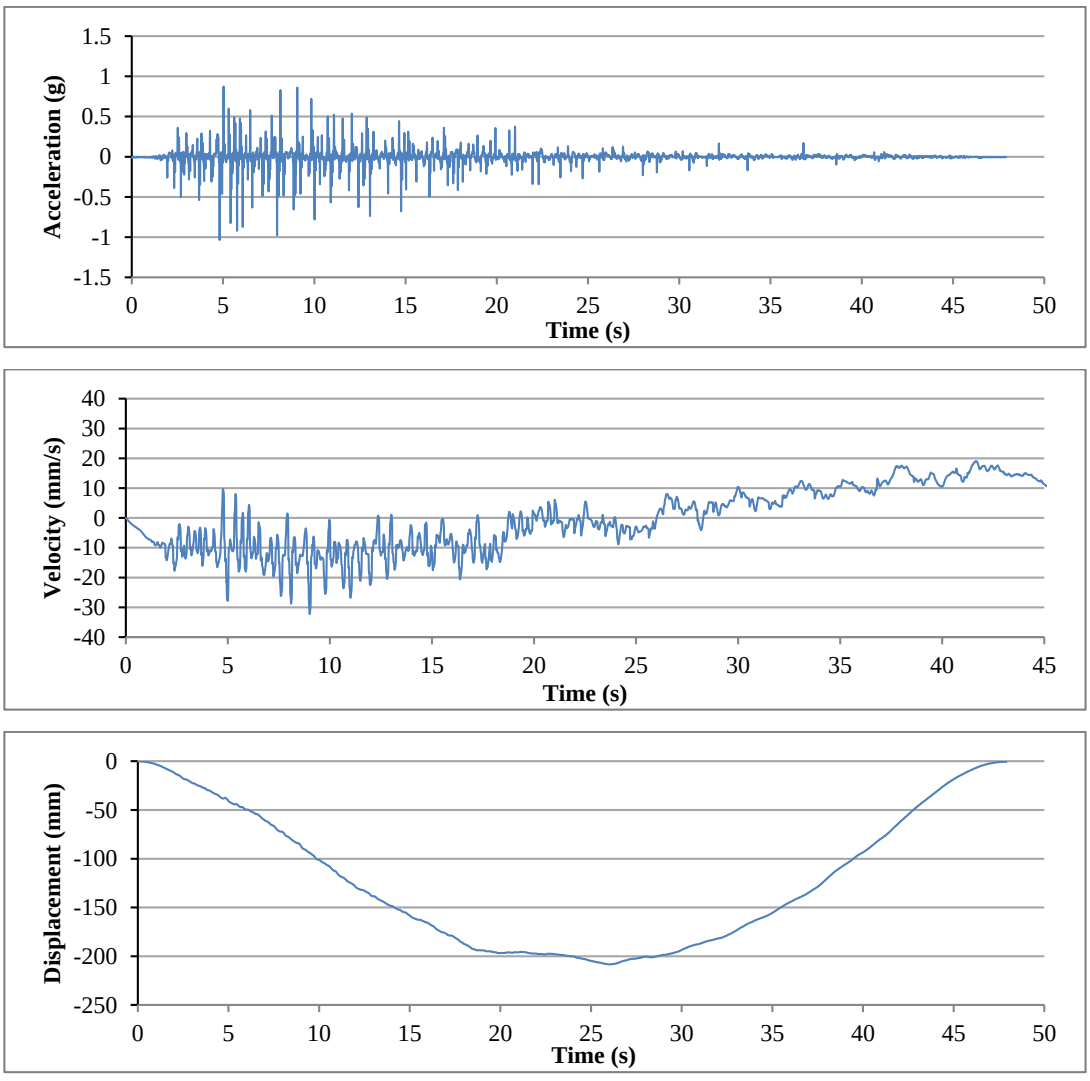

Figure 4.5 Raw Acceleration, Velocity and displacement time histories recorded at base slab of 3-story model under “San Fernando” ground motion scaled to 0.3 g

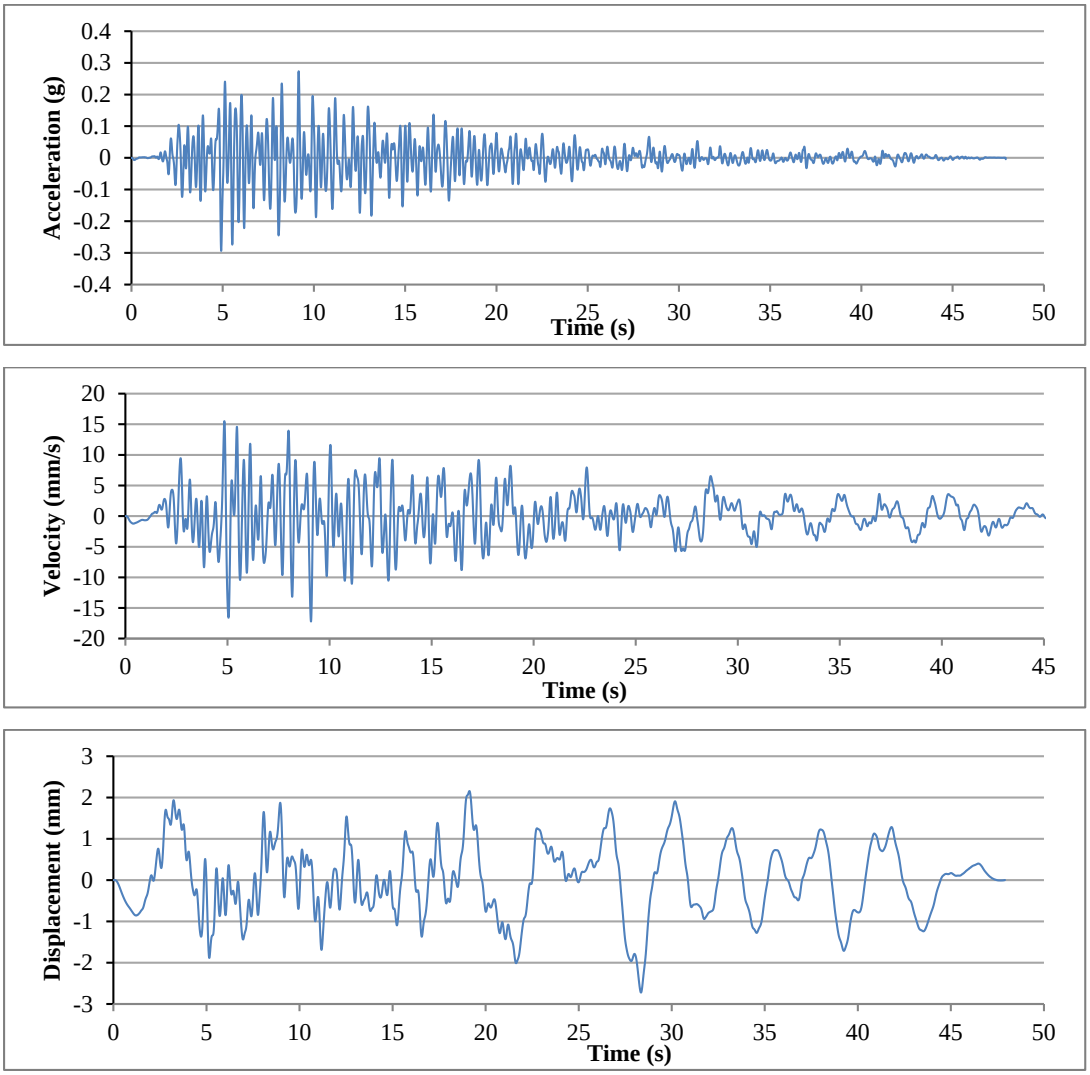

Figure 4.6 Filtered Acceleration, velocity and displacement time histories recorded at base slab of 3-story model under "San Fernando" ground motion scaled to 0.3 g

4.1 Result of Tests with Harmonic Motions

The test results of the experiments with harmonic loading combinations are shown in Figures 4.7 to 4.10 for harmonic motions with 1 Hz, 2 Hz, 3 Hz, and 4 Hz frequencies, respectively. Horizontal axis of Figures 4.7 to 4.10 shows the absolute maximum value of the measured accelerations at each floor. The vertical axis of these figures shows the H/L, which is defined as ratio of height of each floor to the total height of the model (0 at the base and 1 at the top). Each motion is denoted by fXaYY where X stands for the frequency of input motion and YY shows the

maximum acceleration of that particular motion. For instance, ‘f1a0.24’ is the motion with the frequency of 1 Hz and the acceleration of 0.24g.

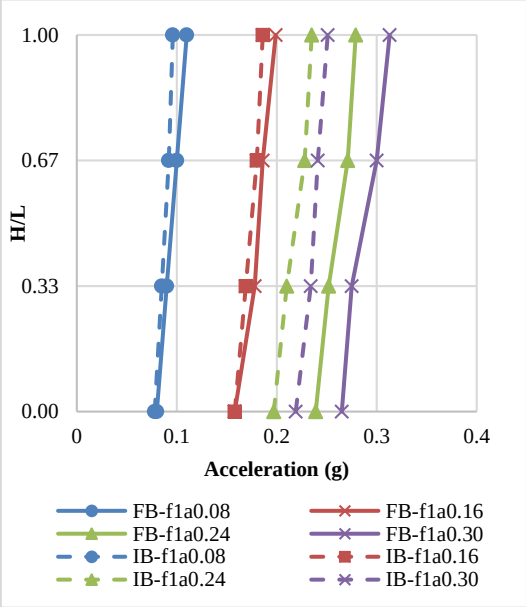

Figure 4.7 Acceleration vs. H/L under f=1 Hz

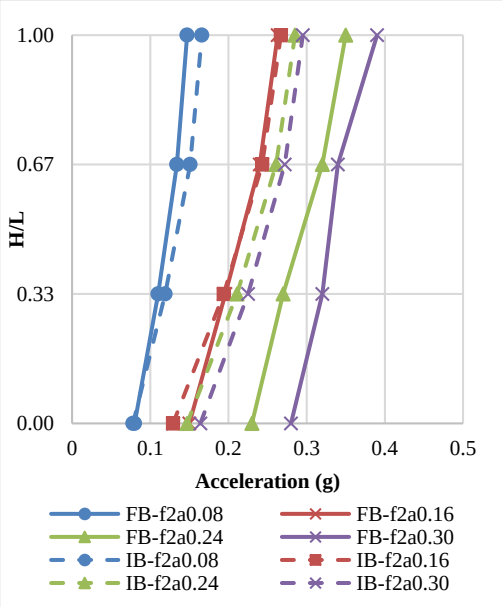

Figure 4.8 Acceleration vs. H/L under f=2 Hz

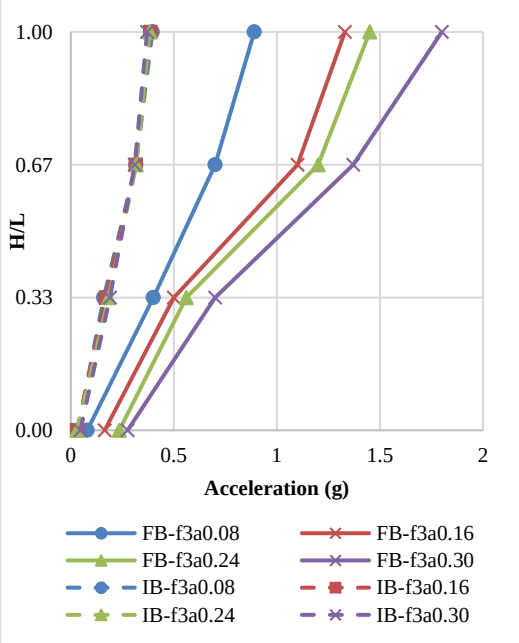

Figure 4.9 Acceleration vs. H/L under f=3 Hz

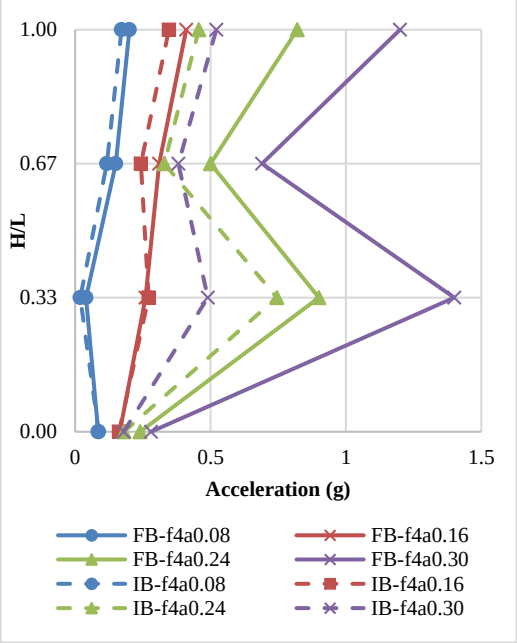

Figure 4.10 Acceleration vs. H/L under f=4 Hz

Figures 4.7 – 4.10 show that:

- When the input acceleration levels are small (e.g. blue and red curves in Figures 4.7, 4.8, and 4.10), the accelerations measured in FB and IB conditions are approximately the same. Insignificant reduction in the accelerations in each floor indicates that the base isolation system is not utilized (or triggered) for small acceleration levels (for motions with a_{max} = 0.08 and 0.16g).
- If the input acceleration is higher than 0.16g, the accelerations measured for IB cases at the top floor are significantly smaller than the accelerations measured at the top floor for FB cases, showing that the base isolation system effectively reduced the ground shaking levels.
- When the frequency of the input motion is close to the natural frequency of the system, the amplification of the response (the floor accelerations) is very large, (measured top floor accelerations for FB case are close to or larger than 1g in Figure 4.8). For this case, the base isolation system reduces the measured accelerations even for small shaking levels.
- The maximum accelerations are measured at the top floor in each test, except for f=4 Hz FB tests (green and purple lines in Figure 4.10). It is notable that the mode of the building model shifts to higher vibrational periods for these tests with large base accelerations.
- Amount of decrease in the base acceleration due to the base isolator is highly dependent on the frequency of the input motion. As the input motion frequency "f" gets closer to the natural frequency "f_n" of the model (as increases from 1 Hz to 4 Hz for this model), the reduction in the accelerations for IB condition relative to FB condition is higher.
- The composite liner system is most effective for motions with frequencies close to the natural frequency of the model namely, f = 2 Hz and f = 3 Hz motions recalling that the natural frequency of the model was f_n = 3.13 Hz.
- Test results for 4-story building model are consistent with the findings of Kalpakcı (2013) for 2-story and 4-story building models. Comparison of the results presented here and the tests results from Kalpakcı (2013) is provided in Chapter 5.

4.2 Result of Tests with Scaled Ground Motions

Maximum floor accelerations measured during the tests with modified time histories are plotted vs. H/L in Figures 4.11-4.16 for the recordings from Landers, Coalinga, Chalfant Valley, Northridge, Loma Prieta and San Fernando earthquakes, respectively (see Table 3.2 for details of ground motions).

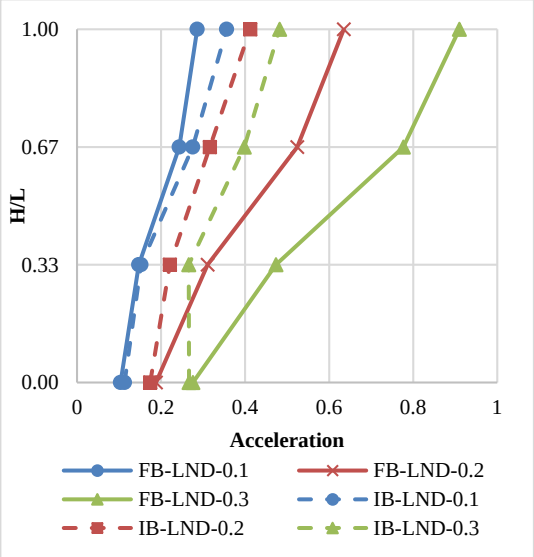

Figure 4.11 Acceleration vs. H/L under Landers motions (f= 1Hz)

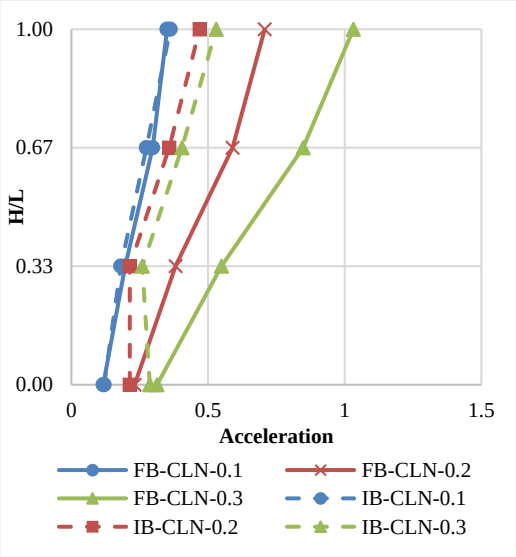

Figure 4.12 Acceleration vs. H/L under Coalinga motions (f= 1Hz)

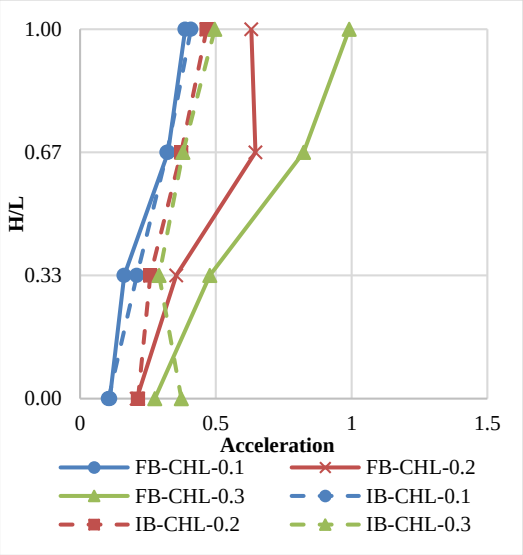

Figure 4.13 Acceleration vs. H/L under Chalfant Valley motions (f= 2Hz)

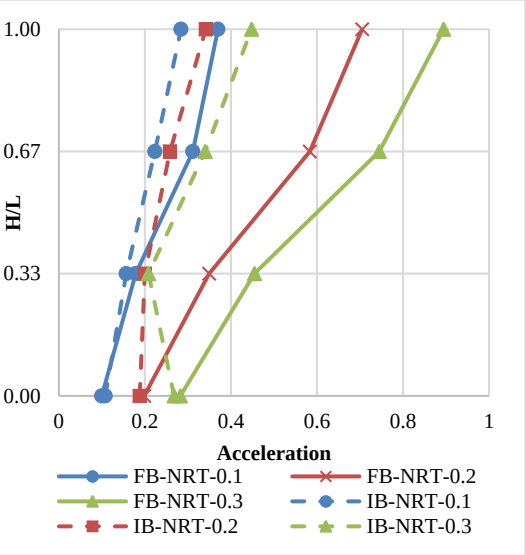

Figure 4.14 Acceleration vs. H/L under Northridge motions (f= 2Hz)

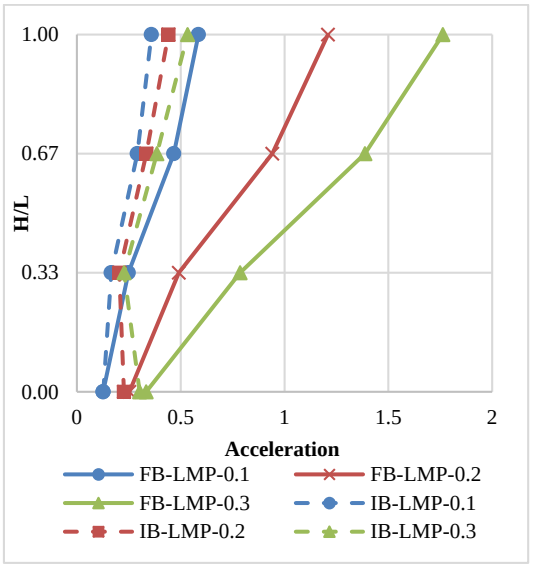

Figure 4.15 Acceleration vs. H/L under Loma Prieta motions (f= 4Hz)

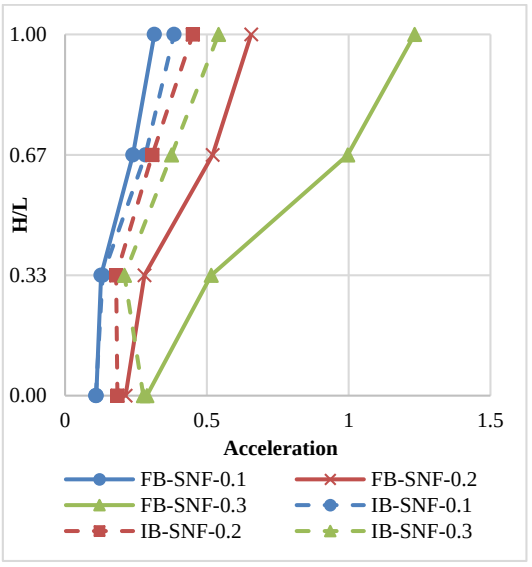

Figure 4.16 Acceleration vs. H/L under San Fernando motions (f= 4Hz)

According to Figures 4.11-4.16:

- Results of the tests with scaled ground motions are not significantly different from the results of the tests with harmonic motions. Again, the floor accelerations measured in FB and IB conditions for small shaking levels (a_{max}=0.1g) are close to each other, indicating that the base isolation system is not triggered (solid and broken blue lines in Figures 4.11-4.16).
- The composite liner system effectively reduces the floor accelerations for the tests with a_{max}=0.2g and a_{max}=0.3g.
- As the predominant frequency of the input motion increases from f=1 Hz to 4 Hz the efficiency of the seismic isolator increases. When the predominant frequency of the input motions is close to the natural frequency of the experimental model (motions with predominant frequency of f= 4 Hz shown in Figures 4.15 and 4.16) the isolator system works well even for small acceleration levels and the floor accelerations in IB case are significantly smaller than the floor accelerations in FB conditions.
- The change in vibrational period (mode) observed in harmonic tests with f=4 Hz in FB conditions (Figure 4.10) is not observed in the tests with input motions with the same predominant frequency (Figures 4.15 and 4.16).

Mean response spectra measured at the top and the base floors in FB and IB cases are presented in Figures 4.17 through 4.25. In these figures, the mean spectra are calculated for the input motions scaled to the same maximum acceleration level and with the same predominant frequency. For example, Figure 4.17 shows the mean spectra of the time histories from Landers and Coalinga earthquakes (with f=1 Hz) scaled to a_{max}=0.1g that are recorded at the base and at the top floors in FB and IB cases. Green and orange lines in each figure show that the response spectra recorded at the base floor in IB and FB cases are similar to each other, especially in the long period range. Minor differences are observed in the spectral accelerations for periods close to the natural period of the system.

When the top and base spectra are compared, a very significant amplification in the spectral acceleration values for 0.2-0.5 second periods (f=2-5 Hz) are observed in each test (purple lines in Figures 4.17-4.25). This substantial increase in the response can be explained by the effect of structural response of the building model on the frequency content of the recorded ground motions. Test results show that the base isolation system has a significant effect on this amplification. Contribution of the base isolation system is not visible in Figures 4.17, 4.18 and 4.19 since the ground shaking levels in these tests are small and the base isolation system is not triggered. However, the base isolation system clearly reduces the amplification in 2-5 Hz spectral accelerations in the tests with a_{max}=0.2g and a_{max}=0.3g (blue lines in Figures 4.20-4.25).

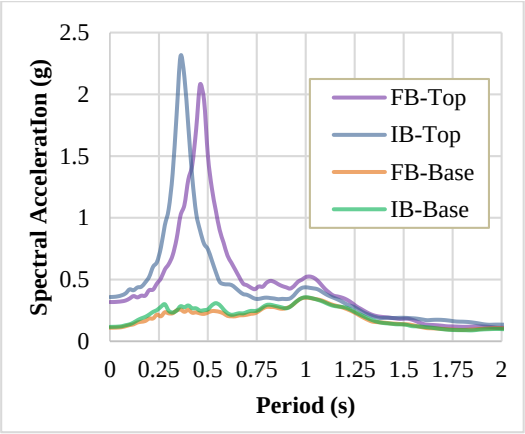

Figure 4.17 Mean Response Spectra for motions with f=1Hz scaled to 0.1g at top and base of the 3-story model

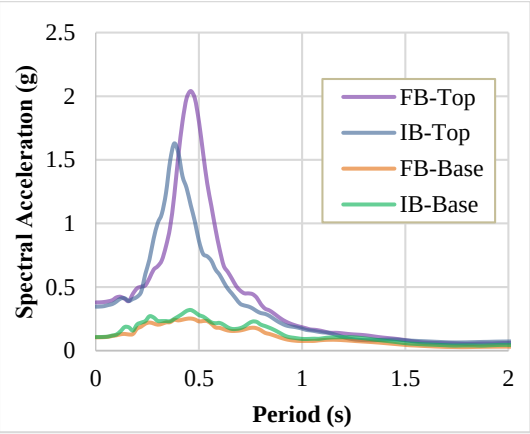

Figure 4.18 Mean Response Spectra for motions with f=2Hz scaled to 0.1g at top and base of the 3-story model

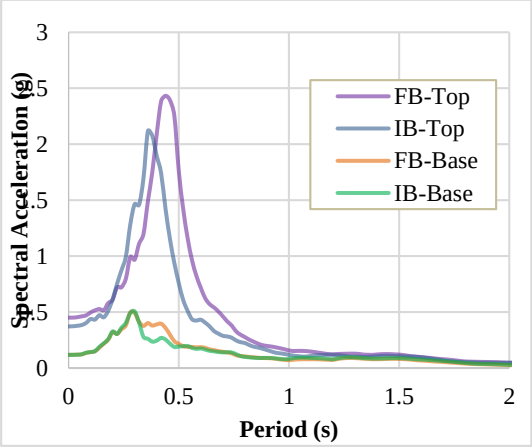

Figure 4.19 Mean Response Spectra for motions with f=4Hz scaled to 0.1g at top and base of the 3-story model

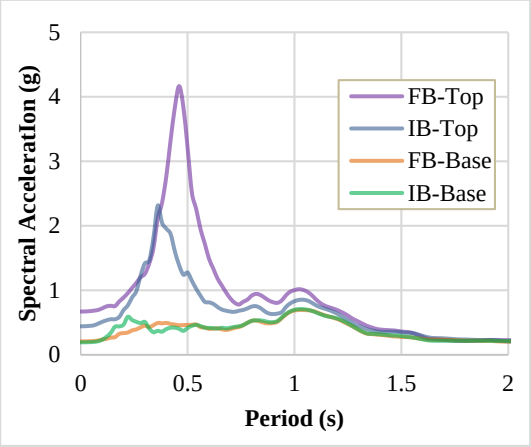

Figure 4.20 Mean Response Spectra for motions with f=1Hz scaled to 0.2g at top and base of the 3-story model

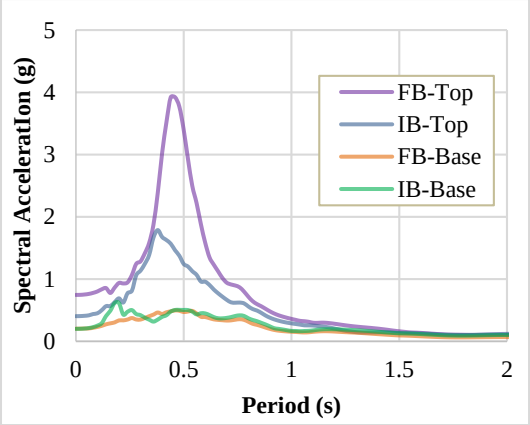

Figure 4.21 Mean Response Spectra for motions with f=2Hz scaled to 0.2g at top and base of the 3-story model

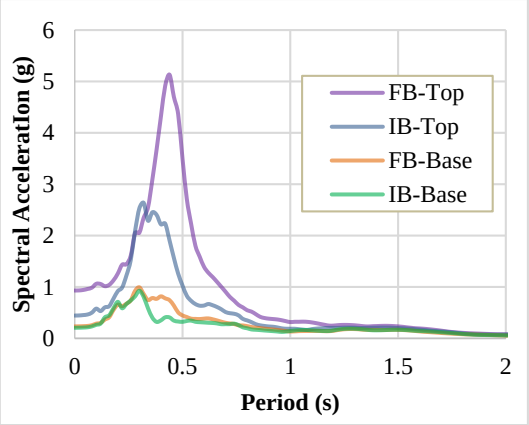

Figure 4.22 Mean Response Spectra for motions with f=4Hz scaled to 0.2g at top and base of the 3-story model

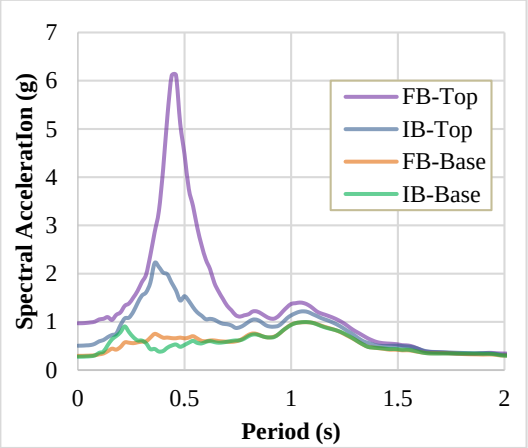

Figure 4.23 Mean Response Spectra for motions with f=1Hz scaled to 0.3g at top and base of the 3-story model

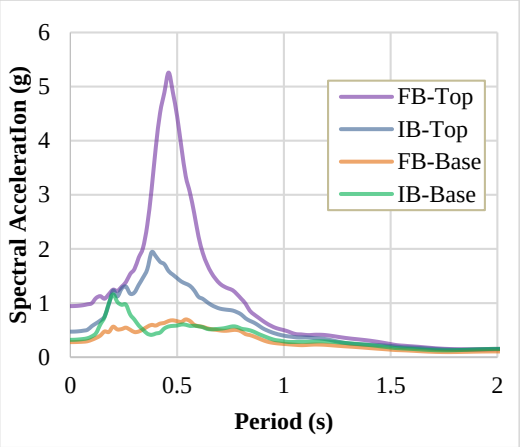

Figure 4.24 Mean Response Spectra for motions with f=2Hz scaled to 0.3g at top and base of the 3-story model

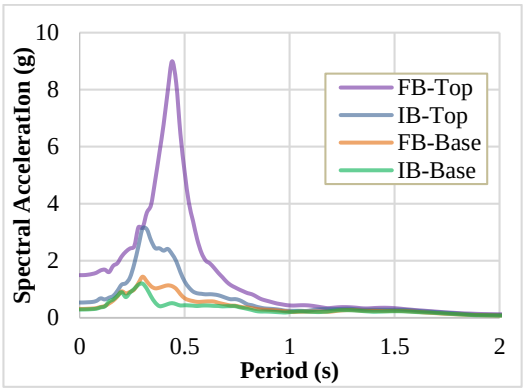

Figure 4.25 Mean Response Spectra for motions with f=4Hz scaled to 0.3g at top and base

4.3 Verification of Fixed Base Model in CSI SAP2000 Software

The building model used in these experiments was prepared using the scale of 1:12. Same 4-story building model is also created in CSI SAP2000 software (https://www.csiamerica.com/) but the scale is modified as shown in Figure 4.25. For the SAP2000 model, the floor dimensions are taken as 4.2×6.0 m and the story height is selected as 2.70 m. Slab thickness is defined as 15 cm and columns dimension are determined in way that the natural frequency of the SAP2000 model would be identical to the natural frequency of the building model (f_n= 3.13 Hz). By assigning 47×70 cm dimensions to columns, the desired natural frequency is obtained in SAP2000. Please note that only the fixed base condition is modelled, since the seismic isolator system used in this study cannot be defined in SAP2000.

The response of the SAP2000 model is analyzed using the same set of scaled ground motion recording used in the experiments. Acceleration-time history at each floor is calculated using SAP2000 software and compared with the maximum floor accelerations measured during the experiments as shown in Figures 4.26 – 4.31. In these figures, the solid lines show the values calculated in SAP2000 whereas the broken lines represent the measured values in experiments. According to Figures 4.26-4.31, calculated accelerations in SAP2000 software and the measured accelerations during the experiments at base are the same. However, most of the calculated and measured accelerations are different for the top floor: the measured accelerations are greater than the calculated ones almost for all ground motions.

These differences might be related to the scale of the SAP2000 model. Even if the natural frequency of the SAP2000 model is the same as that of the real model, dimensions of the models are quite different.

The response spectra at the top and the base measured during the experiments are compared with the response spectra calculated by SAP2000 at the same ground motion (LMP) and at the same shaking level (0.2g) as shown in Figure 4.32. This figure clearly shows that the significant amplification in the spectral acceleration values for 0.2-0.5 second periods (f=2-5 Hz) observed in the experiments are also estimated by the SAP2000 software. The peak of the response spectrum at the top estimated in SAP2000 is slightly shifted to the shorter periods and significantly higher when compared to the experimental test results.

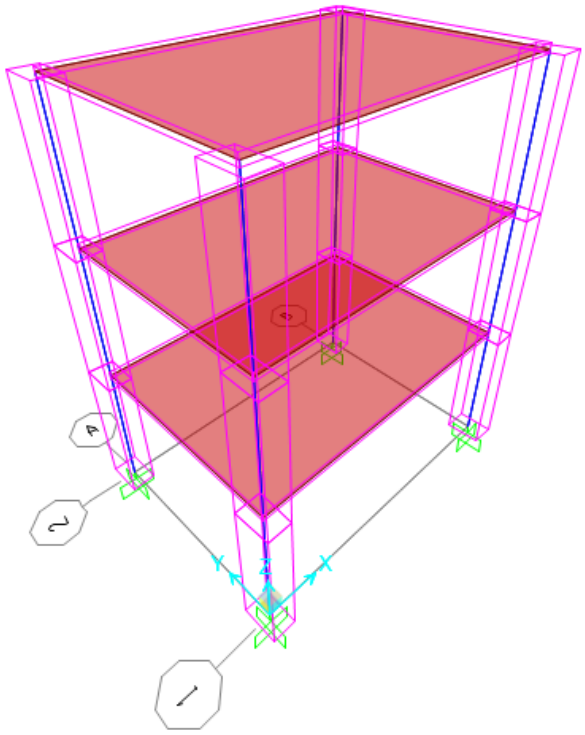

Figure 4.26 SAP2000 Model

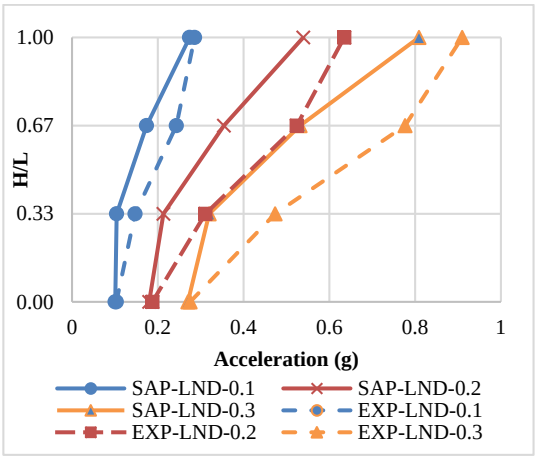

Figure 4.27 Acceleration vs. H/L under Landers motions in SAP2000 and Experiments

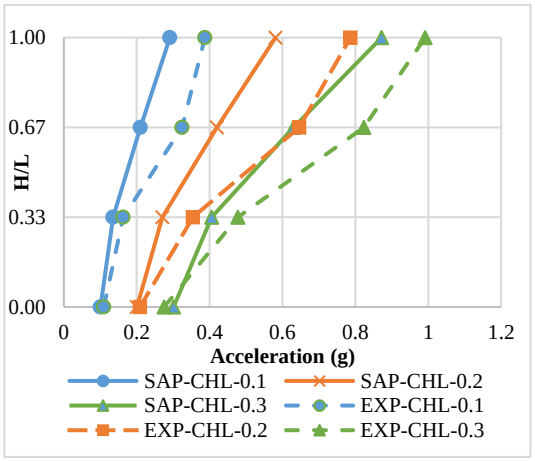

Figure 4.28 Acceleration vs. H/L under Chalfant Valley motions in SAP2000 and Experiments

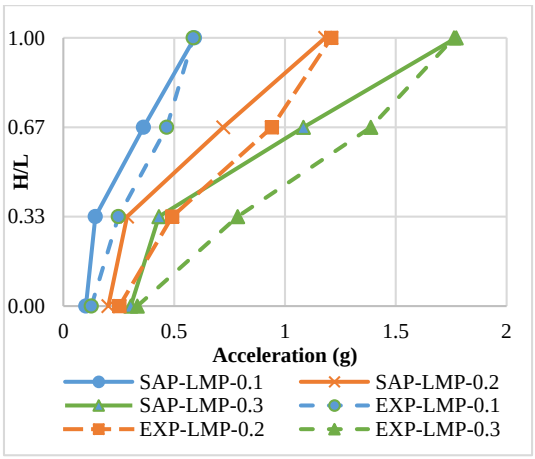

Figure 4.29 Acceleration vs. H/L under Loma Prieta motions in SAP2000 and Experiments

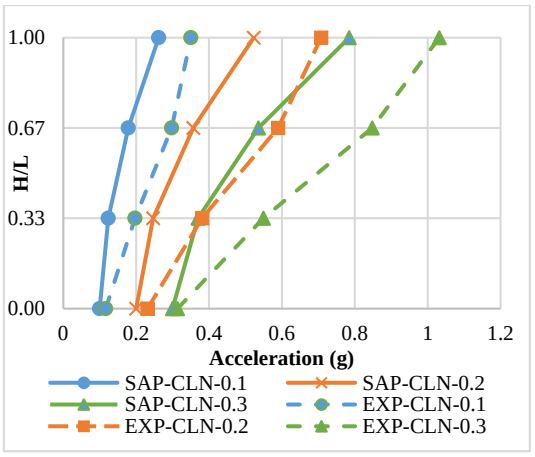

Figure 4.30 Acceleration vs. H/L under Coalinga motions in SAP2000 and Experiments

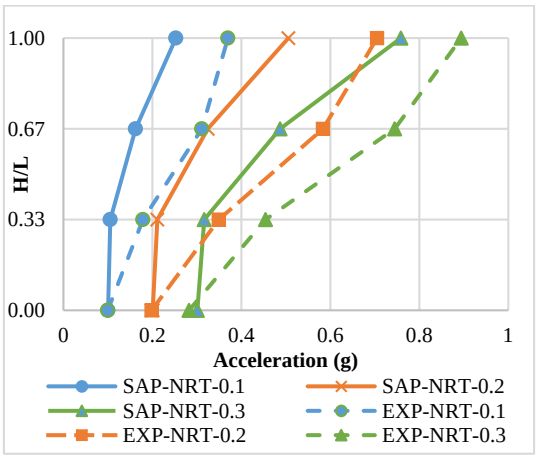

Figure 4.31 Acceleration vs. H/L under Northridge motions in SAP2000 and Experiments

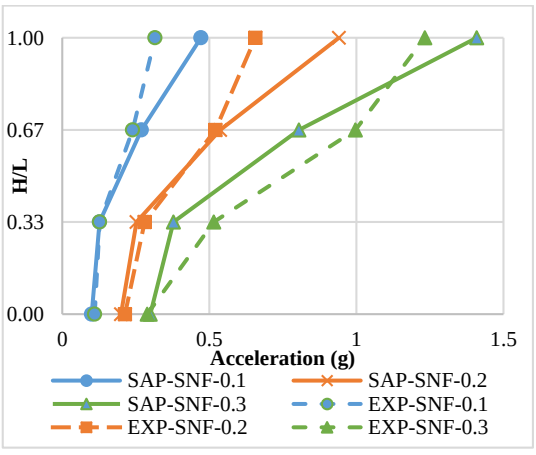

Figure 4.32 Acceleration vs. H/L under San Fernando motions in SAP2000 and Experiments

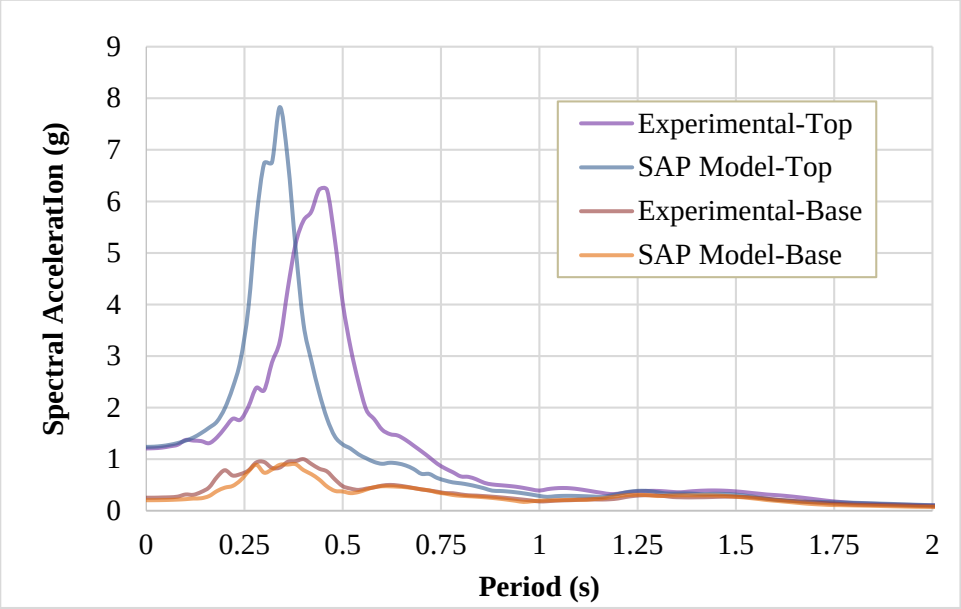

Figure 4.33 Comparison of the response spectra at the top and at the base gathered from SAP2000 model and the experiments for the ground motion from Loma Prieta earthquake scaled to a_{max}=0.2g (LMP-0.2)

CHAPTER 5

COMPARISON OF THE CURRENT TEST RESULTS WITH PREVIOUSLY PERFORMED EXPERIMENTS

Details of the experiments performed by Kalpakcı (2013) using a 2-story model with the natural frequency of 4.35 Hz and 4-story model with the natural frequency of 2.33 Hz are provided in Chapter 2. This chapter is devoted to the comparison of the current test results of the 3-story model (natural frequency of 3.13 Hz) with the previous test results in terms of the measured accelerations in FB and IB experiments.

5.1 Comparison of Test Results for Harmonic Motions

The accelerations at each floor level measured during the tests with harmonic loading combinations are compared in Figures 5.1 to 5.4. Horizontal axis of Figures 5.1 to 5.4 shows the ratio between the absolute maximum value of the measured accelerations in IB and FB conditions at each floor (a_{IB}/a_{FB}). When the base isolation system has no effect on the accelerations, a_{IB}/a_{FB} is equal to or close to one. Values lower than one indicate the level of efficiency for the base isolation system. The vertical axis of these figures shows the H/L, which is defined as ratio of height of each floor to the total height of the model (0 at the base and 1 at the top). Figure 5.1 shows that the base isolation system was not triggered in any of the tests with small shaking levels (f=1 Hz and a_{max}=0.08g) since the a_{IB}/a_{FB} is equal to one at each floor. Figure 5.2 shows the test results with the same frequency but for the highest shaking level (f=1 Hz and a_{max}=0.3g). For this case, the reduction in the acceleration at each floor is almost the same for each model (a straight line through H/L), however the efficiency of the composite liner system changes with the natural frequency of the model, being highest for the 4-story model.

When the frequency of the input harmonic motion is increased (f=3 Hz in Figures 5.3 and 5.4), the base isolation system was triggered for the 3-story and 4-story models even if the ground shaking levels are small (a_{max}=0.08g for Figure 5.3) since the

input motion frequency is closer to the natural frequency of the system. The a_{IB}/a_{FB} is constant at each slab of the 2-story model but floor-to-floor variations in the reduction of acceleration are observed in the other cases. Figure 5.4 (a_{max}=0.08g) is consistent with Figure 5.3 in terms of the variations in floor accelerations. The base isolation system was triggered in each case and the efficiency of the system increases as the natural frequency of the system gets closer to the frequency of the loading.

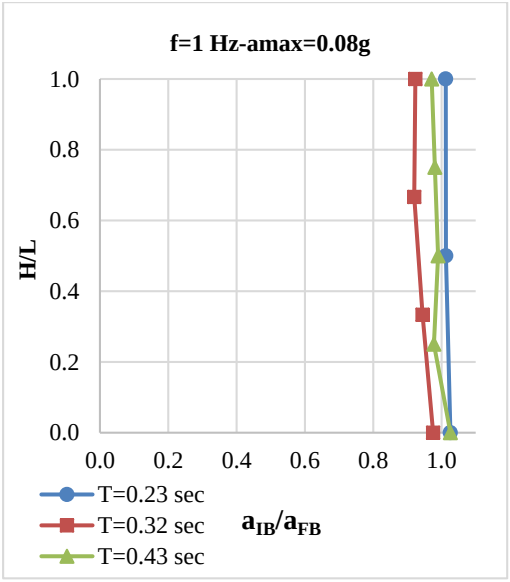

Figure 5.1 a_{IB}/a_{FB} vs. H/L for f1a0.08 motion

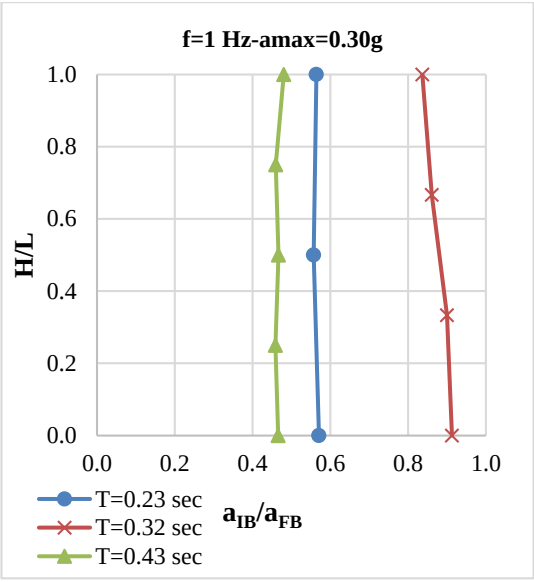

Figure 5.2 a_{IB}/a_{FB} vs. H/L for f1a0.30 motion

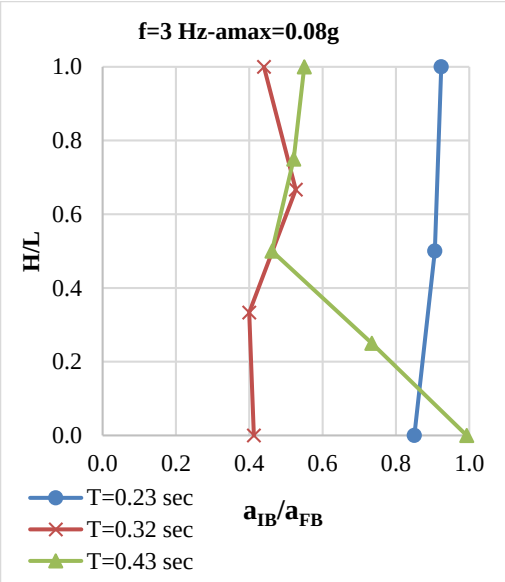

Figure 5.3 a_{IB}/a_{FB} vs. H/L for f3a0.08 motion

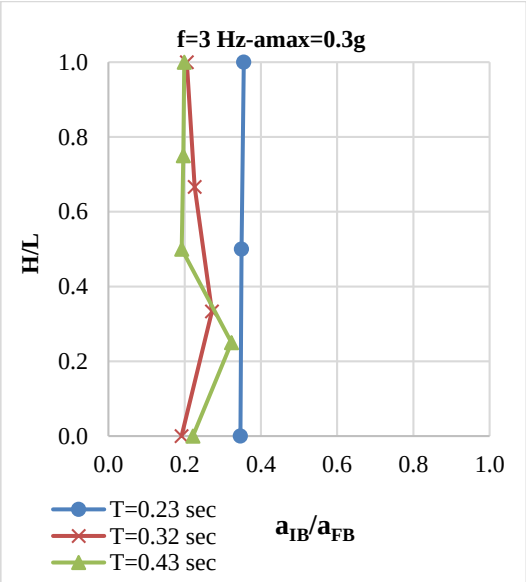

Figure 5.4 a_{IB}/a_{FB} vs. H/L for f1a0.30 motion

To further analyze the effect of the interaction between the natural frequency of the loading and the natural frequency of the model, average reduction in acceleration at the top and at the base for all ground shaking levels are presented in Figures 5.5 to 5.8 for f=1, 2, 3 and 4 Hz harmonic motions, respectively. When the frequency of the loading is outside the natural frequency of the models, the efficiency of the composite liner system is not dependent on the frequency of the loading as shown in Figure 5.5. However, for f=2, 3 and 4 Hz tests, the a_{IB}/a_{FB} has its peak when f_n is close to f (Figures 5.6-5.8).

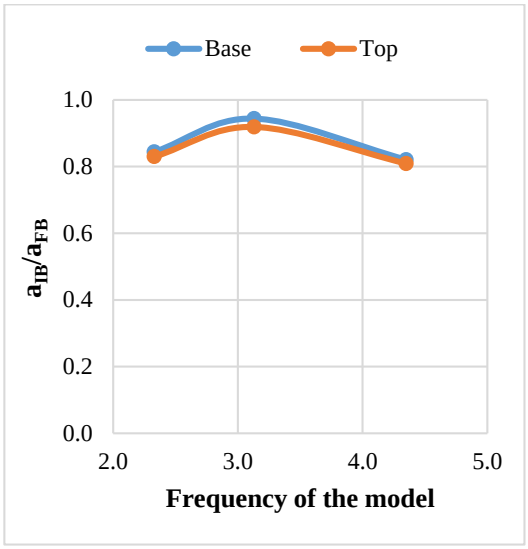

Figure 5.5 Mean of a_{IB}/a_{FB} vs freq. of model at top and base for f=1 Hz motions

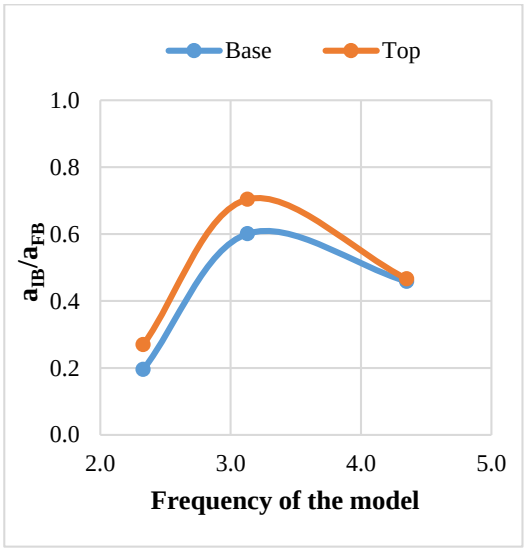

Figure 5.6 Mean of a_{IB}/a_{FB} vs freq. of model at top and base for f=2 Hz motions

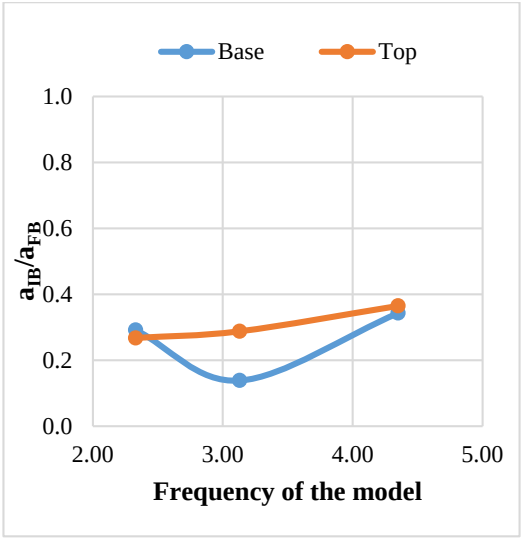

Figure 5.7 Mean of a_{IB}/a_{FB} vs freq. of model at top and base for f=3 Hz motions

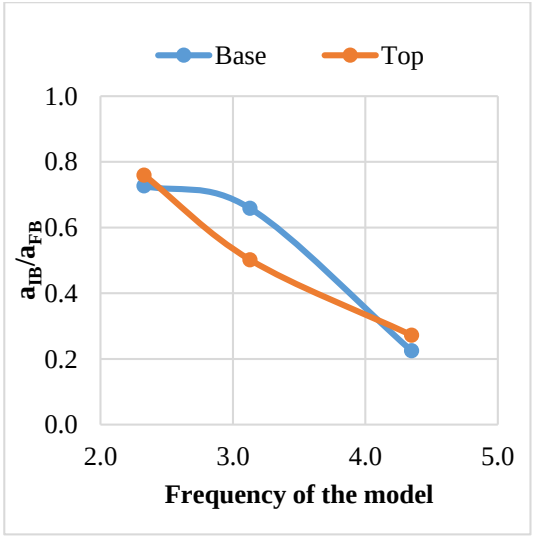

Figure 5.8 Mean of a_{IB}/a_{FB} vs freq. of model at top and base for f=4 Hz motions

5.2 Comparison of Test Results for Ground Motions

Similar to the tests with the harmonic motions, the ratio of the absolute maximum value of the measured accelerations in IB and FB conditions at each floor (a_{IB}/a_{FB}) is plotted vs. H/L ratio for different models under the same ground motions. Two cases- the ground motions from Landers and Loma Prieta earthquakes for different ground shaking levels are provided in Figures 5.9 to 5.14. These plots are not similar to Figures 5.1-5.4 since the interaction between the natural frequency of the model and the predominant frequency of the ground motion are not substantial for real ground motions. The a_{IB}/a_{FB} is approximately equal to one at the base for each model and the efficiency of the composite liner system increases as the ground shaking level increases. Floor accelerations at the 2-story (blue lines) and 3-story (red lines) models are similar in each plot whereas, the maximum reduction in the floor acceleration is generally observed at the middle floors of the 4-story model (green lines).

When compared to the test results with harmonic motions (Figures 5.1-5.4), the reduction in the maximum accelerations at the base in the tests with ground motions (Figures 5.9-5.14) is systematically smaller even if the isolation system was triggered for that particular test. To understand the impact in other spectral accelerations, the average normalized response spectra measured at the base in FB and IB conditions in 2, 3 and 4-story models are compared for each ground motion through Figures 5.15 to 5.20 separately for reverse and strike slip earthquakes. These figures indicate that: i) the average normalized spectra in IB conditions are almost always smaller than the average normalized spectra in FB conditions (especially in the large period range), ii) the mechanism of the earthquake does not have a noteworthy effect on the efficiency of the base isolation system, and iii) behavior of the 2-story, 3-story and 4-story models are not significantly different. Therefore, average normalized spectra for different mechanism events can be combined for a better understanding in the efficiency in the reduction of accelerations as shown in Figure 5.21, 5.22 and 5.23 for 2-story, 3-story and 4-story models, respectively. According to Figure 5.23, the normalized spectral accelerations in FB and IB conditions are very close to each other for 2-story model. Still, the normalized spectral accelerations decreased from 2.24 to 1.60 (≈28%) at the first mode natural period of the tested model.

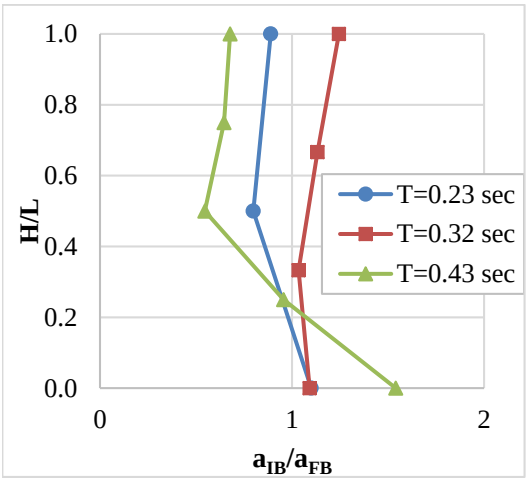

Figure 5.9 a_{IB}/a_{FB} vs. H/L for LND_0.1 motion

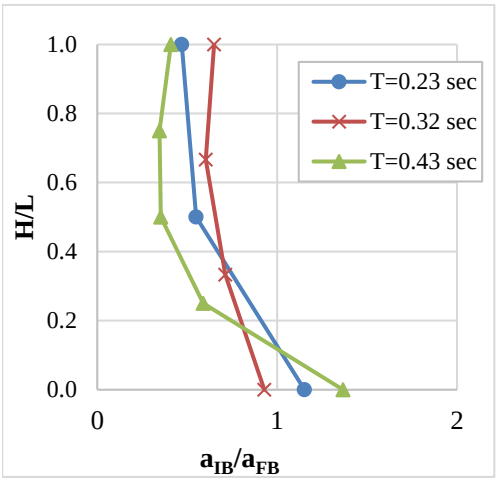

Figure 5.10 a_{IB}/a_{FB} vs. H/L for LND_0.2 motion

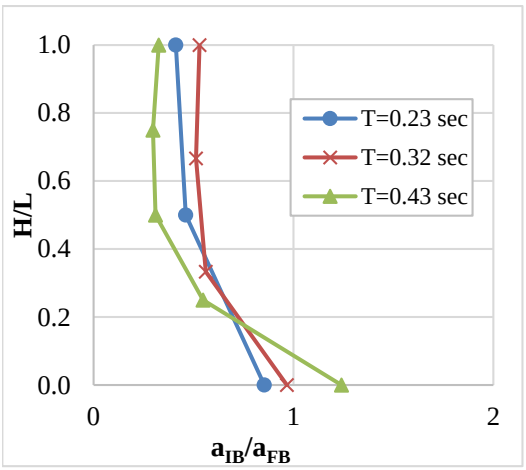

Figure 5.11 a_{IB}/a_{FB} vs. H/L for LND_0.3 motion

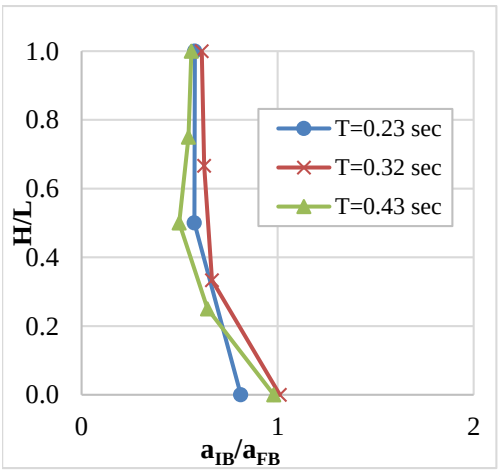

Figure 5.12 a_{IB}/a_{FB} vs. H/L for LMP_0.1 motion

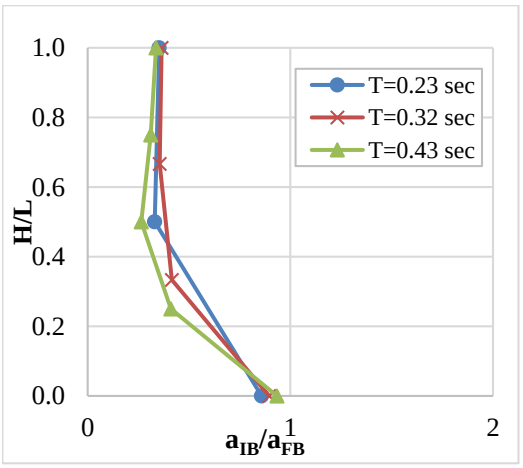

Figure 5.13 a_{IB}/a_{FB} vs. H/L for LMP_0.2 motion

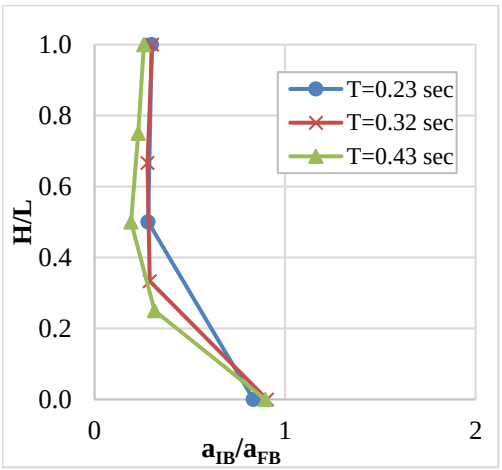

Figure 5.14 a_{IB}/a_{FB} vs. H/L for LMP_0.3 motion

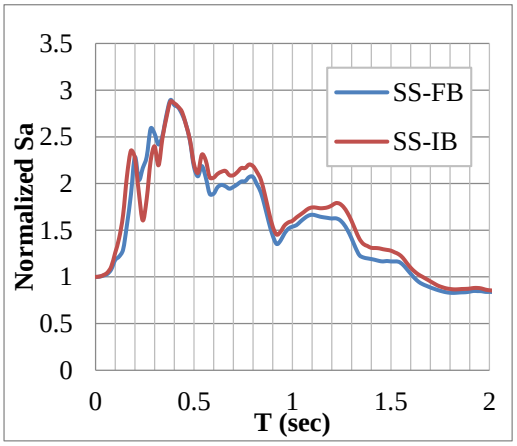

Figure 5.15 Normalized Response Spectra for 2-Story Model under Strike-Slip Ground Motions

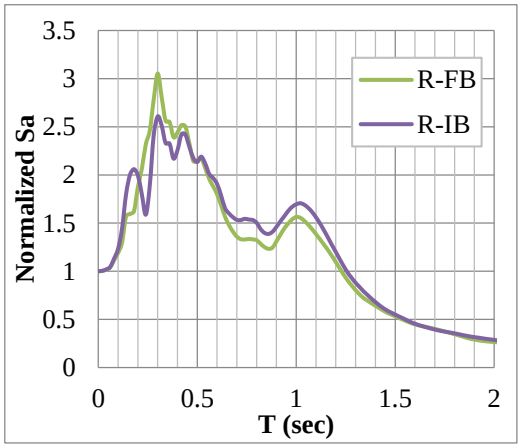

Figure 5.16 Normalized Response Spectra for 2-Story Model under Reverse Ground Motion

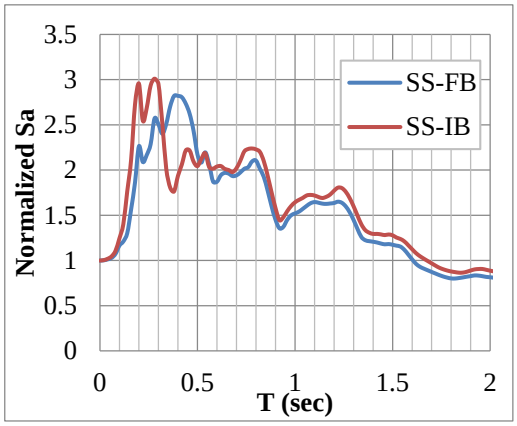

Figure 5.17 Normalized Response Spectra for 3-Story Model under Strike-Slip Ground Motion

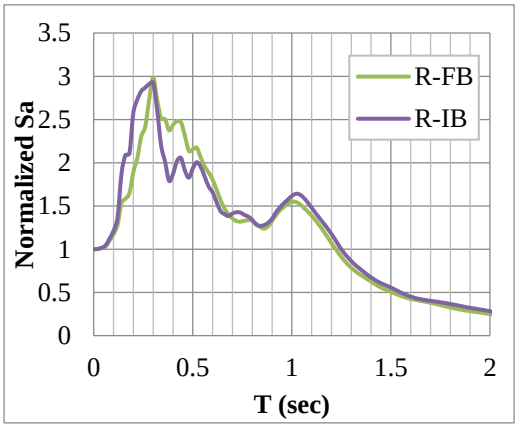

Figure 5.18 Normalized Response Spectra for 3-Story Model under Reverse Ground Motion

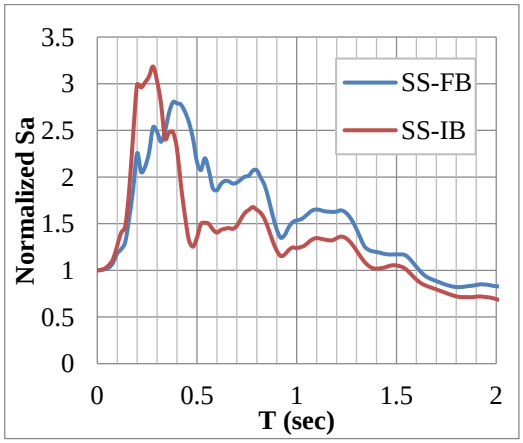

Figure 5.19 Normalized Response Spectra for 4-Story Model under Strike-Slip Ground Motion

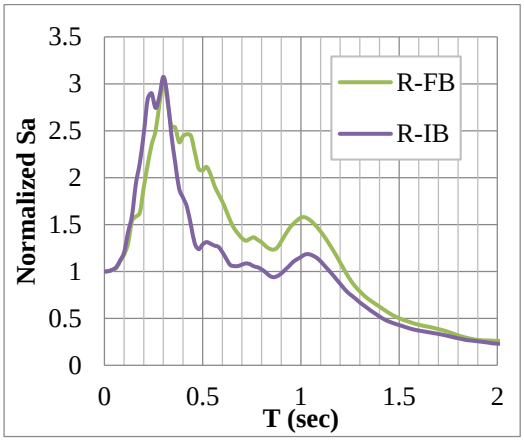

Figure 5.20 Normalized Response Spectra for 4-Story Model under Reverse Ground Motion

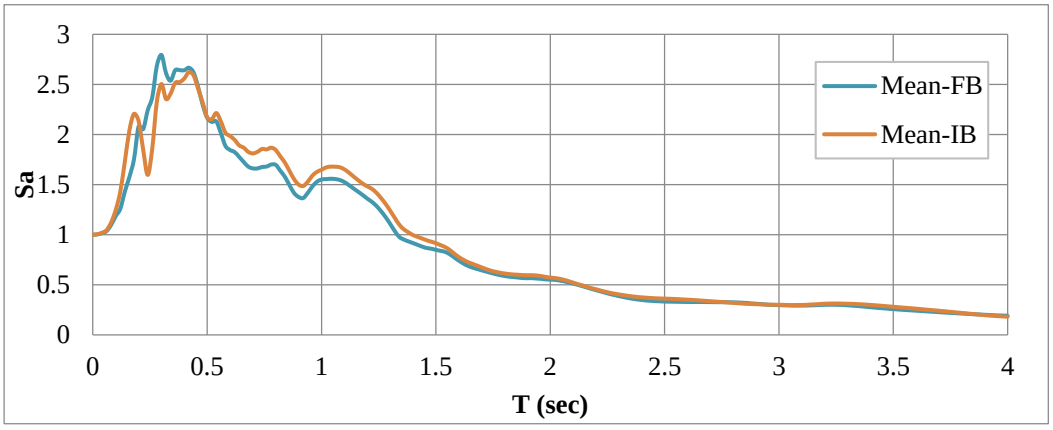

Figure 5.21 Mean of Normalized Response Spectra for 2-Story Model under Strike-Slip and Reverse Ground Motions

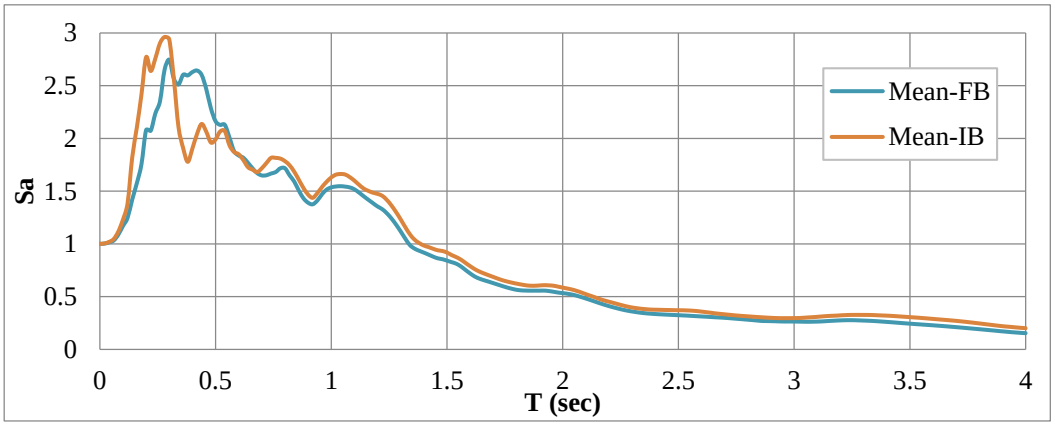

Figure 5.22 Mean of Normalized Response Spectra for 3-Story Model under Strike-Slip and Reverse Ground Motions

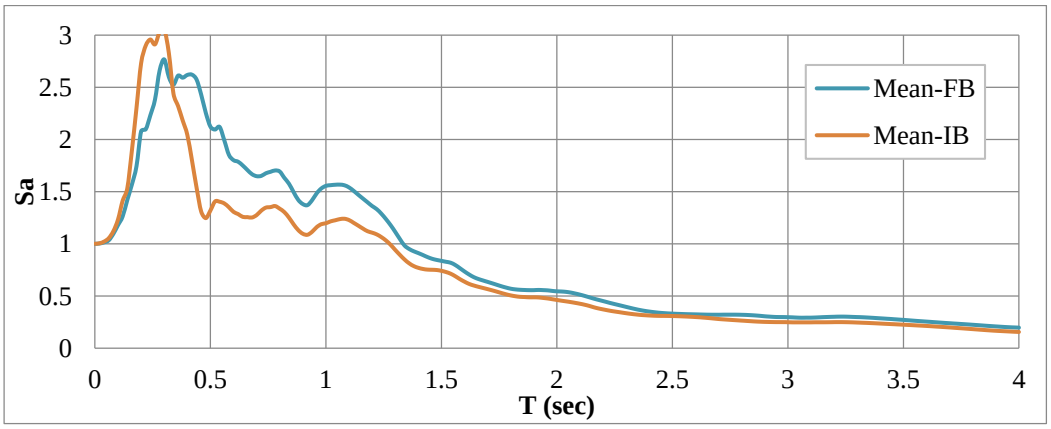

Figure 5.23 Mean of Normalized Response Spectra for 4-Story Model under Strike-Slip and Reverse Ground Motions

The difference between the spectral accelerations of FB and IB conditions were more significant for 3-story model (Figure 5.22). Moreover, the decrease in spectral accelerations were not only observed at the natural frequency of the tested model but also spread over a larger period range. It should be mentioned that a slight increase was observed in spectral accelerations of IB case with respect to the FB case in the low period range (T=0 – 0.3 sec). For the 4-story model, the decrease in spectral accelerations were much more remarkable as compared to other models and were spread over a larger period range (Figure 5.23). Similar to the previous case, the spectral accelerations in T = 0 – 0.30 sec range were slightly higher for IB case as compared to the FB case.

Finally, the mean normalized response spectra for all of the tested models and ground motion combinations for FB and IB cases are calculated to clearly observe the reduction in the accelerations due to the seismic isolation system when it was subjected to a random motion in Figure 5.24. According to this figure, the corner periods (T_A, T_B) of the plateau were shifted (decreased) and the range between these values were narrowed down for the IB case when compared to the FB case. This fact provided a significant decrease in spectral accelerations between T ≈ 0.30 – 0.75 sec. For periods less than 0.30 second, the spectral accelerations are slightly higher for IB cases while the values of FB and IB cases almost coincide after T > 0.75sec spectral periods.

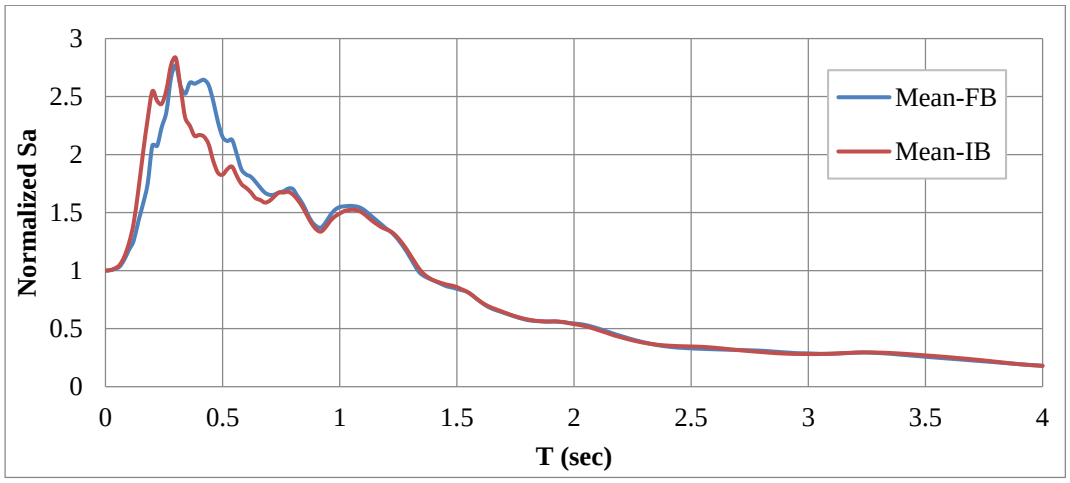

Figure 5.24 Mean of Normalized Response Spectra for All Models under Strike-Slip and Reverse Ground Motions

The test results under modified and scaled ground motions are not as influenced by the resonance effects as the tests results with harmonic motions do since the empirical ground motions contains a large range of frequencies. When the test results from all three models are combined, a significant reduction in spectral accelerations between T ≈ 0.30 – 0.75 sec are observed. To model this reduction, the design envelope recommended in Turkish Earthquake Code (TEC, 2007) was taken as a reference point (Figure 5.25) and the necessary parts were modified to make it fit better to mean spectra for FB and IB cases as shown in Figures 5.26 and 5.27. For FB case, the formulation given in TEC (2007) was directly used with the same corner periods (T_A = 0.25 sec and T_B = 0.45 sec) (Figure 5.26 and Equations 5.1-5.4). For IB case, the characteristic periods obtained for the FB case were scaled by 0.75 (Equations 5.5-5.8) and a slight modification was made for T > T_B (Figure 5.27). The idealized response spectra for FB and IB cases are compared in Figure 5.28.

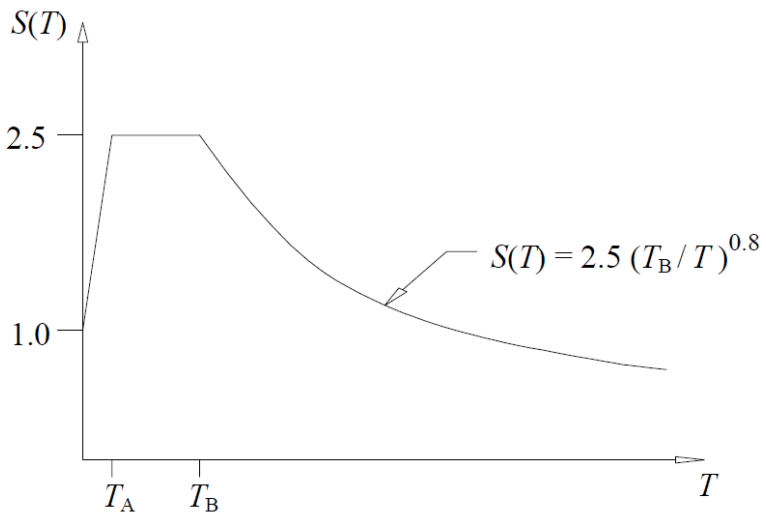

Figure 5.25 Special Design Acceleration Spectra According to Turkish Earthquake Code 2007

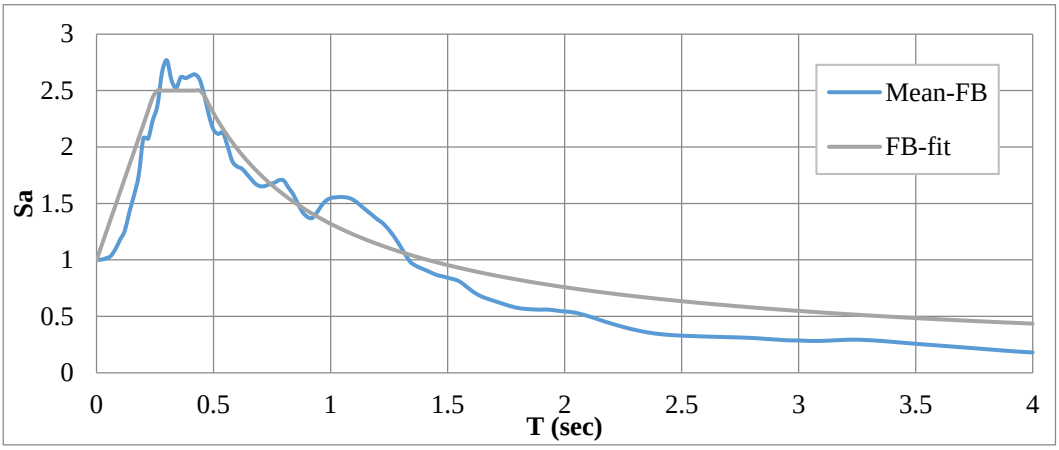

Figure 5.26 Fitted curve to Mean of Normalized Response Spectra for All Models in FB Condition

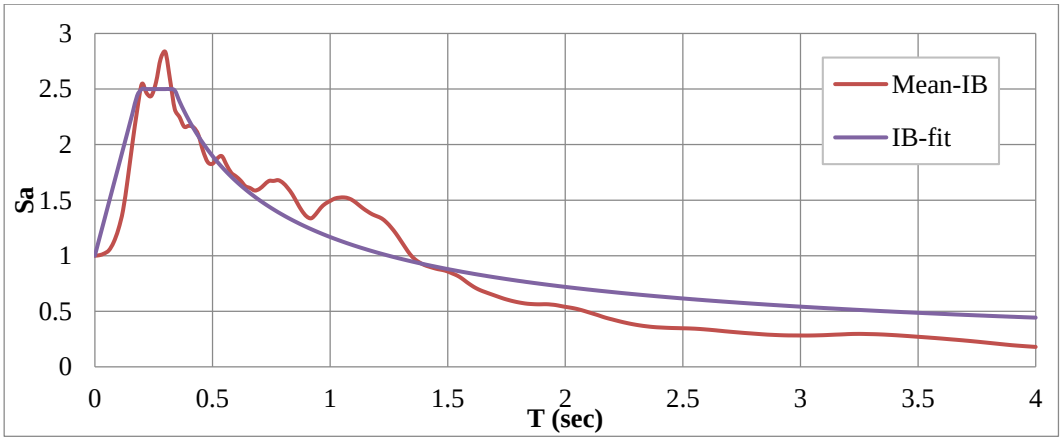

Figure 5.27 Fitted curve to Mean of Normalized Response Spectra for All Models in IB Condition

For FB condition:

$$T_{A,FB} = 0.25 \quad T_{B,FB} = 0.45 \tag{5.1}$$

$$S(T) = 1 + 1.5\frac{T}{T_{A,FB}} \qquad (0 \le T \le T_{A,FB}) \tag{5.2}$$

$$S(T) = 2.5 \qquad (T_{A,FB} < T \le T_{B,FB}) \tag{5.3}$$

$$S(T) = 2.5\left(\frac{T_{B,FB}}{T}\right)^{0.8} \qquad (T < T_{B,FB}) \tag{5.4}$$

For IB condition:

$$T_{A,IB} = 0.75.T_{A,FB} \qquad T_{B,IB} = 0.75.T_{B,FB} \tag{5.5}$$

$$S(T) = 1 + 1.5\frac{T}{T_{A,IB}} \qquad (0 \le T \le T_{A,IB}) \tag{5.6}$$

$$S(T) = 2.5 \qquad (T_{A,IB} < T \le T_{B,IB}) \tag{5.7}$$

$$S(T) = 2.5\left(\frac{T_{B,IB}}{T}\right)^{0.7} \qquad (T < T_{B,IB}) \tag{5.8}$$

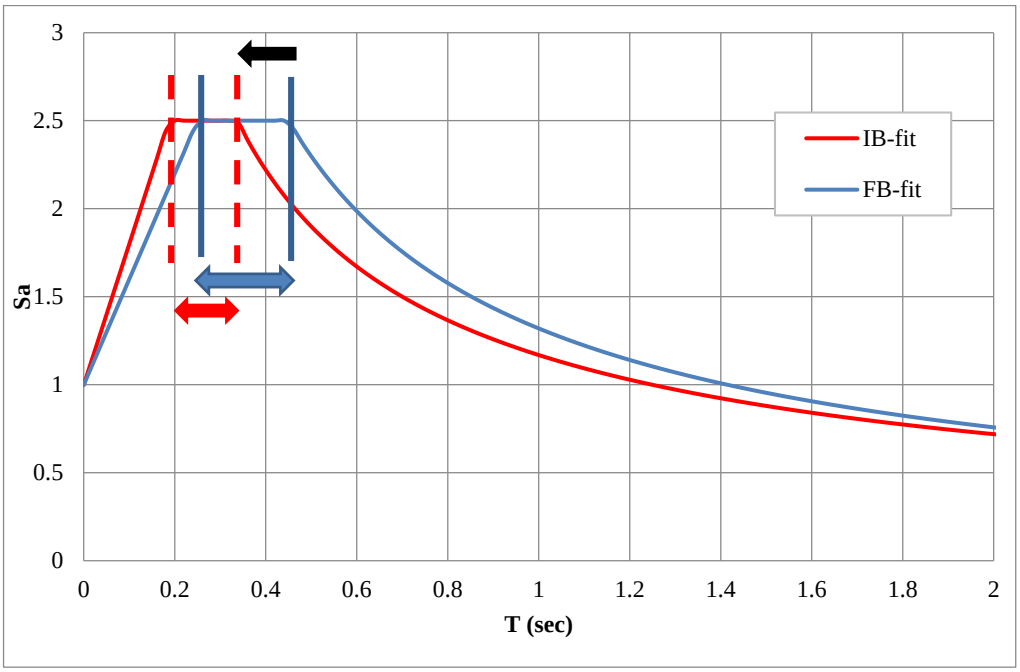

Figure 5.28 Fitted Curves for Mean of Normalized Response Spectra for FB and IB conditions

CHAPTER 6

SUMMARY AND CONCLUSIONS

Within the content of this study, a 3-story building model is designed and tested by employing harmonic and real/modified ground motions in the shaking table test set-up that is located in the Soil Mechanics Laboratory of Middle East Technical University. One of the main objectives is to analyze the seismic response of the model in fixed based (where the model is fixed to the shaking table) and isolated base (where the model is allowed to move over the composite liner system designed as a base isolation system) conditions. Therefore, tests are repeated in these altered base conditions using harmonic ground motions with different frequencies and amplitudes. Since the interaction between the natural frequency of the system and the frequency of the harmonic motion was found to be profound in the previous attempts (similar 2-story and 4-story models were tested by Kalpakcı, 2013), special attention was given to the natural frequency of the model. Model dimensions were modified in a trial-and-error process to achieve a natural frequency around 3 Hz, which lies in the middle of the frequency range of previous models. To reduce the effect of selected frequency of harmonic motion on the response of the model, real acceleograms that are richer in frequency content are also employed in the tests.

One of the main findings of Kalpakcı (2013) was related to the cut-off or triggering amplitude of the ground motion: when the ground shaking levels are smaller than a certain level, the composite liner system was found to be ineffective in reducing the floor accelerations. This behavior is also observed in the experiments with harmonic and real ground motions that were conducted in this study. The minimum threshold acceleration, which is the minimum value necessary to trigger the base isolation system, was measured to be around $a_t \approx 0.08g$ by Kalpakcı (2013); that is consistent with the value stated in Yegian and Kadakal (2004) for rigid models. However, this value was measured as low as $a_t \approx 0.03g$ in this study for 3Hz motion frequency. This difference is attributed to the fact that the model was nearly in resonance during

shaking for 3Hz input motion frequency since the first-mode natural frequency of the model is 3.13Hz.

One of the major findings of this study is related to the interaction between the natural frequency of the loading and the natural frequency of the model. When the frequency of the harmonic loading is away from the natural frequency of the models, the efficiency of the composite liner system is not dependent on the frequency of the harmonic loading. But when these two frequencies are close to each other, the seismic isolation system became more efficient, especially in the tests with harmonic motions. A function which defines the reduction in the floor accelerations provided by the composite liner system based on the natural frequency of the superstructure and the input motion frequency of the harmonic loading cannot be derived since the system's behavior is rather influenced by the resonance effects. Additionally, the system was not triggered for some of the motions and higher modes of shaking were observed in some of the experiments. By combining the results of tests with scaled ground motions the efficiency of the composite liner system in reducing the spectral accelerations in a range of frequencies were evaluated and a mean response spectra was derived to define the behavior of the isolation system under ground motion excitation

Since this experiments use models with different scales in dimension and weight when compared to the real structures, test results presented here is only a preliminary evaluation of the efficiency of geotextiles / geomembrane interface as base isolation. For further experimental studies, the size and edge effects might be investigated by testing different sizes of small blocks beneath the foundation. Also, analytical calculations could be performed and compared in order to verify the results of these experiments.

REFERENCES

Akkar S, Kale Ö, Yenier E, Bommer JJ. (2011). The high-frequency limit of usable response spectral ordinates from filtered analogue and digital strong-motion accelerograms. *Earthq Eng Struct Dyn.*, 40(12):1387-1401. doi:10.1002/eqe.1095.

Chiou, B., Darragh, R., Gregor, N., and Silva, W. (2008). "NGA Project Strong-Motion Database," Earthq. Spectra 24, 23-44.

Douglas J, Boore DM. (2010). High-frequency filtering of strong-motion records. *Bull Earthq Eng.*,9(2):395-409. doi:10.1007/s10518-010-9208-4.

Kalpakcı, V. (2013). Seismic Isolation of Foundations by Composite Liners. Middle East Technical University, PhD Dissertation.

Kalpakcı, V. (2015). Utilization of Geosynthetic Material Interfaces for Reduction of Cyclic Motion Induced Accelerations. *Adv Mater Res.*;1105:361-364. doi:10.4028/www.scientific.net/AMR.1105.361.

Naeim F, Mayes R (2001). Chapter 14 Design of Structure with Seismic Isolation. In: *The Seismic Design Handbook.* Boston, MA: Springer US;. doi:10.1007/978-1-4615-1693-4.

SeismoSignal v5.1.2 and SeismoSignal v2016, Seismosoft Ltd, available from: http://seismosoft.com/seismosignal

SeismoSpect v2.1.2 and SeismoSpect v2016, Seismosoft Ltd, available from: http://seismosoft.com/seismospect

SAP2000 Software v14, Computers and Structures, Inc. (CSI), available from: https://www.csiamerica.com/products/sap2000

Turkish Earthquake Code (2007) Specification for structures to be built in disaster areas. Ministry of Public Works and Settlement, Ankara.

Yegian MK, Lahlaf AM. (1992). Dynamic Interface Shear Strength Properties of Geomembranes and Geotextiles. *J Geotech Eng.*, 118(5):760-779. doi:10.1061/(ASCE)0733-9410(1992)118:5(760)

Yegian MK, Kadakal U, Catan M. (1999). Geosynthetics for Earthquake Hazard Mitigation. In: *Geosynthetics '99: Specifying Geosynthetics and Developing Design Details*. https://trid.trb.org/view.aspx?id=657415

Yegian MK, Kadakal U. (2004). Foundation Isolation for Seismic Protection Using a Smooth Synthetic Liner. *J Geotech Geoenvironmental Eng*.,130(11):1121-1130. doi:10.1061/(ASCE)1090-0241(2004)130:11(1121).

APPENDIX A

SAMPLE INPUT MOTION

A part of the code for Landers earthquake scaled to a_{max} = 0.2g is given below ("X" stands for position in "mm" and "F" is velocity in "mm/s")

G90 (Routine code)
G01 (Start code)
X 0.0000 F 0.0400
X 0.0000 F 0.1200
X 0.0001 F 0.2800
X 0.0002 F 0.5600
X 0.0005 F 1.0400
X 0.0009 F 1.6800
X 0.0015 F 2.4800
X 0.0024 F 3.2400
X 0.0034 F 4.1200
X 0.0046 F 4.8800
X 0.0060 F 5.6800
X 0.0077 F 6.5600
X 0.0096 F 7.8800
X 0.0121 F 9.8400
X 0.0153 F 12.8400
X 0.0196 F 17.0400
X 0.0252 F 22.4800
X 0.0325 F 29.1600
X 0.0417 F 37.0400
X 0.0532 F 45.7600
X 0.0670 F 55.2800
X 0.0833 F 65.2000
X 0.1021 F 75.0800
X 0.1232 F 84.4400
X 0.4325 F 82.4800
X 0.4536 F 84.4400
X 0.4759 F 89.2400
X 0.5003 F 97.2800
X 0.5273 F 108.1600
X 0.5577 F 121.7600
X 0.5921 F 137.3200
X 0.6307 F 154.4000
X 0.6738 F 172.4400
X 0.7215 F 190.9200
X 0.7739 F 209.6400
X 0.8310 F 228.4000
X 0.8928 F 247.0800
X 0.9591 F 265.4400
X 1.0298 F 282.6000
X 1.1038 F 295.8800
X 1.1790 F 301.0400
X 1.2522 F 292.5600
X 1.3187 F 265.9600
X 1.3737 F 220.1600
X 1.4135 F 159.2000
X 1.4364 F 91.6400
X 1.4433 F 27.5200
X 1.4369 F 25.6800
X 1.4205 F 65.4800
X 1.3966 F 95.6800

X 0.1463 F 92.6000
X 0.1711 F 98.9600
X 0.1968 F 103.0400
X 0.2230 F 104.8400
X 0.2492 F 104.6400
X 0.2750 F 103.0000
X 0.3000 F 100.2800
X 0.3242 F 96.8400
X 0.3475 F 92.9600
X 0.3697 F 89.0400
X 0.3911 F 85.5600
X 0.4119 F 83.1200
X 1.3655 F 124.3600
X 1.3251 F 161.7200
X 1.2709 F 216.6000
X 1.1972 F 294.8400
X 1.0978 F 397.4000
X 0.9677 F 520.5200
X 0.8040 F 655.0800
X 0.6073 F 786.4000
X 0.3837 F 894.7600
X 0.1441 F 958.2800
X -0.0952 F 957.3600
X -0.3153 F 880.2400

APPENDIX B

PROPERTIES OF SHAKING TABLE AND MEASUREMETN DEVICES

Table B.1 Properties of shaking table used in METU soil laboratory

Engine:	Rated Torque 24 Nm	Rated Power 6600 W
Dimensions:	Externally 2m x 4m	Laminar Tank 1m x 1.5m
Motion:	Maximum Stroke ± 300mm	Maximum Acceleration 0.3 g

Table B.2 specification of data logger used in experiments

Device:	TESTBOX 2010
Type:	Data Logger
Producer:	TDG
Origin:	Turkey
Resolution:	24-bit
Connection:	Ethernet
Channel:	16
Sampling Speed:	500 Hz
Excitation Voltage:	5V - 12V
Measuring Voltage:	± 30 mV to ± 12 V
Safe Temperature Range:	10 to 35 ^{0}C

Table B.3 Specification of measurement devices used in experiments

Device:	AS1-GA	ASW-1A	LPT 600
Type:	Accelerometer	Accelerometer	Displacement Sensor
Producer:	KYOWA	KYOWA	OPKON
Origin:	Japan	Japan	Turkey
Rated Capacity:	± 1g	± 1g	600 mm
Nonlinearity:	≤ ± 1% of RO	≤ ± 1% of RO	≤ ± 0.05%
Hysteresis:	≤ ± 1% of RO	≤ ± 1% of RO	≤ ± 0.01%
Rated Output (RO):	0.5 mV/V	0.5 mV/V	-
Safe Overload Rating:	300%	300%	-
Safe Excitation Voltage:	6V AC / DC	6V AC / DC	12 - 30V DC
Safe Temperature Range:	-15 to 65 ^{0}C	-15 to 65 ^{0}C	-20 to 80 ^{0}C
Resonance Frequency:	70 Hz	40 Hz	-
Displacement Speed:	-	-	≤ 5 m/s

APPENDIX C

GEOMEMBRANE AND GEOTEXTILE PROPERTIES

Table C.4 Material Properties of nonwoven heat-bonded Geotextile (Typar-3601)

PROPERTY	TEST METHOD	METRIC
Weight - Typical	ASTM D-5261	203 g/sm
Tensile Strength	ASTM D-4632	1,068 N
Elongation @ Break	ASTM D-4632	60%
Puncture Strength	ASTM D-4833	298 N
CBR Puncture	ASTM D-6241	1,647 N
Trapezoidal Tear	ASTM D-4533	400 N
Apparent Opening Size	ASTM D-4751	0.10 mm
Permittivity	ASTM D-4491	0.10 Sec-1
Water Flow Rate	ASTM D-4491	611 l/min/sm
UV Resistance @ 500 Hours	ASTM D-4355	70%

Table C.5 Physical and Mechanical Properties of UHMWPE Geomembrane (TIVAR 88-2)

Physical and Mechanical Properties	Metric	Comments
Specific Gravity	0.933 g/cc	ASTM D792
Water Absorption	<= 0.010 %	Immersion, 24hr; ASTM D570(2)
Hardness, Shore D	64	ASTM D2240
Tensile Strength	37.9 MPa	ASTM D638
Elongation at Break	200%	ASTM D638
Tensile Modulus	0.669 GPa	ASTM D638
Flexural Yield Strength	20.7 MPa	ASTM D790
Flexural Modulus	0.724 GPa	ASTM D790
Compressive Strength	20.0 MPa	10% Def.; ASTM D695
Compressive Modulus	0.552 GPa	ASTM D695
Shear Strength	33.1 MPa	ASTM D732
Izod Impact, Notched	NB	ASTM D256 Type A
Coefficient of Friction	0.08	Dry vs. Steel; QTM55007
Sand Slurry	11	1018 Steel = 100

Table C.6 Chemical Resistance Properties of UHMWPE Geomembrane (TIVAR 88-2)

Chemical Resistance Properties	**Metric**
Acids, Strong (pH 1-3)	Limited
Acids, Weak	Acceptable
Alcohols	Acceptable
Alkalies, Strong (pH 11-14)	Acceptable
Alkalies, Weak	Acceptable
Chlorinated Solvents	Acceptable
Conductive / Static Dissipative	No
Continuous Sunlight	Limited
Hot Water / Steam	Limited
Hydrocarbons - Aliphatic	Acceptable
Hydrocarbons - Aromatic	Unacceptable
Inorganic Salt Solutions	Acceptable
Ketones, Esters	Limited

APPENDIX D

TIME HISTORIES OF INPUT GROUND MOTIONS

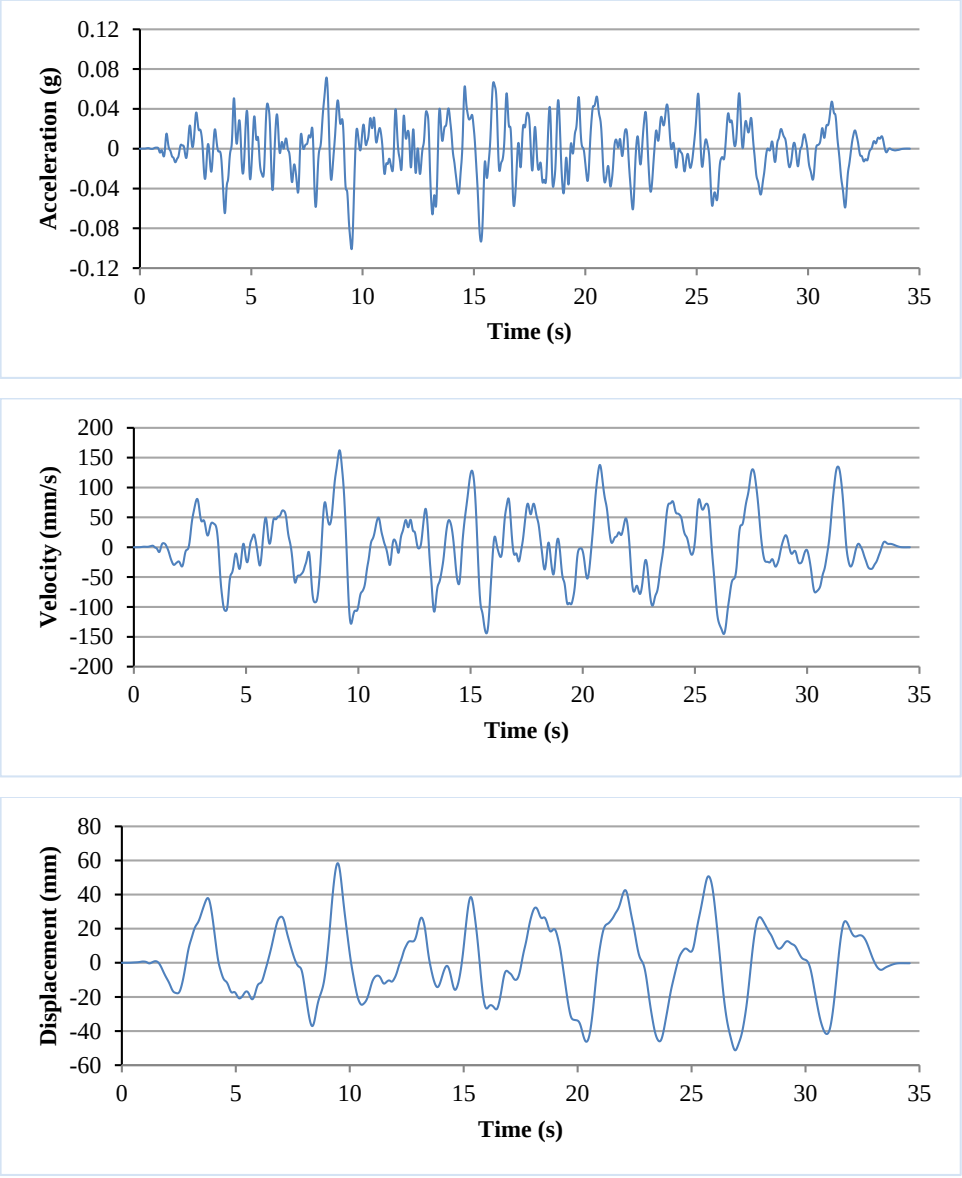

Figure D.1 Acceleration, velocity and displacement time histories for “Landers” ground motion scaled to 0.1 g

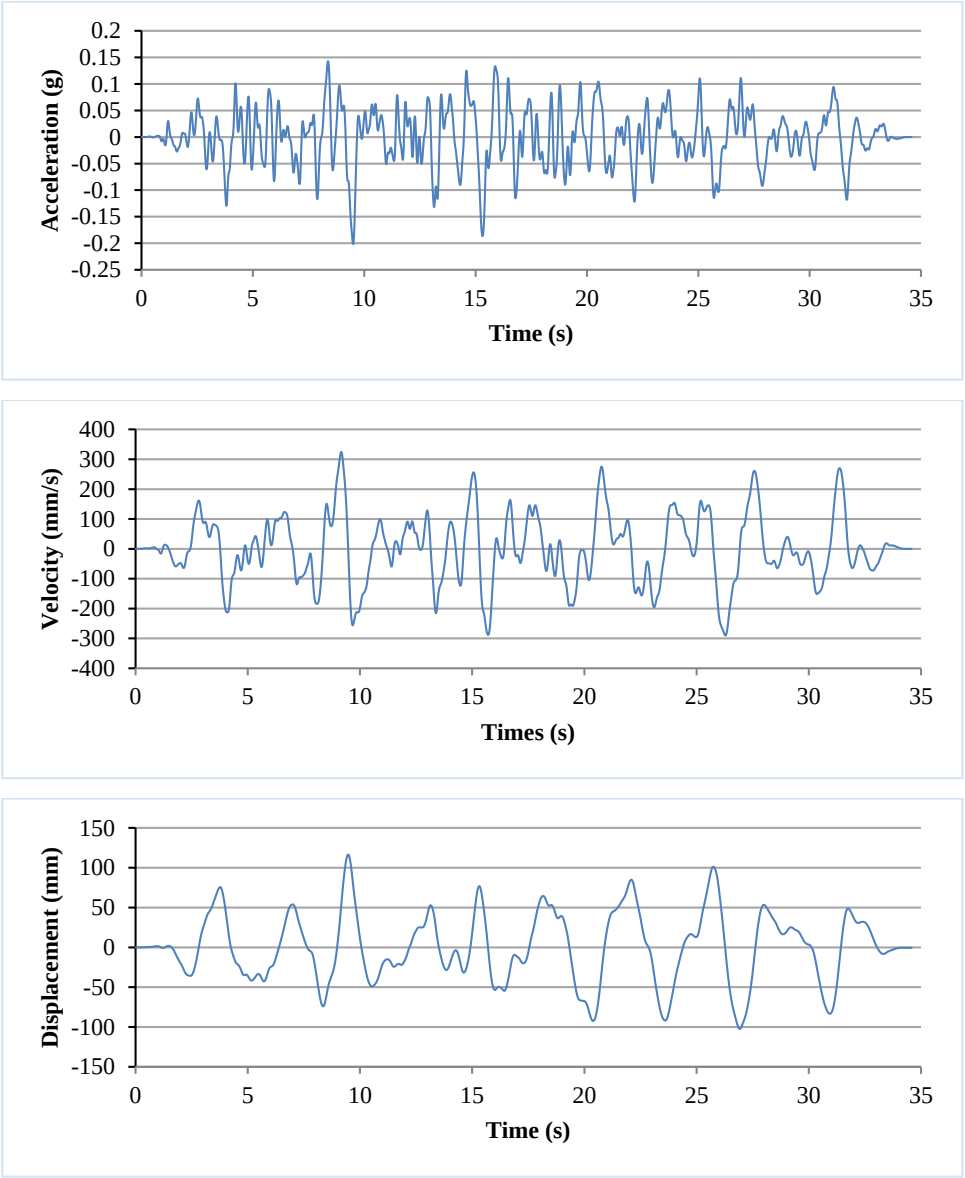

Figure D.2 Acceleration, velocity and displacement time histories for “Landers” ground motion scaled to 0.2 g

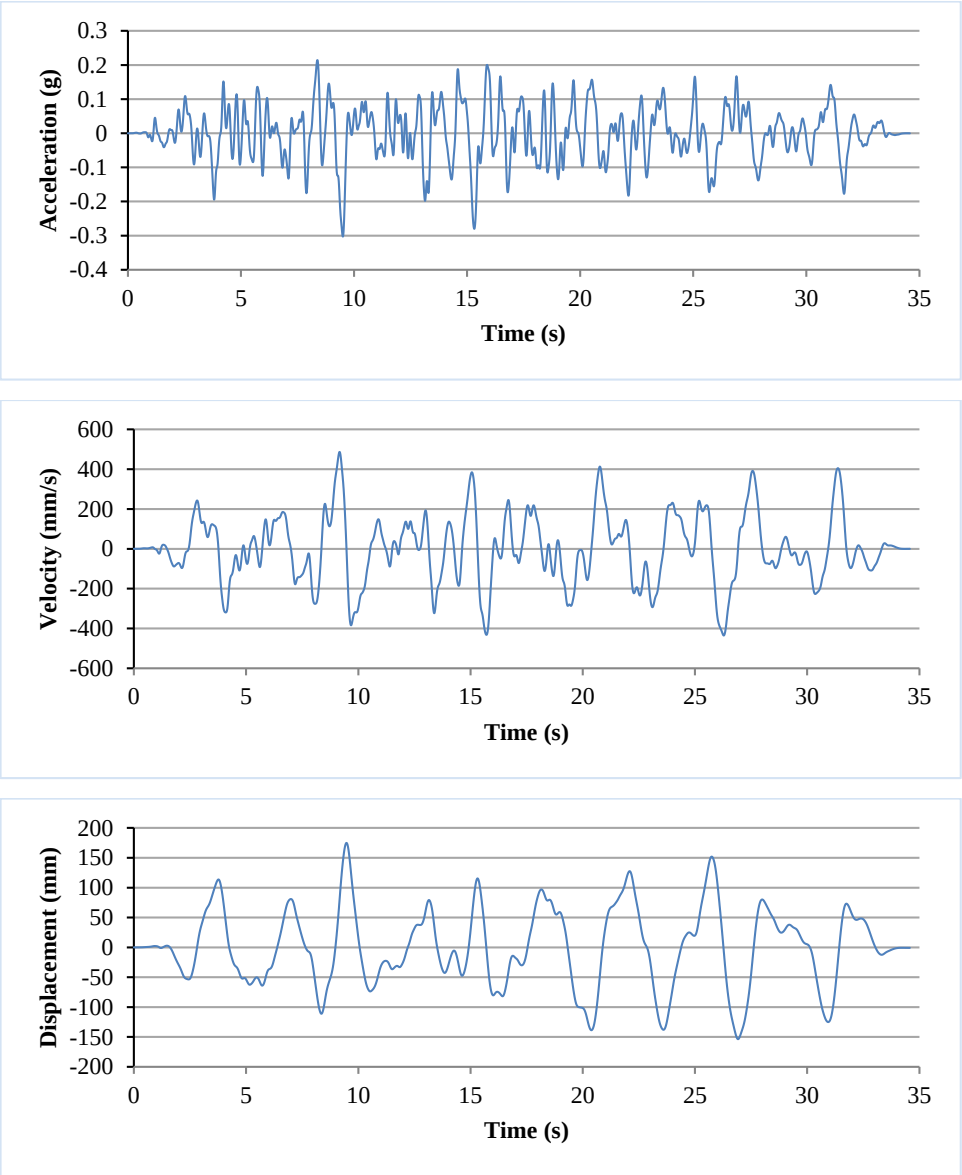

Figure D.3 Acceleration, velocity and displacement time histories for “Landers” ground motion scaled to 0.3 g

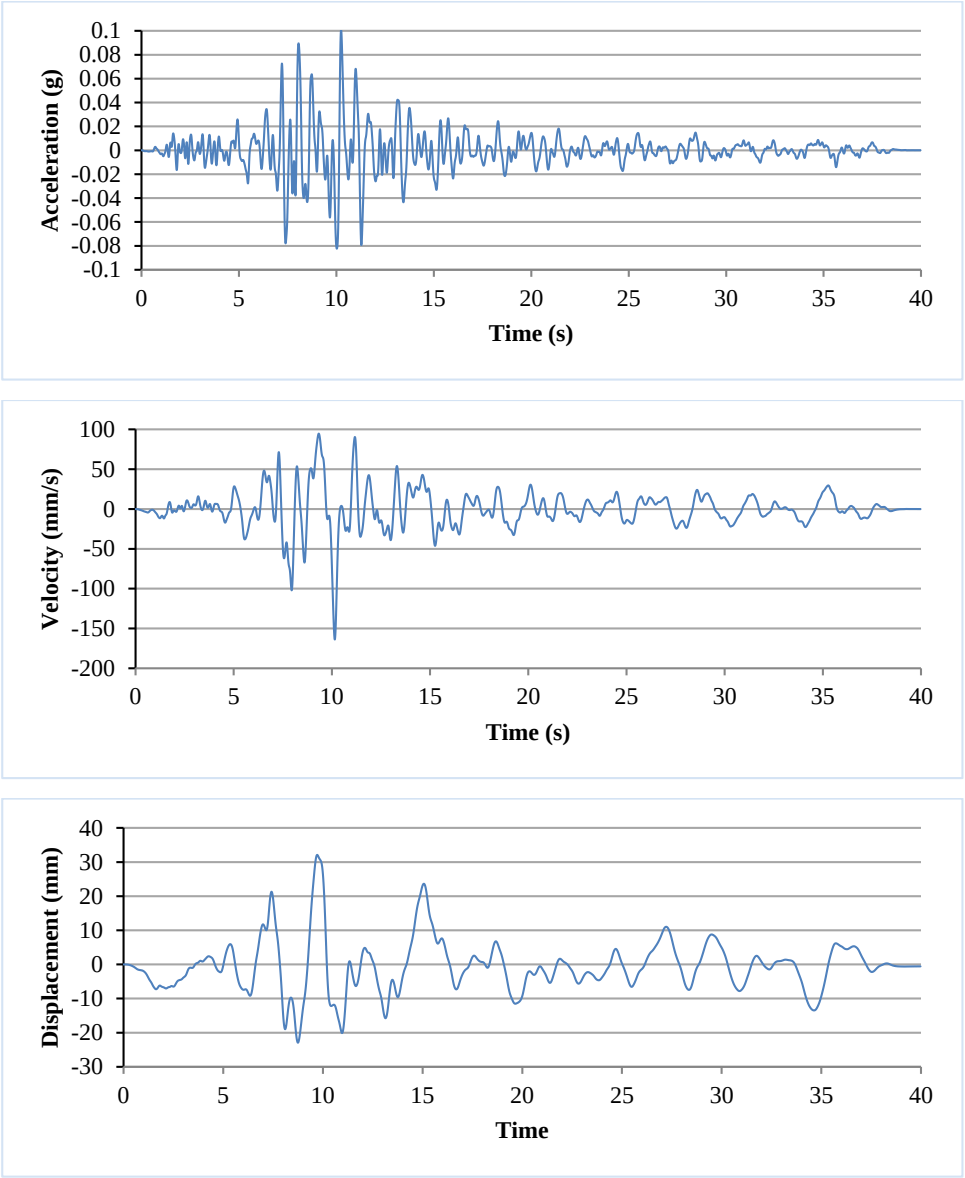

Figure D.4 Acceleration, velocity and displacement time histories for “Chalfant Valley” ground motion scaled to 0.1 g

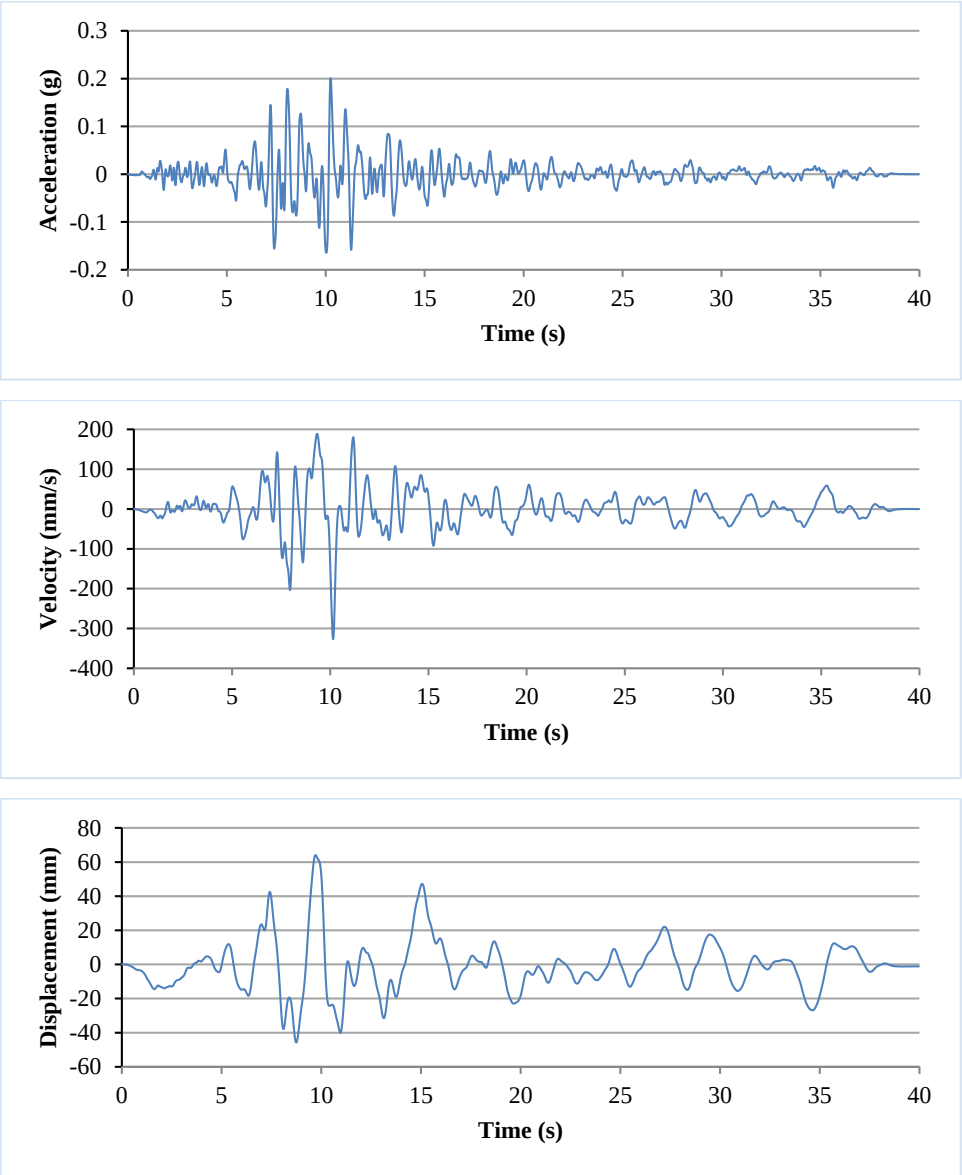

Figure D.5 Acceleration, velocity and displacement time histories for “Chalfant Valley” ground motion scaled to 0.2 g

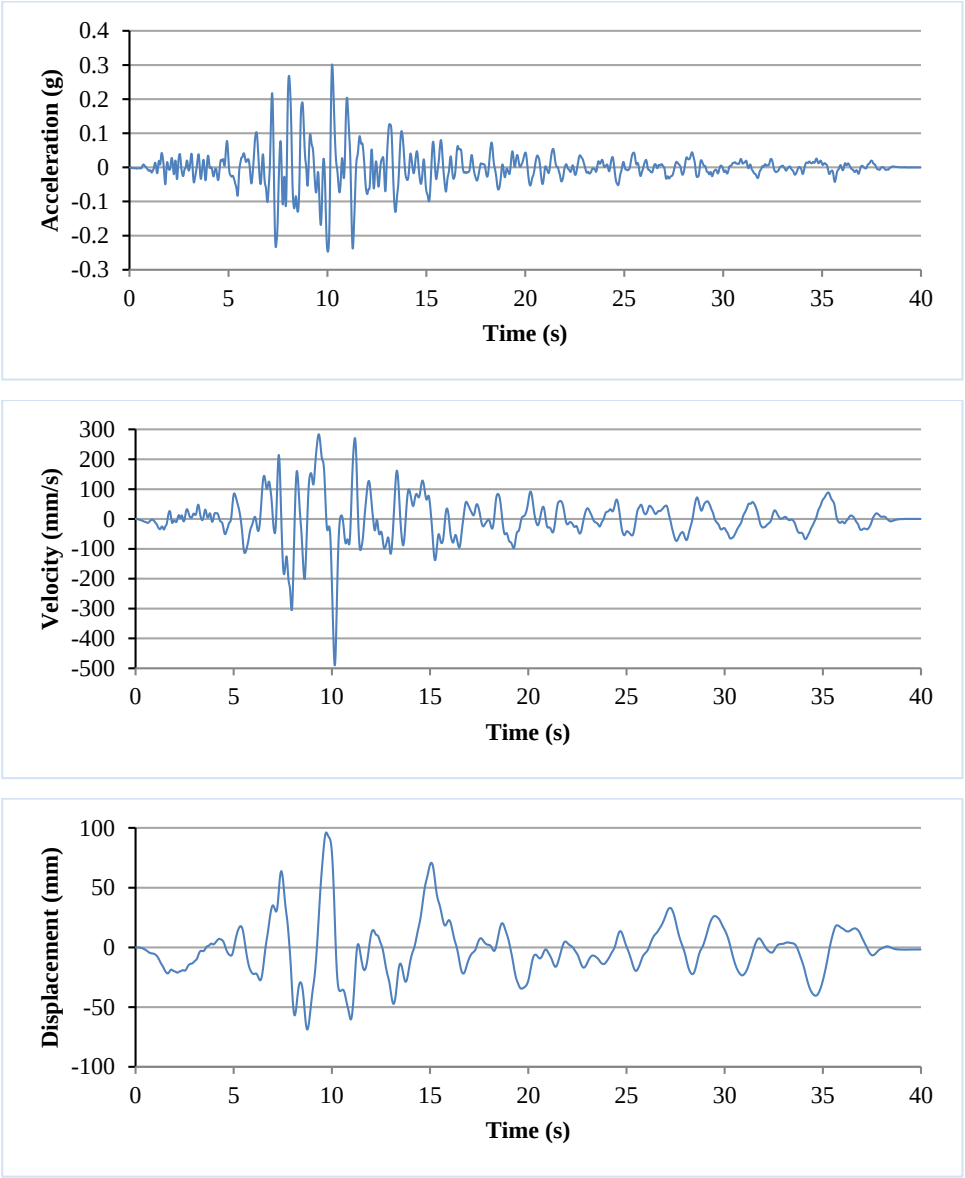

Figure D.6 Acceleration, velocity and displacement time histories for “Chalfant Valley” ground motion scaled to 0.3 g

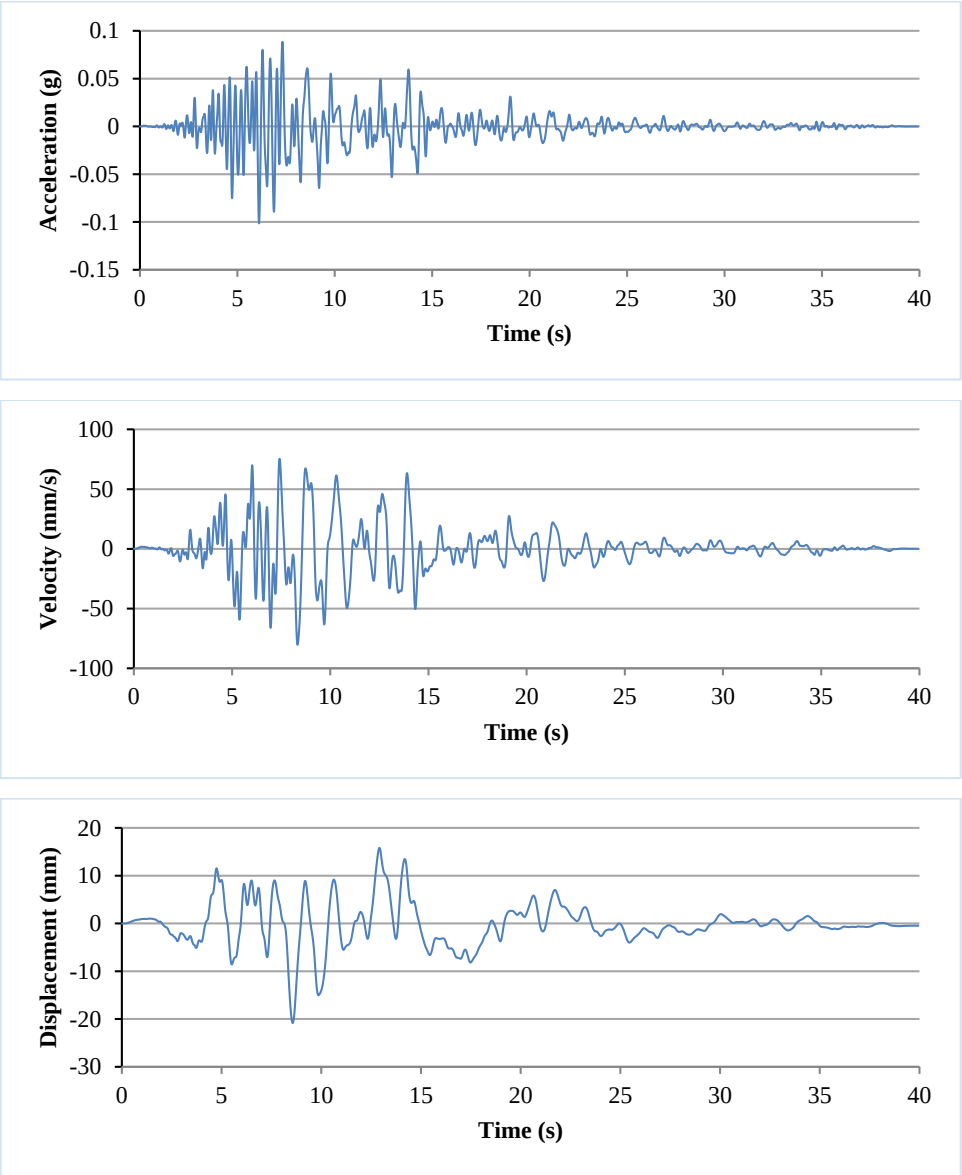

Figure D.7 Acceleration, velocity and displacement time histories for “Loma Prieta” ground motion scaled to 0.1 g

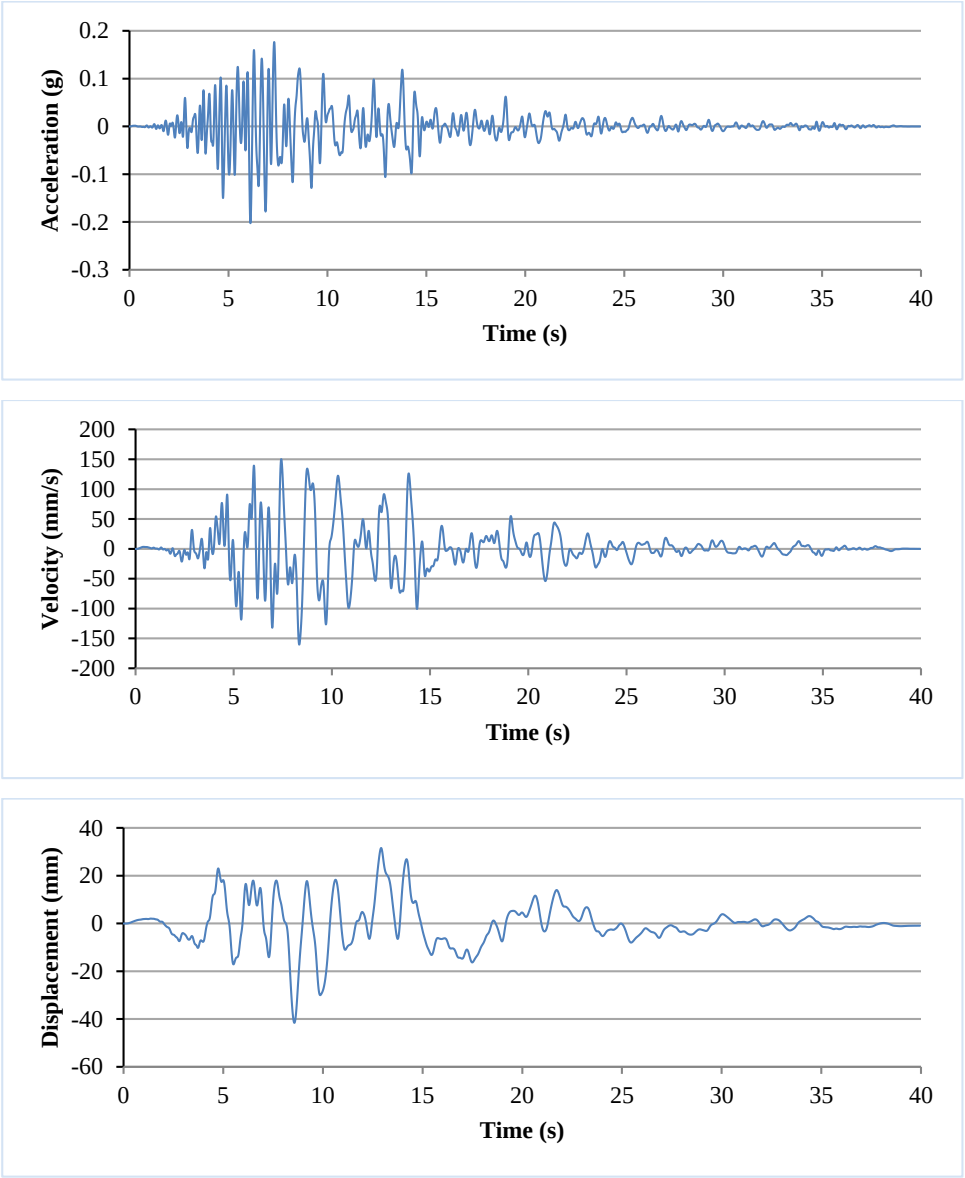

Figure D.8 Acceleration, velocity and displacement time histories for “Loma Prieta” ground motion scaled to 0.2 g

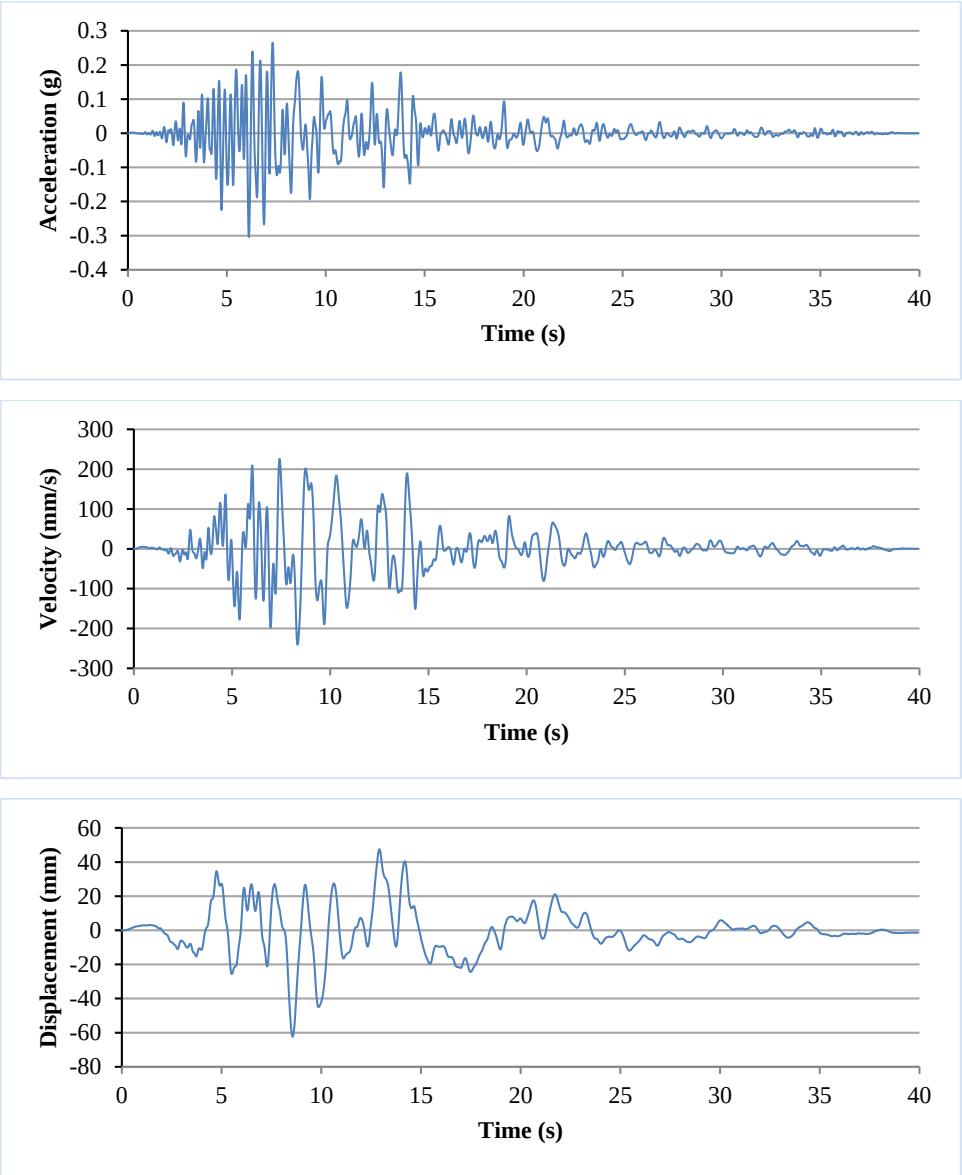

Figure D.9 Acceleration, velocity and displacement time histories for “Loma Prieta” ground motion scaled to 0.3 g

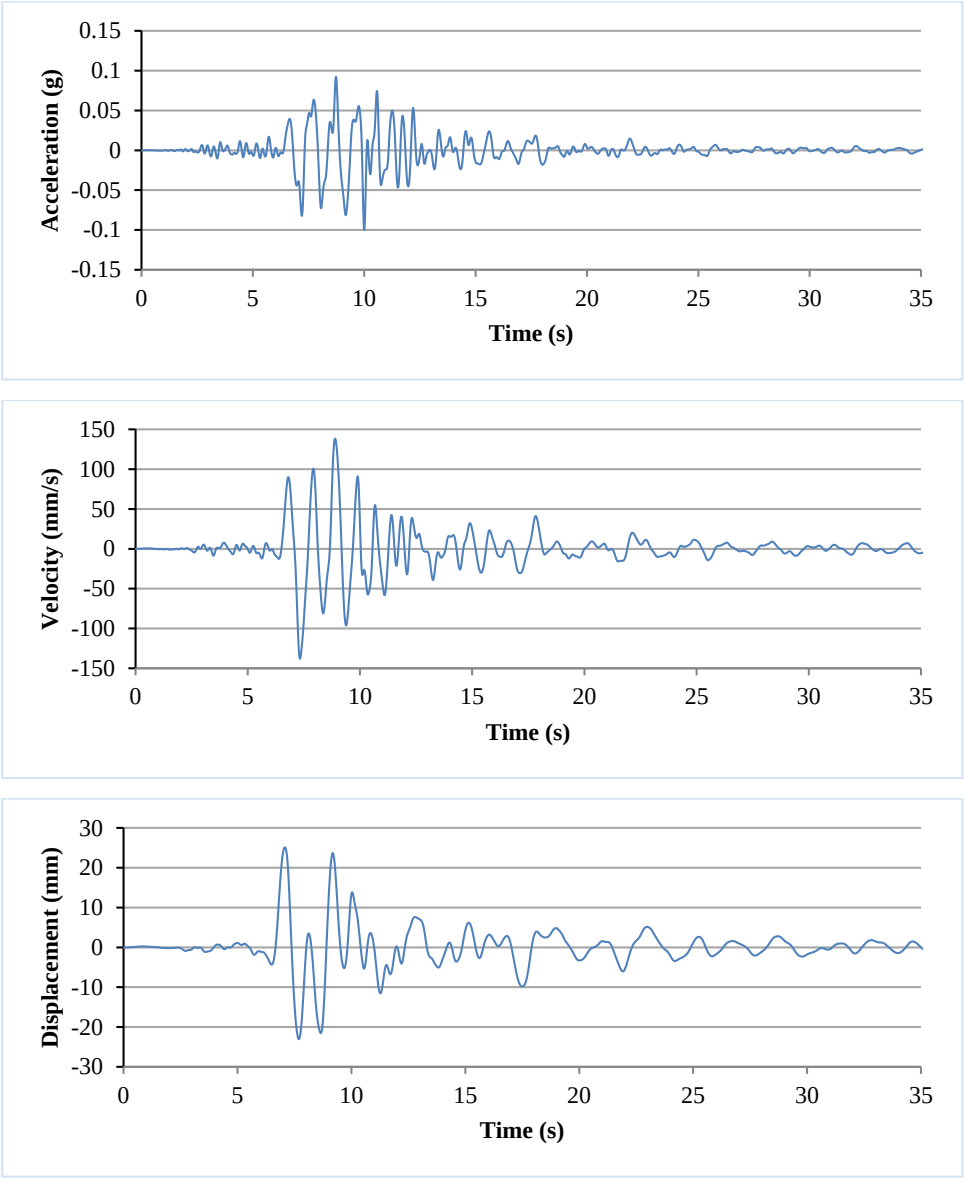

Figure D.10 Acceleration, velocity and displacement time histories for “Coalinga” ground motion scaled to 0.1 g

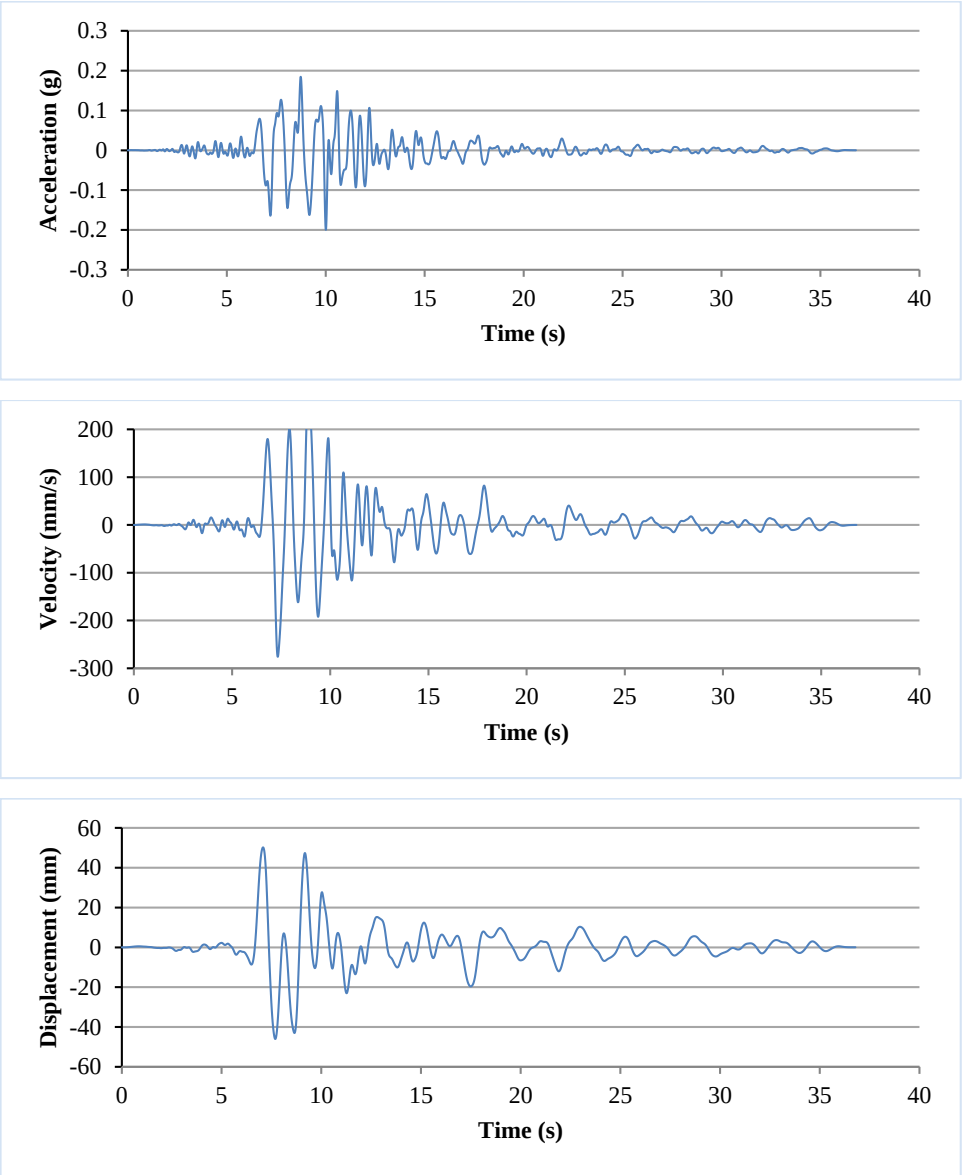

Figure D.11 Acceleration, velocity and displacement time histories for “Coalinga” ground motion scaled to 0.2 g

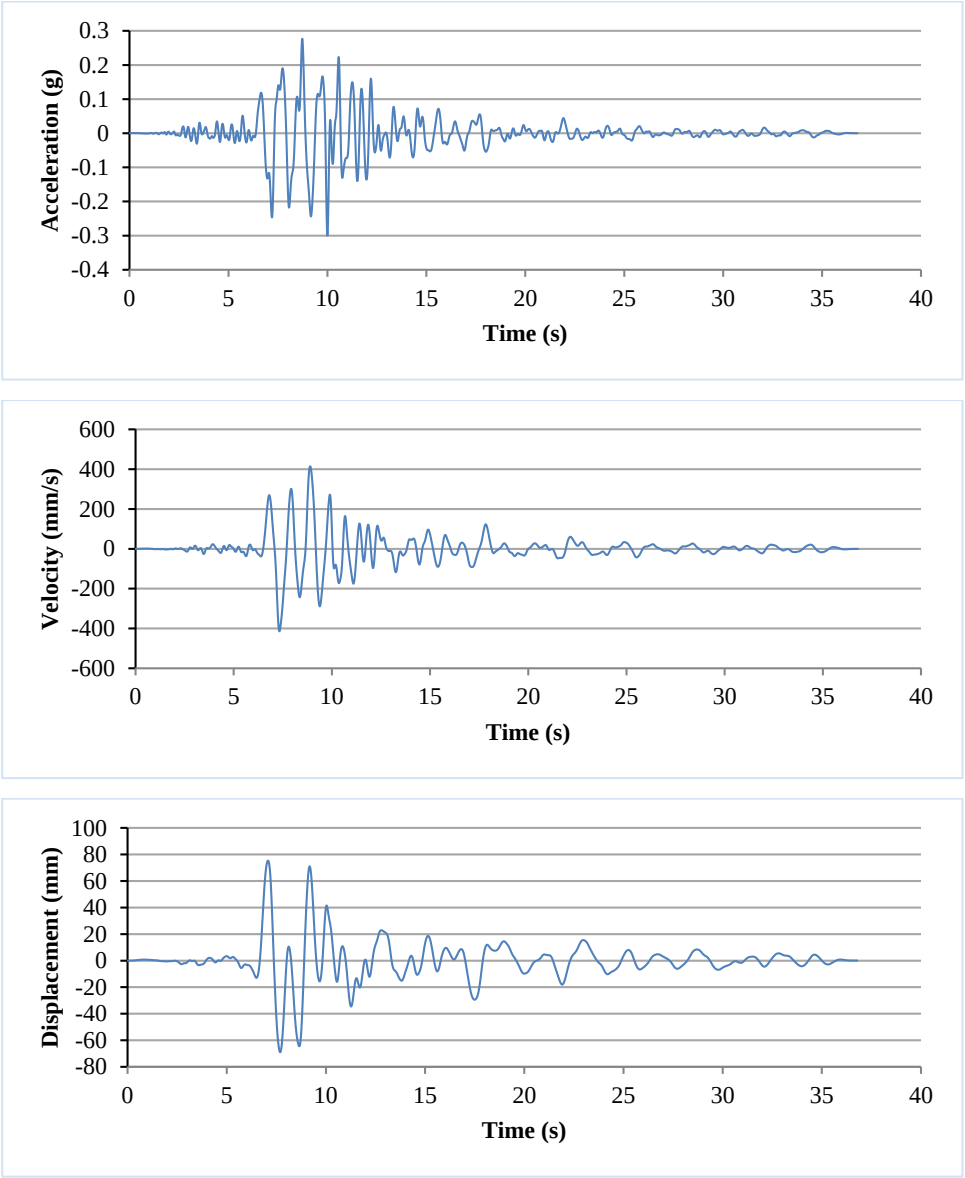

Figure D.12 Acceleration, velocity and displacement time histories for “Coalinga” ground motion scaled to 0.3 g

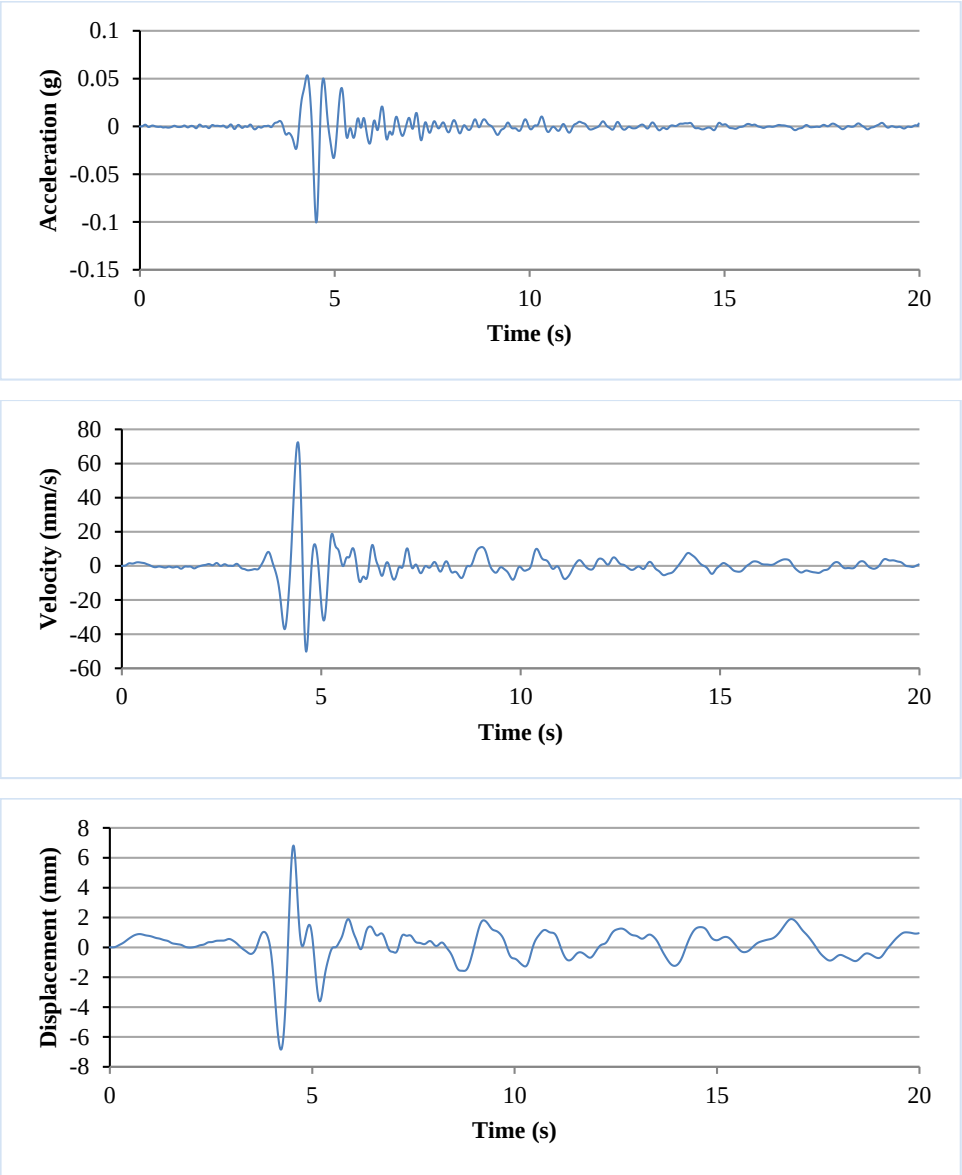

Figure D.13 Acceleration, velocity and displacement time histories for “Northridge” ground motion scaled to 0.1 g

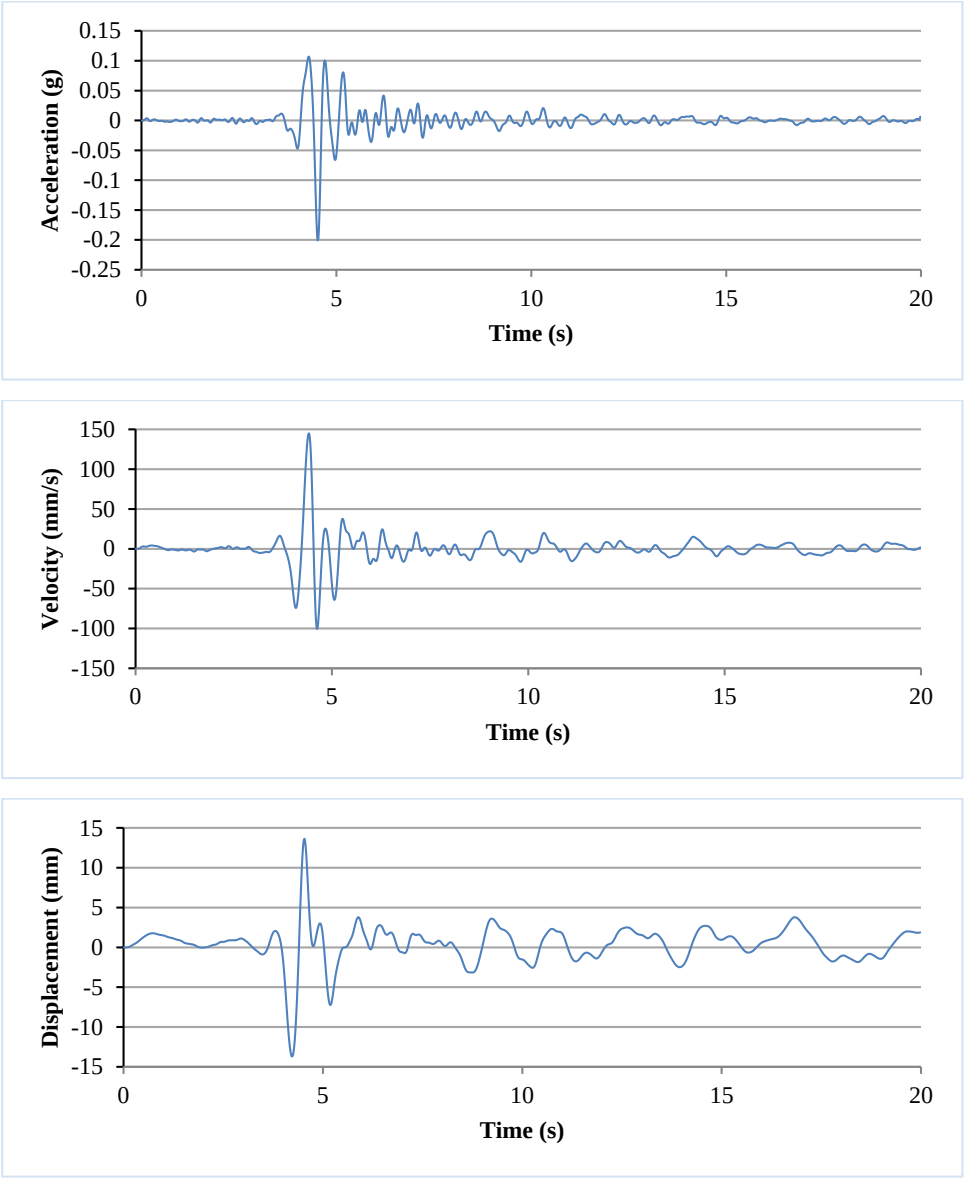

Figure D.14 Acceleration, velocity and displacement time histories for “Northridge” ground motion scaled to 0.2 g

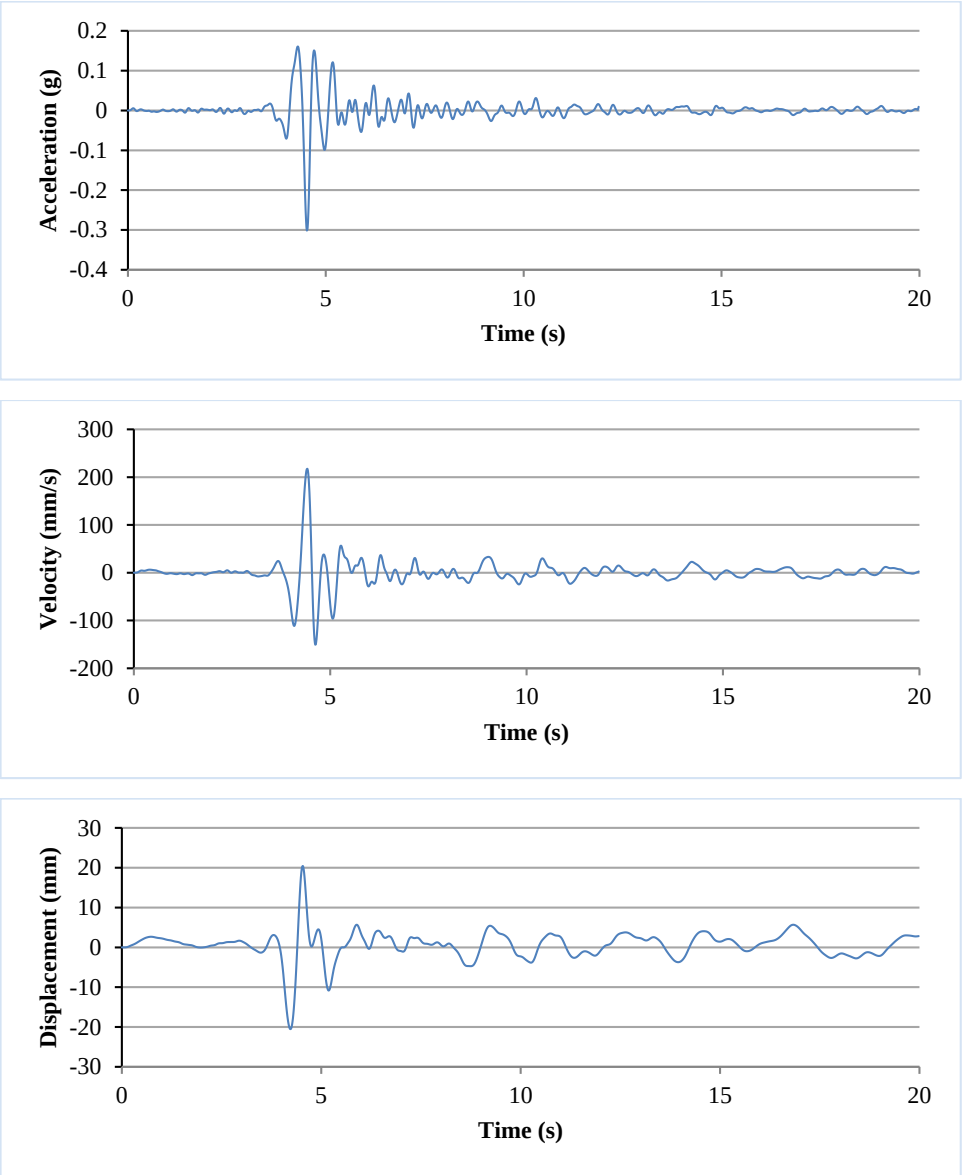

Figure D.15 Acceleration, velocity and displacement time histories for “Northridge” ground motion scaled to 0.3 g

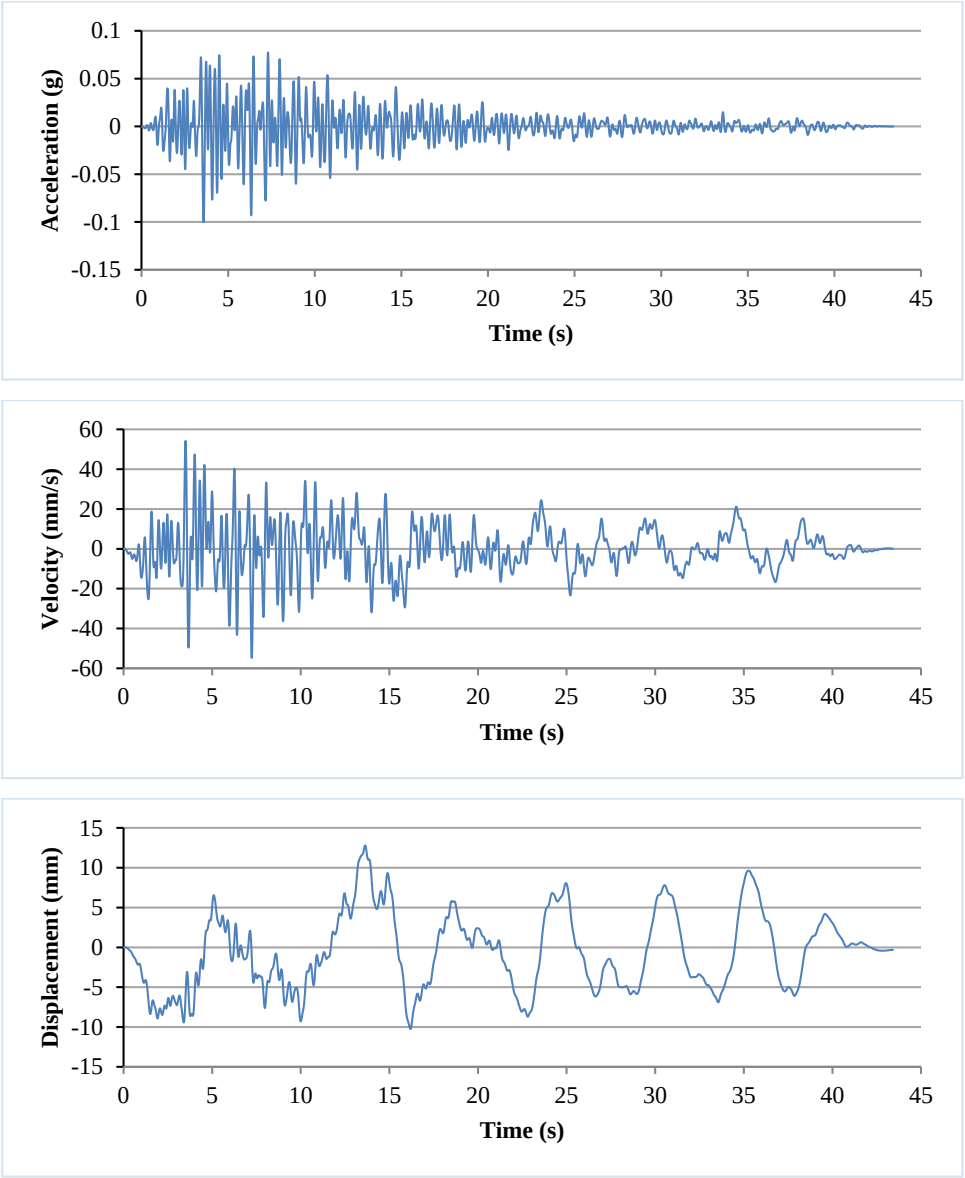

Figure D.16 Acceleration, velocity and displacement time histories for “San Fernando” ground motion scaled to 0.1 g

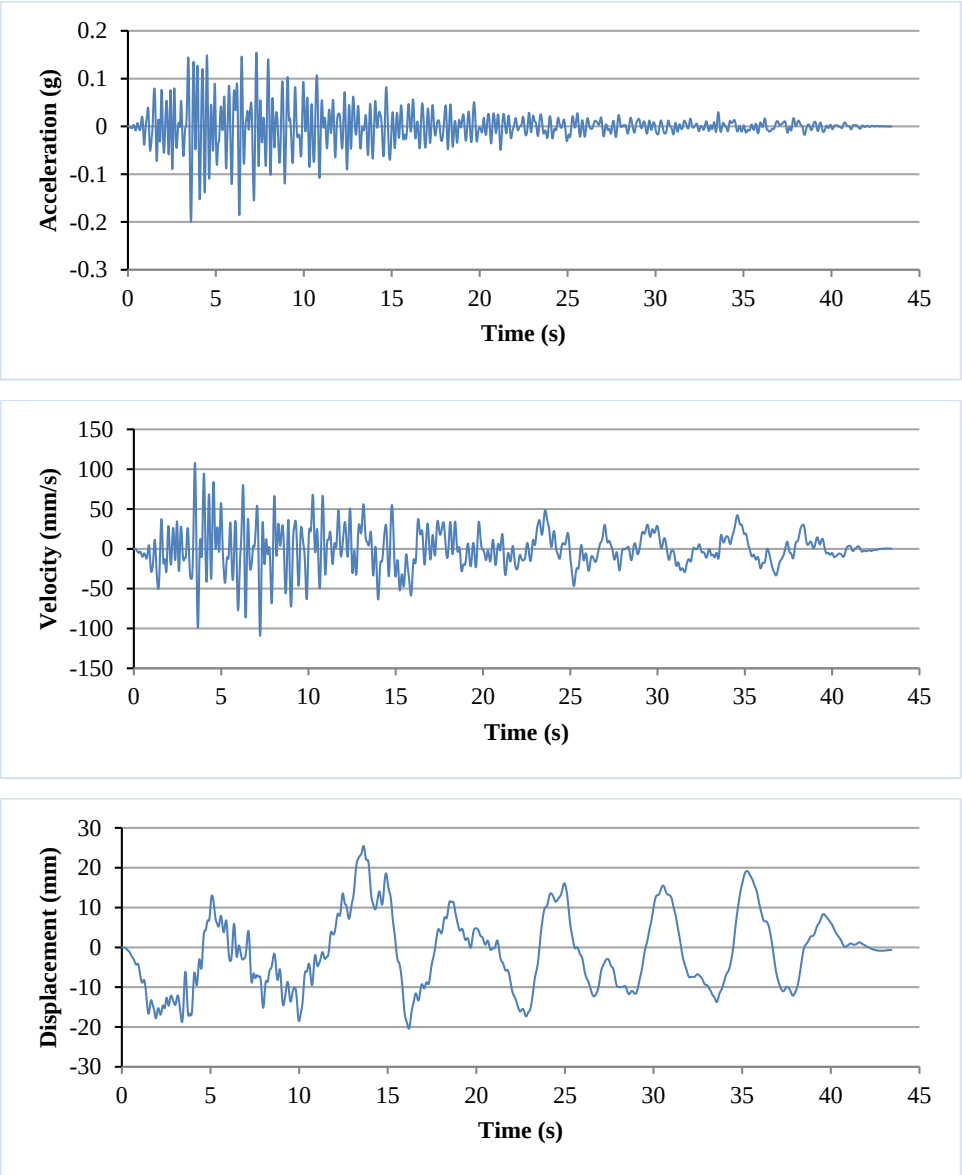

Figure D.17 Acceleration, velocity and displacement time histories for “San Fernando” ground motion scaled to 0.2 g

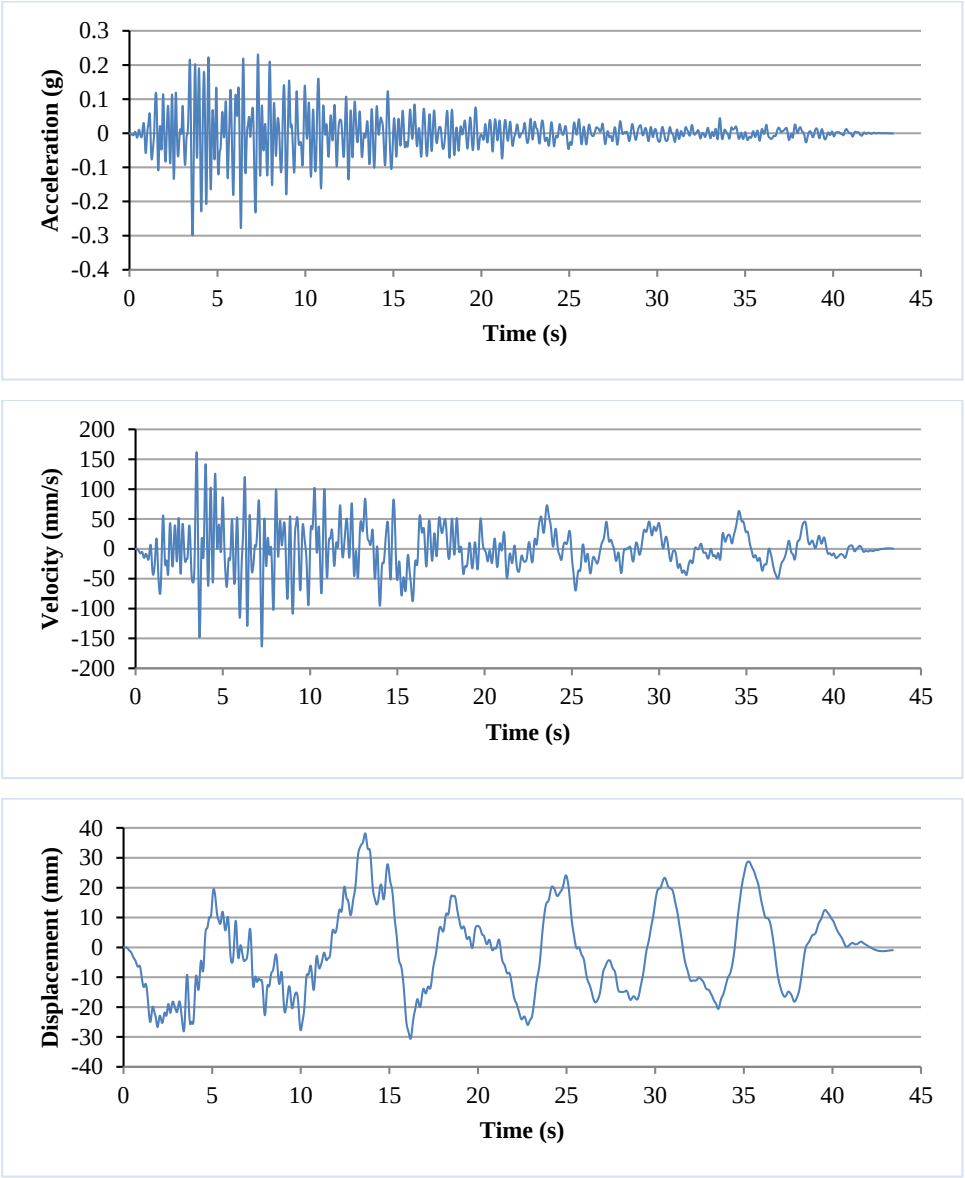

Figure D.18 Acceleration, velocity and displacement time histories for “San Fernando” ground motion scaled to 0.3 g